Institut für Experimentelle Pneumologie

der Universität München

Direktor: Prof. Dr. med. Oliver Eickelberg

Aus dem

Comprehensive Pneumology Center

des Helmholtz Zentrum München

Direktor: Prof. Dr. med. Oliver Eickelberg

IMMUNE CELL CHARACTERIZATION IN THE LUNG AFTER ACUTE AND CHRONIC CIGARETTE SMOKE EXPOSURE IN A MOUSE MODEL OF COPD

Dissertation

zum Erwerb des Doktorgrades der Humanbiologie

an der Medizinischen Fakultät der

Ludwig-Maximilians-Universität zu München

vorgelegt von

Katrin Hager

aus

Eilenburg

2016

Mit Genehmigung der Medizinischen Fakultät

der Universität München

Berichterstatter:	Prof. Dr. med. Oliver Eickelberg
Mitberichterstatter:	Prof. Dr. Albrecht Bergner
	Prof. Dr. Jürgen Behr
Mitbetreuung durch den promovierten Mitarbeiter:	Dr. Ali Önder Yildirim
Dekan:	Prof. Dr. med. dent. Reinhard Hickel

Tag der mündlichen Prüfung: 21.10.2016

Eidesstattliche Versicherung

Ich, Katrin Hager, erkläre hiermit an Eides statt, dass ich die vorliegende Dissertation mit dem Thema

„Immune cell characterization in the lung after acute and chronic cigarette smoke exposure in a mouse model of COPD“

selbständig verfasst, mich außer der angegebenen keiner weiteren Hilfsmittel bedient und alle Erkenntnisse, die aus dem Schrifttum ganz oder annähernd übernommen sind, als solche kenntlich gemacht und nach ihrer Herkunft unter Bezeichnung der Fundstelle einzeln nachgewiesen habe.

Ich erkläre des Weiteren, dass die hier vorgelegte Dissertation nicht in gleicher oder in ähnlicher Form bei einer anderen Stelle zur Erlangung eines akademischen Grades eingereicht wurde.

_____ _____

Ort, Datum Unterschrift Doktorandin/Doktorand

Table of Contents

List of Abbreviations

%	percent
ANA	antinuclear antibodies
BAL	bronchoalveolar lavage
CAT	COPD assessment test
CCL	Chemokine (C-C motif) ligand
CCR	C-C chemokine receptor
CD	cluster of differentiation
Chit	chitotriosidase
Chi3l	Chitinase 3-like protein
CO	carbon monoxide
COPD	chronic obstructive pulmonary disease
CS	cigarette smoke
CSC	cigarette smoke condensate
CSE	cigarette smoke extract
CXCL	chemokine (C-X-C motif) ligand
CXCR	C-X-C chemokine receptor
DC	dendritic cell
DMSO	dimethyl sulfoxide
DNA	desoxyribonucleic acid
EAE	experimental autoimmune encephalomyelitis
et al.	*et alii*
Fc	fragment crystallisable
FDC	follicular dendritic cell
FEV	forced expiratory volume
FoxP3	forkhead box P3
FVC	forced vital capacity
G-CSF	granulocyte colony-stimulating factor
GM-CSF	granulocyte-macrophage colony-stimulating factor
GOLD	global initiative for chronic obstructive lung disease
h	hour
HEV	high endothelial venule
HPV	human papillomavirus
iBALT	inducible bronchus-associated lymphoid tissue
IBD	inflammatory bowl disease
IFN	interferon
Ig	immunoglobulin
IL	interkeukin
iNOS	inducible nitric oxide synthase
IRF	interferon-regulatory factor
KC	keratinocyte-derived cytokine
Ko	knockout
L	ligand
Lm	mean linear intercept
LF	lymphoid follicle
LPS	lipopolysaccharide
M1	classically activated macrophage
M2	alternatively activated macrophage
m^3	cubic meters
MCP	monocyte chemoattractant protein
mg	milligram
MIP	macrophage inflammatory protein 2
MMP	matrix metalloproteinase
mMRC	modified Medical Research Council
µMT	B cell deficient
mRNA	messenger RNA
MS	multiple sclerosis
NFκB	nuclear factor 'kappa-light-chain-enhancer' of activated B-cells
NE	neutrophil elastase
NO	nitric oxide
PBS	phosphate buffered saline
PCR	polymerase chain reaction
PE	phycoerythrin
PM	particulate matter
R	receptor
RA	rheumatoid arthritis
RNA	ribonucleic acid
ROR	retinoic orphan nuclear receptor
ROS	reactive oxygen species
SHS	secondhand smoke
Sv	airspace wall surface to volume ratio
TGFβ	transforming growth factor β
Th	T helper cell
TIMP1	TIMP metallopeptidase inhibitor 1

TLO	tertiary lymphoid organ
TLR	toll-like-receptor
TNFα	tumor necrosis factor α
TPM	total particulate matter
Treg	regulatory T cell
Wt	wildtype
WHO	World Health Organization

List of Publications

- "*Inflammaging increases susceptibility to cigarette smoke-induced COPD"*, Gerrit John-Schuster, Stefanie Günther, Katrin Hager, Thomas Conlon, Oliver Eickelberg, Ali Önder Yildirm, **Oncotarget**, 2015 May 29. [Epub ahead of print]

- *"Cigarette smoke-induced iBALT mediates macrophage activation in a B cell-dependent manner in COPD"*, Gerrit John-Schuster*, Katrin Hager*, Thomas Conlon, Martin Irmler, Johannes Beckers, Oliver Eickelberg, Ali Ö. Yildirim, **American Journal of Physiology-Lung Cellular and Molecular Physiology**, 307 L692-L706, 2014.
* Authors contributed equally to this work

- *"The composition of cigarette smoke determines inflammatory cell recruitment to the lung in COPD mouse models"*, Gerrit John, Katrin Kohse, Jurgen Orasche, Ahmed Reda, Jurgen Schnelle-Kreis, Ralf Zimmermann, Otmar Schmid, Oliver Eickelberg, Ali Önder Yildirim, **Clinical Science,** 126 (3), 207-221, 2013.

- *"Acute cigarette smoke exposure impairs proteasome function in the lung",* Sabine H van Rijt, Ilona E Keller, Gerrit John, Katrin Kohse, Ali Önder Yildirim, Oliver Eickelberg, Silke Meiners, **American Journal of Physiology-Lung Cellular and Molecular Physiology,** 303 (9), L814-L823, 2012.

- *"All-trans retinoic acid results in irregular repair of septa and fails to inhibit proinflammatory macrophages",* Carola Seifart, Jai Prakash Muyal, Alexandra Plagens, Ali Önder Yildirim, Katrin Kohse, Veronika Grau, Sabine Sandu, Christian Reinke, Thomas Tschernig, Claus Vogelmeier, Heinz Fehrenbach, **European Respiratory Journal**, 38 (2), 425-439, 2011.

1 Introduction

1.1 Definition of COPD

Chronic obstructive pulmonary disease (COPD) is a major global health problem, since an estimated 64 million people suffered from COPD in 2004 (Mathers et al., 2008). In 2005 more than 3 million people died of COPD, which is equal to 5% of all global deaths this year. The World Health Organization (WHO) ranked COPD as the third common cause of death worldwide and estimates that it will be the third by 2020 (WHO, 2008). Furthermore, COPD is one of the leading causes for hospitalization and health care incurrence (Buist et al., 2007; Gershon et al., 2010; Hall et al., 2010). COPD is a highly under-diagnosed disease and often diagnosed in a late stage. Cigarette smoking is the major cause for COPD in the industrialized countries where it accounts for 80 – 90 % of the cases (Barnes et al., 2003) . Earlier diagnosis would be important for aggressive smoking cessation efforts and by this may lead to a reduction in the burden of COPD symptoms (Tinkelman et al., 2007). In developing countries other environmental pollutants such as indoor air pollution from combustion of biomass/traditional fuels and coal are important causes of COPD (Dennis et al., 1996). Next to CS and air pollution, genetic predispositions are risk factors for developing COPD. The lack of proteinase inhibitor α-1-antitrypsin in the lung and a polymorphism of the promoter region of the pro-inflammatory cytokine tumor necrosis factor-α (TNF-α) have been associated with COPD development (WHO, 1997). Inflammatory changes are detectable in lungs of all smokers, independently of disease development, but in COPD inflammatory processes seem to be abnormal (Chung and Adcock, 2008). Deregulated inflammatory responses can subsequently cause mucus hypersecretion (chronic bronchitis) (Sommerhoff et al., 1990)), tissue destruction (emphysema) (Lee et al., 2007; Sullivan et al., 2005; Turato et al., 2002) as well as disruption of repair- and defense mechanisms (Rennard, 2007). Together these pathological changes lead to increased resistance to airflow in the small conducting airways, and increased compliance and reduced elastic recoil in the lungs. Consequences are progressive airflow limitations and air trapping, which are the hallmarks of COPD. In general, inflammatory and structural changes persist even after smoking cessation and increase with disease severity.

1.2 COPD classification

Since all COPD patients exhibit airflow limitation with reduced expiratory flow rates, the GOLD committee defines COPD on the basis of spirometric criteria. The severity of air flow limitation is determined by measuring the forced expiratory volume in one second (FEV1) and its ratio to the forced vital capacity (FVC) that can be expired without time limit. Both parameters are reliable screening tools because both are affected by airway obstruction and by emphysema. The GOLD committee designates that an FEV1/FVC ratio of less than 70% indicates COPD. Depending on FEV1/FVC ratios in combination with FEV1 alone the GOLD committee defines 4 severity stages of COPD (Table 1). Cessation of cigarette smoking has a beneficial effect at any age, but can only delay and not stop COPD progression (Hogg, 2008; Pauwels et al., 2001; Rabe et al., 2007) .

Table 1: Spirometric classification of COPD severity based on post-bronchodilator FEV_1

COPD GOLD stage	Spirometric data
Stage I: Mild	FEV1/FVC < 0.70 FEV1 ≥ 80% predicted
Stage II: Moderate	FEV1/FVC < 0.70 50% ≤ FEV1 < 80% predicted
Stage III: Severe	FEV1/FVC < 0.70 30% ≤ FEV1 < 50% predicted
Stage IV: Very Severe	FEV1/FVC < 0.70 FEV1 < 30% predicted or FEV1 < 50% predicted plus chronic respiratory failure*

*respiratory failure: arterial partial pressure of oxygen (PaO_2) less than 8.0 kPa (60 mm Hg) with or without arterial partial pressure of CO_2 ($PaCO_2$) greater than 6.7 kPa(50 mm Hg) while breathing air at sea level.
(adapted from: The Global Strategy for the Diagnosis, Management, and Prevention of Chronic Obstructive Pulmonary Disease, Global Initiative for Chronic Obstructive Lung Disease (GOLD) (2006))

In 2011 the GOLD committee approved that the extent of symptoms, health status impairment and risk of exacerbations can poorly be predicted by the FEV1 alone. As a first step towards personalized therapy a reorganization of treatment objectives into two categories (relief of present symptoms and reduction in the risk of future adverse health effects) was conducted. The new system (Table 2) aimed at increasing the match between clinical assessment and specific treatment options. Therefore, amongst others the COPD assessment test (CAT), which is a questionnaire assessing the impact of COPD (cough, sputum, chest tightness, dyspnea) on health status and the modified Medical Research Council (mMRC) dyspnoea scale were implemented.

Table 2: New GOLD classification and therapy

<table>
<tr><td>Patient Group</td><td>A
(low risk, less symptoms)</td><td>B
(low risk, more symptoms)</td><td>C
(high risk, less symptoms)</td><td>D
(high risk, more symptoms)</td></tr>
<tr><td rowspan="2">Burden of Symptoms</td><td colspan="2">GOLD I - GOLD II (FEV>50% predicted) and/or 0-1 exacerbation p.a. and no hospitalization for exacerbation; and</td><td colspan="2">GOLD III - GOLD IV (FEV<50% predicted) and/or ≥ 2 exacerbations p.a. or ≥ 1 with hospitalization for exacerbation; and</td></tr>
<tr><td>CAT score < 10 or mMRC grade 0-1</td><td>CAT score ≥ 10 or mMRC grade ≥ 2</td><td>CAT score 10 or mMRC grade 0-1</td><td>CAT score ≥ 10 or mMRC grade ≥ 2</td></tr>
<tr><td rowspan="4">Treatment</td><td colspan="4">active reduction of risk factor(s) e.g. influenza vaccination; short-acting bronchodilator (when needed) →</td></tr>
<tr><td></td><td colspan="3">regular treatment with one or more long-acting bronchodilators (when needed); rehabilitation →</td></tr>
<tr><td></td><td></td><td colspan="2">inhaled glucocorticosteroids if repeated exacerbations →</td></tr>
<tr><td></td><td></td><td></td><td>long term oxygen if chronic respiratory failure; consideration of surgical treatments →</td></tr>
</table>

(Adapted from: The Global Strategy for the Diagnosis, Management, and Prevention of Chronic Obstructive Pulmonary Disease, Global Initiative for Chronic Obstructive Lung Disease (GOLD) 2009 & 2015)

1.3 Pathophysiology of COPD

The three main hallmarks of COPD pathophysiology are airway obstruction, chronic bronchitis and emphysema, as defined by the Global Initiative for Chronic Obstructive Lung Disease Guidelines (GOLD) (Pauwels et al., 2001). Airway obstruction, which in COPD is mainly irreversible, results from a combination of small airway narrowing (small airway obstruction), increased inflammation of the airways and mucus production (chronic bronchitis) (Cosio et al. 1978) and destruction of lung parenchyma (emphysema) accompanied by loss of lung elastic recoil (Colebatch et al., 1973; Penman et al., 1970). Chronic bronchitis is described as inflammation located in the epithelium of the central airways, which also affects mucus-producing glands (Mullen et al., 1985; Saetta et al., 1997). These inflammatory processes subsequently lead to mucus hypersecretion, defects in the mucociliary clearance, and disruption of the epithelial barrier. Cells of the innate and the adaptive immune system are involved in these processes (Lacoste et al., 1993; Saetta et al., 1993, 1997). The thickening of bronchial walls which is associated with chronic bronchitis is mainly due to increased connective tissue deposition and there is evidence that growth factors such as transforming growth factor-β (TGF-β) are responsible for this circumstance (Vignola et al. 1997; Hogg 2004). Although the terms chronic bronchitis and airway obstruction are often used in the same context, obstruction is preferentially found in the smaller conducting airways (Hogg et al. 1968; Van Brabandt et al. 1983; Yanai et al. 1992). Although the accumulation of inflammatory exudates in the small-airway lumen might be related to an extension of chronic bronchitis into the small airways, results of several studies give evidence that this is not the case. It was shown by two clinical trials that the development of airflow limitation is not predicted by the presence of chronic bronchitis (Fletcher et al., 1976; Vestbo and Lange, 2002). In addition, pathological studies indicate that inflammation of central and peripheral airways can occur independently of each other (Mullen et al., 1985). These data lead to the conclusion that chronic bronchitis is independent of disease processes occurring in the small airways, which are responsible for airway obstruction in COPD patients (Hogg et al., 2004). Beside small airway disease and chronic bronchitis, COPD is characterized by emphysema. Emphysema is defined as “abnormal permanent enlargement of air spaces distal to terminal bronchioles, accompanied by destruction of their walls without obvious fibrosis.” (ATS, 1962; Snider et al., 1985). Emphysematous changes lead to reduction of elastic recoil, which is the force responsible for driving expiratory flow (Mead et al., 1967). Furthermore, emphysema worsens diffusion capacity by reducing gas exchange area (Pauwels et al., 2001; Rodriguez-Roisin et al., 2009).

COPD symptoms include: shortness of breath (dyspnea), wheezing, chest tightness, chronic cough that induces sputum, blueness of the lips or fingernail beds (cyanosis), frequent respiratory infections, lack of energy and, at later stages, loss of weight.

1.4 Immunopathogenesis of COPD

Inhalation of toxic particles firstly leads to activation of the innate immune system, which provides the first line of defense and is important to maintain sterility in the lower respiratory tract (Hogg, 2008). Components of the innate immune system of the lung include the mucuciliary clearance apparatus, the epithelial barrier and the innate immune cells (Green et al., 1977; Knowles and Boucher, 2002). Chronic CS exposure leads to reduced mucociliary clearance, increased mucus production (Cohen et al., 1979; Vastag et al., 1984) and disruption of the tight junctions (Hulbert et al., 1981; Jones et al., 1980; Simani et al., 1974) that form the epithelial cell barrier. Consequently, this results in an invasion of polymorphonuclear cells, mononuclear phagocytes, and natural killer cells into the damaged tissue (Kumar et al., 2005). Dendritic cells bridge innate and adaptive immune response by

presenting antigen to lymphocytes located in T and B cell zones within lymphoid follicles (Hogg, 2008; Hogg et al., 2004).

CS and other air pollutants lead to an activation of neutrophils and epithelial cells in the respiratory tract via the activation of toll like receptors (TLRs) and the induction of oxidative stress (Brusselle et al., 2011). Subsequently, neutrophils and epithelial cells release multiple chemoattractants, mainly chemokines to attract more neutrophils and monocytes as well as T lymphocytes (Becker et al., 2002; Fujii et al., 2001, 2002; Gilmour et al., 2001). All types of activated cells secrete inflammatory mediators and additionally, several cell types, including neutrophils and epithelial cells release proteases such as neutrophil elastase (NE) and matrix metalloproteinases (MMPs) (Caughey, 1994; Lieberman, 2003; Shapiro, 2012; Taggart et al., 2005). An increase of proteases leads to a protease-antiprotease imbalance and hence, on the one hand to destruction of connective tissue in the lung parenchyma, resulting in emphysema (Churg and Wright, 2005; MacNee, 2005) and on the other hand to stimulation of mucus hypersecretion (chronic bronchitis) (Nadel, 2000; Sommerhoff et al., 1990; Takeyama et al., 1998). TGF-β release by macrophages and epithelial cells stimulates fibroblast proliferation, leading to fibrosis in the small airways (Epstein et al., 1994; Wynn, 2011).

Moreover, the adaptive part of the immune system has been shown to be involved in COPD pathogenesis. For instance, an association between increased numbers of CD8+ T cells and the severity stage of COPD has been observed (O'Shaughnessy and Ansari, 1997; Saetta et al., 1999). Usually, activated CD8+ T cells have a protective function by releasing proteolytic enzymes which induce cell death of virus-infected cells, but in the case of COPD they are described to be involved in the destruction of lung parenchyma (Cosio et al., 2002; Majo et al., 2001). Furthermore, CD4+ T cells show increased numbers in the airways and lungs of smokers with COPD (Finkelstein et al., 1995). At least two types of effector CD4 T helper (Th) cell subsets accumulate in the lungs of patients with stable COPD: Th1 and Th17 cells (Grumelli et al., 2004; Di Stefano et al., 2009). Th1 cells release interferon-γ (IFN-γ) and promote the recruitment of inflammatory cells into the lung (Grumelli et al., 2004). IL-18, which promotes Th1 cell development, is highly expressed in alveolar macrophages, CD8+ T cells, and alveolar and bronchiolar epithelial cells in the lungs of patients that suffer from severe COPD (Imaoka et al., 2008). Th17 cells, which are characterized by the secretion of IL-17A, IL-17F, IL-22 and IL-23, play a central role in the defense against extracellular pathogens but are also involved in autoimmunity (Miossec et al., 2009). Th17 cells promote the accumulation of neutrophils at the site of tissue injury by inducing epithelial cells to produce antimicrobial peptides (such as β-defensins) (Kao et al., 2004), chemokines and the granulocyte growth factors GM-CSF and G-CSF (Traves and Donnelly, 2008). Di Stefano et al. demonstrated that COPD patients have increased numbers of IL-23+ cells in bronchial epithelium and IL-17+ cells in bronchial submucosa (Di Stefano et al., 2009). A distinct T helper effector cell lineage are regulatory T cells (Treg), which regulate inflammatory processes and inhibit autoimmunity. Tregs exert their suppressive functions on other T cells or antigen presenting dendritic cells via cell-cell contacts or the secrection of anti-inflammatory cytokines such as IL-10 and TGF-β (Tang and Bluestone, 2008). Tregs are characterized by the expression of the surface marker CD25 and the transcription factor Foxp3. Decreased numbers of regulatory T cells, lower Foxp3 mRNA expression levels and less secretion of IL-10 have been shown in the whole lung of COPD specimens compared to controls (Brusselle et al., 2011; Lee et al., 2007). In summary, COPD appears to represent an amplification of the normal response of the respiratory mucosa to inhaled irritants associated with limited regulatory control.

1.5 The key immune cells involved in COPD

1.5.1 B cells and inducible bronchus-associated lymphoid tissue in COPD

Aside from T cells also B cell numbers have been shown to be increased in the large airways of COPD patients (Gosman et al., 2006). The presence of B cells points to an antigen-driven specific immune response that contributes to the inflammatory process and the development and perpetuation of COPD (Brandsma et al., 2009; Lee et al., 2007). Increasing evidence suggests that antigens triggering this specific immune response in COPD patients might not only include tobacco smoke residues but also extracellular matrix components resulting from smoke-induced lung tissue destruction (Brandsma et al., 2009; Feghali-Bostwick and Gadgil, 2008). Lee et al. provided the most conclusive results supporting a role of autoimmune components in COPD and described immune responses against lung elastin as shown by the presence of anti-elastin antibodies and specific Th1 responses in patients with emphysema (Lee et al., 2007). However, these results could not be confirmed by more recent studies performed by Cottin et al. and Greene et al. (Brandsma et al., 2011; Cottin et al., 2009; Greene et al., 2010). Furthermore, autoimmune responses against airway epithelial cells, endothelial cells, several immunogenic peptides, and cytokeratin have also been described for COPD (Brandsma et al., 2011). These findings and the fact that immune cells persist even after smoking cessation (Hogg et al., 2004; Rutgers et al., 2000; Wright et al., 1983) nevertheless support the hypothesis that COPD might have an autoimmune component characterized by inflammatory responses against auto- and neo-antigens. Moreover, especially in patients with severe and very severe COPD, B cells are found in organized structures called tertiary lymphoid follicles organs (TLO) (Hogg et al., 2004). Lymphoid follicles are special anatomical structures which are well organized and consist of memory and naïve B cells, T lymphocytes, dendritic cells and follicular dendritic cells (FDCs) which allow priming, clonal expansion of B cells and T cells, antigen retention, somatic hypermutation, affinity maturation and immunoglobulin (Ig) class switching (Aloisi and Pujol-Borrell, 2006; Kroese et al., 1990; MacLennan, 1994). Lymphoid neogenesis is a dynamic process starting with slight lymphocyte infiltrates which result in aggregates or even organized B cell follicles with germinal centers and distinct T cell areas containing DCs and high endothelial venules (HEVs) (Aloisi and Pujol-Borrell, 2006; Armengol et al., 2001; Hjelmström, 2001; et al., 2005; Salomonsson et al., 2003). Via HEVs extravasation of B and T cells is regulated. In COPD, TLOs in the lung contain aggregates of B cells surrounded by T cells. The T cells are mainly CD4+ (80-90%) and only 10-20% CD8+ (Hogg, 2004; Hogg et al., 2004; van der Strate et al., 2006). B cells found in these follicles are mainly IgM positive and IgD negative, a fact leading to the assumption that these B cells are activated to some extent. Furthermore, many cells in these infiltrates express the surface marker CD27, a marker for memory B cells (Zubler, 2001). As already found in other tissues affected by chronic inflammation, TLOs in COPD arise from lymphoid neogenesis and therefore belong to the inducible bronchus-associated lymphoid tissue (iBALT). iBALT is defined as ectopic lymphoid tissue, which is formed in response to chronic infection or inflammation and collects antigens from the airways. It induces local inflammatory responses and is responsible for the maintenance of memory cells in the lungs (Brusselle et al., 2009; Randall, 2010). In COPD patients the presence and size of iBALT structures in the lung correlate with disease severity (Hogg et al., 2004). Similar observations were made for mice exposed to tobacco smoke (van der Strate et al., 2006). Thus, iBALT is likely to be involved in COPD pathogenesis, however its definite role is still unknown. In general, iBALT might protect from microbial colonization and infection of the lower respiratory tract. Two recent studies addressed the question of lymphoid neogenesis in the COPD lung and emphasized an important role for CXCL13. Litsiou et al. discovered an involvement of CXCL13 in lymphoid neogenesis in COPD

patients by promoting B cell migration to ectopic sites of lymphoid tissue formation. Additionally, upregulation of lymphotoxin on B cells, which in turn further induces CXCL13 in a positive feedback loop, was reported (Litsiou et al., 2013). Chronic CS exposure of mice leads to increased CXCL13 levels in BAL and lung tissue and subsequently to B cell chemotaxis as well (Bracke et al., 2013). Furthermore, Bracke et al. observed increased CXCL13 levels in lung tissue and induced sputum of COPD patients. By prophylactic and therapeutic administration of a CXCL13 neutralizing antibody in a COPD mouse model they could inhibit iBALT formation. In the absence of iBALT these mice showed less BAL inflammation and were partially protected against destruction of alveolar walls (Bracke et al., 2013). In line with these findings, recently published results by Morisette et al. showed the persistence of iBALT even after smoking cessation. The authors observed a strong association of iBALT structures with antinuclear antibodies (ANAs) (Morissette et al., 2014). Interestingly, CCR7 deficient mice spontaneously develop iBALT. The authors reason that this phenomenon is caused by absent homing of Tregs via the homing receptor CCR7 to the lung-draining bronchial lymph nodes. Adoptive transfer of Wt Treg cells to $CCR7^{-/-}$ recipients attenuated iBALT (Kocks et al., 2007). Thus, Treg cells seem to be involved in controlling iBALT formation. Demoor et al. conducted a study exposing $CCR7^{-/-}$ mice chronically to CS, and emphysematous changes in $CCR7^{-/-}$ mice caused by CS-exposure were not significant compared to $CCR7^{-/-}$ mice under filter air conditions. However, compared to Wt mice, $CCR7^{-/-}$ mice showed a significant airspace enlargement on baseline level (Demoor et al., 2009). Altogether, these findings strongly point to an important role of iBALT structures in COPD pathogenesis.

Aside from their involvement in lymphoid neogenesis and their antibody-producing capacity, B cells can also function as antigen-presenting cells and provide costimulatory signals to T cells (DiLillo et al., 2011). Furthermore, the secretion of a variety of cytokines enables B cells to influence the differentiation and polarization of T cells, macrophages and dendritic cells during immune reactions. For instance IL-10 producing B cells with an immune modulatory role are described for EAE (experimental autoimmune encephalomyelitis), the murine model for multiple sclerosis (MS) (Fillatreau et al., 2002). B cells directly stimulate IFN-γ secretion and proliferation of Th1 cells (Harris et al., 2005). Since B cells secrete TGF-β as well as IL-6 (Pistoia, 1997), which are described to be critical for Th17 differentiation, they might also be involved in bolstering Th17 responses. Depletion of B cells in RA (rheumatoid arthritis) patients decreases Th17 responses, as measured by the number of Th17 cells in synovial tissue as well as expression of Rorγt and IL-22 (van de Veerdonk et al., 2011). B cells are also capable of modulating macrophage effector functions via cytokine secretion, which has been described to be important for the outcome of various models of infection, inflammation and cancer (Biswas and Mantovani, 2010; Moseman et al., 2012; Wong et al., 2010). B cell derived IL-10 negatively regulates the expression of pro-inflammatory genes such as TNF-α, CCL3 and IL-1-β, and up-regulates IL-10 expression in LPS stimulated macrophages (Wong et al., 2010). Furthermore, Popi et al. observed that innate-like B1 B cells down-regulate macrophage activities, including phagocytic capacity and the release of nitric oxide as well as hydrogen peroxide. Using transwell experiments with macrophages and B1 cells from either IL-10 knockout mice or Wt mice Popi et al. demonstrated that only Wt B1 cells were able to influence the phagocytic potential of Wt macrophages (Popi et al., 2004). These observations indicate that B1 cells via IL-10 have the ability to influence macrophages via the secretion of soluble mediators. In a transgenic mouse model of multistage epithelial carcinogenesis using K14-HPV16 mice, B cells were shown to foster pro-tumoral properties of macrophages via activation of Fcγ receptors on macrophage surfaces. IgGs secreted by B cells interact with Fcγ receptors on resident and recruited macrophages and promote M2 polarization since macrophages isolated from HPV16/$FcR\gamma^{+/-}$ versus HPV16/$FcR\gamma^{-/-}$ skin revealed a significant upregulation of M2 characterizing genes (IL-13, CD163, CCL17, IL-4, and Ym1) (Andreu

et al., 2010). Results from Wong et al. support the hypothesis of B cell mediated M2 polarization via IL-10 secretion. Wong and colleagues have shown that B1-induced M2 polarization was prevented by inhibition of IL-10 (Wong et al., 2010) .

1.5.2 **Macrophages in COPD**

Macrophages play a central role in the inflammatory processes in COPD and account for most of the features of the disease pathogenesis. Former studies involving the depletion of either neutrophils or macrophages have shown that only mice deprived of macrophages are protected against emphysema development. Similarly, the absence of MMP12, mainly produced by macrophages, protects mice against loss of alveolar structures even though they still can produce neutrophil elastase (Brusselle, 2009; Hautamaki et al., 1997). The role of different macrophage phenotypes in COPD is the topic of several recently conducted studies.
M1 or classically activated macrophages are activated when exposed to IFN-γ or TNF-α and are under the influence of the transcription factor IRF5. They are characterized by generating reactive oxygen species (ROS) and nitric oxide (NO) and by amplifying Th1 responses by secreting pro-inflammatory cytokines such as IL-12, IL-1β and TNFα thereby contributing to host defense against intracellular pathogens (Biswas and Mantovani, 2010; Krausgruber et al., 2011). In contrast, M2 macrophages are induced by IL-4 and IL-13 (Gordon, 2003; Stein et al., 1992) under the influence of the transcription factor IRF4 (Satoh et al., 2010). They are associated with protection against helminthes and with physiological and pathological tissue remodeling (Boorsma et al., 2013; Martinez et al., 2009; Mosser and Edwards, 2008). Thus, M2 macrophages are also considered as wound-healing macrophages.

Relating to an involvement of different macrophage phenotypes in COPD pathogenesis, conflicting data exist. Several studies point to a role for M1 macrophages or dysregulated M1 macrophages in the development of COPD. CS, the most important risk factor for COPD, contains lipopolysaccharide (LPS) which activates macrophages in the lung resulting in increased iNOS espression (Stedman, 1968). Upregulated iNOS expression in turn is an indicator for M1 activation. iNOS subsequently leads to increases in ROS and NO causing further oxidative stress adding to the oxidative stress originating from CS per se and contributing to COPD (Ito, 2009; Montuschi et al., 2000; Paredi et al.; Rahman et al., 2002). Additionally smoking induces pro-inflammatory M1 derived cytokines such as TNF-α, IL-6, IL-8 and IL-1β (Demirjian et al., 2006; Doz et al., 2008; Facchinetti et al., 2007; Karimi et al., 2006; Walters et al., 2005; Yang et al., 2006), which were also found to be up-regulated in COPD (Bucchioni et al., 2003; Sapey et al., 2009; Yamamoto and Yoneda, 1997). In experimental settings over-expression of TNF-α in mouse lung tissue was shown to induce development of chronic inflammation and emphysema (Fujita et al., 2001; Thomson et al., 2012; Vuillemenot et al., 2004). However, therapeutic application of anti-TNF-α antibodies in humans seems to be ineffective in COPD treatment (Matera et al., 2010). Another M1 cytokine, IL-1-β, was found to cause lung inflammation, emphysema, mucus metaplasia, and airway fibrosis when over-expressed in mouse lungs (Lappalainen et al., 2005). Furthermore, over-expressing IFN-γ, a M1 related cytokine produced by CD8+ cells infiltrating lungs in COPD and inducing the M1 phenotype, led to an imbalance of MMPs and antiproteases in mice (Wang et al., 2012). On the other hand, IFNγR and IFN-γ signaling were found to be down-regulated in COPD patients. Another important property of M1 macrophages is phagocytosis, which has been shown to be impaired in COPD and thus contributes to persistence of microorganisms in the exacerbated lung of COPD patients (Berenson et al., 2006; PRIETO et al., 2001; Taylor et al., 2010). In their review article, Boorsma et al. reason that rather a dysregulated M1 macrophage phenotype than an increased or decreased number of M1 macrophages plays a role in

COPD. The authors justify their conclusion with dissonant results for M1 marker molecules or functions, with some being up-regulated under COPD conditions (ROS generation, pro-inflammatory cytokines) and some down-regulated (phagocytosis, IFN-γ responsiveness) (Boorsma et al., 2013). Over-expression of IFN-γ, which induces the M1 phenotype, results in emphysema development just as well as over-expression of the M2 inducer IL-13 (Boorsma et al., 2013). IL-13 producing M2 macrophages were observed in lung tissue of COPD patients, giving a hint that also M2 macrophages are involved in COPD pathogenesis (Kim et al., 2008). Shaykhiev et al. analyzed and compared the transcriptome of alveolar macrophages from healthy smokers, nonsmokers and COPD smokers and demonstrated a smoking-induced reprogramming of alveolar macrophages toward an M1-deactivated, partially M2 polarized phenotype. In mice M2 macrophages characteristically express large amounts of the chitinase-like proteins Ym1 and Ym2 (Chi3l3/4) (Shaykhiev et al., 2009). Using mouse models of chronic obstructive lung diseases, Agapov et al. observed an up-regulation of Ym1 and Ym2 correlating with disease progression. Since Ym1 and Ym2 have no human homologs, Agapov and colleagues also assessed expression levels for each of the potential chitinase and chitinase-like family members that may be found in human lung. In lung tissue obtained from COPD subjects, the authors could detect significantly increased levels of Chit1 compared to control subjects. In immunohistochemically stained lung sections, Chit1+ cells were found to be adjacent to IL-13+ cells. Interestingly, plasma chitinase 1 levels correlated strongly with decline in lung function (Agapov et al., 2009). Woodruff et al. observed an increased frequency of M2 alveolar macrophages in smokers, using MMP12 as a marker for alternative macrophage activation (Woodruff et al., 2005). In summary there is evidence for a role of M2 rather than for M1 macrophages in COPD pathogenesis.

1.6 The role of soluble inflammatory mediators in COPD

Cytokines and chemokines that recruit, activate and promote survival of inflammatory cells in the respiratory tract are the main actors in causing chronic inflammation in COPD. More than 50 cytokines are known to be involved in COPD (Barnes, 2008), but their role remains often unclear.

1.6.1 Proinflammatory cytokines

In the sputum and BAL fluid of COPD patients elevated levels of TNF-α, IL-1β and IL-6 are found. These proinflammatory cytokines amplify inflammatory processes, partly through the activation of NFκB which in turn causes the increased expression of a multitude of inflammatory genes (Barnes, 2009). Many cells, such as macrophages, mast cells, T cells, epithelial cells, and airway smooth muscle cells, are capable to secrete TNF-α (Keatings et al., 1996). Since TNF-α is increased in COPD patients, particularly during exacerbations (Aaron et al., 2001), and is strongly involved in CS-induced emphysema in mice (Churg et al., 2004) it seems obvious that anti-TNF-α strategies may provide therapeutic options. However, infliximab (a chimeric antibody specific for human TNF-α) does not have any positive effects on symptoms, lung function, and exercise performance in patients with COPD in doses that are effective in individuals with rheumatoid arthritis (RA) (Rennard et al. 2007). IL-1β levels are markedly increased in the sputum of COPD patients and correlate with disease severity (Sapey et al., 2009). IL-1β in COPD patients stimulates macrophages to produce cytokines and chemokines as well as MMP9 (Culpitt et al., 2003). Clinical studies of a fully humanized IL-1β antibody (canakinumab) with more than 2000 COPD patients and healthy volunteers did not result in evidence-based findings that might support the use of IL-1β antibody therapy in the treatment of COPD(Rogliani et al., 2015). Furthermore, COPD patients show increased IL-6 concentrations in sputum, exhaled breath and plasma, particularly during exacerbations (Bhomik et al. 2000; Bucchioni

et al., 2003). Tocilizumab, an antibody that blocks IL-6 receptors and which has been successfully applied to treat RA and inflammatory bowel disease (IBD), has yet to be tested in COPD (Barnes, 2009) .

1.6.2 Growth factors

Certain cytokines contributing to pathological changes in COPD by either promoting inflammatory cell survival or differentiation or fostering the proliferation and/or activation of structural cells (Barnes, 2009). One of the COPD-relevant growth factors is GM-CSF which is secreted mainly by macrophages, epithelial cells, and T cells in response to inflammatory stimuli. In COPD, GM-CSF is primarily secreted by alveolar macrophages and might contribute to increased survival of neutrophils and macrophages in the airways (Culpitt et al. 2003). There is a correlation between elevated GM-CSF levels in BAL fluid of COPD patients and increased numbers of neutrophils, particularly during exacerbations (Balbi et al. 1997). Vlahos et al. demonstrated that neutralizing GM-CSF inhibited CS-induced lung inflammation by reducing BAL neutrophils and macrophages as well as TNF-α, MIP-2 and MMP12 mRNA expression (Vlahos et al., 2010). A further study blocking GM-CSF receptor also described attenuated neutrophil influx in CS-exposed mice (Botelho et al., 2011).

1.6.3 Chemokines

In COPD chemokines induce chemotaxis of inflammatory cells from the circulation to the airways (Donnelly and Barnes 2006). CCL2 (Chemokine (C-C Motif) Ligand 2, also known as MCP-1) levels are increased in the sputum, BAL fluid, and lungs of patients with COPD. CCL2 is released by alveolar macrophages, T cells, and epithelial cells (de Boer et al. 2000; Traves et al. 2002). CCL2 activates CCR2 on monocytes and T cells (Deshmane et al., 2009) and might be involved in the accumulation of macrophages in the lungs of COPD patients since it is an effective chemoattractant of monocytes. The chemokine receptor CCR5 binds CCL3 (also known as MIP-1α), CCL4 (also known as MIP-1β), and CCL5, all of them are upregulated in the lungs of individuals with COPD (Curtis et al., 2007; Fuke et al., 2004). The airways of patients with mild to moderate COPD (Stefano et al., 2001) and the sputum of patients with COPD show elevated numbers of CCR5 expressing T cells (Costa et al. 2008). CXCL8 (also known as IL-8 with the murine homologue KC) interacts with CXCR1 and CXCR2, which also binds related CXC chemokines, such as CXCL1 (also known as GRO-α) (Baggiolini et al., 1997). Increased CXCL1 and CXCL8 levels correlate with an increased proportion of neutrophils in induced sputum of patients with COPD (Keatings et al. 1996; Traves et al. 2002). Another CXC chemokine, CXCL13, mentioned above, is produced within lymphoid follicles of patients with COPD and is crucial for the formation of TLOs (Litsiou et al., 2013). Neutralization of CXCL13 partially protects mice against CS-induced inflammation in bronchoalveolar lavage and alveolar wall destruction (Bracke et al., 2013).

1.6.4 Anti-inflammatory cytokines

As described above, most cytokines foster the inflammatory processes in COPD, though some cytokines have inhibitory or anti-inflammatory properties. IL-10, as an efficient anti-inflammatory cytokine, blocks the synthesis of certain cytokines, such as TNF-α and IL-1 (Cassatella et al., 1993; Moore et al., 1993) as well as several chemokines which are increased in COPD. Furthermore, IL-10 inhibits antigen presentation (Ozawa et al. 1996). IL-10 might also have beneficial effects in COPD in

such a way that it impedes MMP-9 production. COPD patients exhibit reduced IL-10 levels in induced sputum samples (Takanashi et al.1999).

1.6.5 Matrix Metalloproteinases (MMP)

MMPs are a large family of zinc-dependent proteinases which are important regulators of the extracellular matrix degradation (Stamenkovic 2003). There is rising evidence for an involvement of MMPs in the COPD pathogenesis (Shapiro 1999). Various polymorphisms of MMP-1, MMP-9, and MMP-12 have been linked to emphysema (Minematsu et al., 2001; Joos et al., 2002; Wallace and Sandford, 2002). The basic principle of the protease–antiprotease hypothesis is that alveolar wall matrix gets attacked by proteases secreted from CS-induced inflammatory cells, thus leading to emphysema (Shapiro, 2003). There is an increased interest in MMPs since it has been demonstrated that MMP-12$^{-/-}$ mice are protected against emphysema induction by chronic CS exposure (Hautamaki et al. 1997). Using a selective inhibitor to block the catalytic activity of MMP-12 in a 4-day acute model resulted in reduced lavage neutrophil numbers by about 50% and lavage macrophages by about 40%. This was accompanied by a reduction of soluble TNF receptors, MIP-1γ, IL-6, KC, CXCL1, CXCL11, tissue inhibitor of metalloproteinase (TIMP)-1 and pro-MMP-9 (Quement et al., 2008). Interestingly, CS-induced emphysema development is not prevented in MMP-9$^{-/-}$ mice, but they are protected against small airway fibrosis (Lanone et al. 2002).

1.7 Cigarette smoke induced experimental models

1.7.1 In vitro models of cigarette smoke exposure

There are two currently used COPD-relevant models to study CS effects in vitro: the cigarette smoke extract (CSE) model and the whole cigarette smoke exposure model, or rather the smoking chamber model.

Cigarette smoke extract model

In this model, CS is generated by means of a smoking machine and the particulate matter is collected. Depending on the method there are different types of extracts that can be collected from CS. The most commonly used CS extracts are total particulate matter (TPM) and cigarette smoke condensate (CSC):

- CSC is usually collected by condensing smoke components using impingers connected to the smoking machine. CS is passed into phosphate-buffered saline or culture medium as the aqueous solvent. The end-product of this method contains water-soluble components from both the particulate and gas/vapor phases of whole smoke.
- CSC may also be collected using electrostatic precipitation
- TPM is collected by transmitting CS through a Cambridge filter pad. The TPM gets trapped on the filter pad and is eluted using a solvent such as dimethyl sulfoxide (DMSO).

Subsequently, CSC or TPM is diluted in a suitable diluent (e.g. culture medium) and cells are directly submerged in medium containing the CSE.

Whole Smoke exposure

In this model, cells are grown at the air-liquid interface and exposed to smoke directly, using a gas exposure chamber (Johnson et al., 2009).

1.7.2 CS-induced COPD mouse models

Human COPD consists of at least three anatomical lesions: emphysema (Colebatch et al., 1973; Penman et al., 1970), small airway remodeling (including goblet cell hyperplasia) (Hogg et al., 2004) and chronic bronchitis (Cosio et al., 1978). In COPD patients any of these features or all of them might be present. Furthermore, some COPD patients develop acute exacerbations (Burge and Wedzicha, 2003; Celli and Barnes, 2007) and to make it even more complicated, COPD is slowly progressive over many years (Pauwels and Rabe, 2004). Animals used to model COPD should have a pulmonary anatomy similar to that of humans. In the best case the model should allow the investigator to mimic all the different lesions of COPD, listed above, during a short period of time. Unfortunately none of the so far described COPD animal models can meet all the listed criteria, but due to human to human variation a human patient would also not meet all of them (Wright et al., 2008). To date, many species have been used including rodents, dogs, guinea-pigs, monkeys, and sheep. Mice are the most suitable species to investigate pathogenic pathways of COPD, given the advances in genetic engineering, the abundance of information about the mouse genome and the variety of antibody probes (Mahadeva and Shapiro, 2002). Also advanced devices for pulmonary function tests enable measuring pressure-volume curves and compliance changes fairly easily in mice. With increasing length of CS exposure abnormalities in lung function progress, such as: increased residual volume, functional residual capacity, total lung capacity, compliance and decreased ratios of FEV/FVC (Wright and Churg, 1990). However, the lesions caused by CS in small laboratory animals can be only slight, even on a microscopic level; thus morphometric analysis is required to assess the degree of damage. For this purpose measurements of air space size (Lm) or surface-to-volume ratio (Sv) are used (Thurlbeck 1994).

In mice characteristic features of human COPD can also be induced by exogenous administration of proteases, chemicals and particulates (Mahadeva and Shapiro, 2002). Given its role as the predominant cause of COPD, animal models using CS exposure appear to be the method of choice. Human features of COPD such as emphysema and small airway remodeling are covered by this model. Other characteristics such as mucus hypersecretion are more problematic. Another important disadvantage of these models is that the induction of either emphysema or small airway disease is an expensive and time-consuming process that takes up to 6 months (Tab.3). Next to the exposure duration, existing CS exposure models vary in the use of either mainstream smoke only or a mixture of side- and main-stream smoke (usually consisting of about 90% sidestream smoke and 10% mainstream smoke). However, the most important limitation of CS models, independent of the used species, the duration of smoke exposure and the composition of CS, is that only mild forms of COPD, probably equivalent to GOLD stage 1 or 2 can be induced (Wright et al., 2008).

Table 3: Pros and cons of cigarette smoke-induced models of COPD

Pros	Cons
Induced by the same insult as in humans	Does not produces the severe disabling disease seen in humans
Induces emphysema, airway remodeling, and vascular remodeling/pulmonary hypertension in selected species	Requires several months of exposure
Induces physiological alterations similar to humans	Lesions do not appear to progress after cessation of cigarette smoke exposure

(Adapted from Wright et al. 2008)

1.8 Aim of the study

It is well accepted that inflammatory processes play an important role in the pathogenesis of COPD. But until now precise mechanisms are not uncovered and anti-inflammatory agents such as corticosteroids, which are thought to improve obstructed airflow by decreasing the chronic inflammation, do not modify the long-term decline in lung function nor mortality. Thus, further studies are needed to identify the main contributing immune cells in order to develop more target-oriented, therapeutic approaches.
This study aimed at describing the kinetics of inflammatory cell recruitment in response to acute sidestream and mainstream as well as chronic CS and in detail to identify how B cells contribute to these kinetics and subsequently to emphysema development.
Therefore, we aimed at:

1) characterizing the time depended recruitment of inflammatory cells in acute sidestream vs. mainstream CS exposure models and under chronic mainstream CS conditions;
2) investigating whether B cells are required for the development of COPD pathogenesis;
3) analyzing the mechanism of B cell-mediated pathogenic effects

Due to its adverse health effects for non-smokers, not only mainstream smoke but also sidestream smoke, more precisely environmental tobacco smoke, mainly composed of exhaled mainstream cigarette smoke (CS) and sidestream CS, is under critical evaluation. Mainstream smoke, side stream smoke, and seconhand smoke (SHS), are nearly identical in their qualitive composition but the quantitative composition of each is different (Leberl et al., 2013). In the enclosed environment some compounds are emitted at up to tenfold increased levels in side stream smoke and SHS when compared with mainstream smoke (Moritsugu, 2007). Side stream smoke has therefore been classified as a Class A carcinogen by the US Environmental Protection Agency (U.S. Environmental Protection Agency 1992). We initially performed a comparison of the dynamics of acute lung inflammation between the acute main- and sidestream CS model. Acute CS exposure models are used to study more direct and early responses to CS. It is now generally accepted that inflammatory responses in CS exposure models proceed in two phases: an acute reaction during the first week of exposure accompanied by an influx of neutrophils and a progressive inflammation after one month of CS exposure consisting of neutrophils, macrophages and lymphocytes (D'hulst et al., 2005; Stevenson et al., 2007; Wan et al., 2010). Several studies have shown that innate immune cells of CS-exposed mice are sufficient for driving inflammatory processes in the lung subsequently initiating COPD like changes (D'hulst et al., 2005a; Stevenson et al., 2007; Wan et al., 2010). These studies suggest the importance of acute CS models to study prompt CS induced inflammatory mechanisms and immune cell activation that potentially contribute to COPD pathogenesis in an early stage of CS exposure. Interestingly, until now mainly mainstream smoke models were used to investigate acute CS induced responses. The only acute sidestream study analyzed oxidative DNA damage in mouse heart, liver and lung tissue after a single CS exposure (Howard et al., 1998). Time- and dose-dependent inflammatory responses after acute mainstream CS exposure have already been described (Morris et al., 2008; Stevenson et al., 2005; Vlahos et al., 2006). But until now, no comprehensive comparison of the dynamics of acute inflammatory processes in the lung between main- and sidestream CS exposure has been performed. Additionally, based on the results of the acute study the mainstream CS model was chosen as the more suitable model for chronic CS exposure studies.
In chronic CS exposure experiments, we monitored functional and structural changes such as lung function decline and loss of alveolar structures in a time-dependent manner and related these

changes to the CS-induced inflammatory kinetics. Since chronic CS exposure leads to the accumulation of B cells organized in iBALT structures, as well as macrophages in the lungs, which might contribute to CS-induced emphysema, we focused on these two immune cell types. By exposing B cell depleted mice to CS we demonstrated that these mice are protected against emphysematous changes. In further experiments this study aimed at investigating the mechanisms by which B cells account for COPD development. We hypothesized that antibody-independent functions of B cells such as their organization in iBALT structures and manipulating other immune cells via the secretion of soluble mediators might be more important with regard to COPD than their antibody-producing capacity. Here, B cells have been shown to influence macrophage polarization towards a phenotype characterized by increased MMP12 production. Thus we hypothesized that CS-induced B cells might cause macrophage accumulation and macrophage-derived MMP12 secretion.

1.9 Research project

The essential methodic tools to examine the dynamics of immunological cells and in more detail the role of B cells in the development of COPD in a CS induced COPD mouse model comprise primarily the COPD mouse model per se. Furthermore, methods to analyze mouse lung function and to quantitatively evaluate morphological changes in lung tissue as well as immunological, molecular and histological methods are required. The analysis of lymphocyte populations and their activation state by flow cytometry and the identification of relevant mediators on mRNA and protein level have been the focus of the study.

1.9.1 Cigarette smoke induced COPD mouse model

For the accomplishment of the presented studies, a CS-induced COPD mouse model was used. Despite the cons listed in Table 1, this model was used due to the facts that both active and second hand CS represent the main risk factors for COPD development, and that CS-induced pathological alterations seen in the experimental mouse model are close to those observed in COPD patients. For the here presented studies pathogen-free C57BL/6 and B cell deficient B6.129S2-*Igh-6*^{tm1Cgn}/J mice (also µMT mice) were used. All mice were housed in rooms maintained at constant temperature and humidity. A 12 hour light/dark cycle was maintained and mice had access to food and water ad libitum. All procedures involving animals were approved by the by the local government for the administrative region of Upper Bavaria and were conducted under strict governmental and international guidelines.
Mice were exposed to CS-generated from 3R4F Research Cigarettes (Tobacco Research Institute, University of Kentucky, Lexington, KY). Control mice for all experiments were kept in a filtered air environment.
The machine is adjusted to produce 89% sidestream and 11% mainstream smoke. The chamber atmosphere was monitored to maintain total particulate matter (TPM) at 250 and 500 mg/m³ and mice were exposed to CS for 50 min twice per day for 3 consecutive days.
To mimic natural human smoking habits the mainstream CS model was used and mice were exposed to active smoke (100% mainstream smoke). The smoke was drawn into the exposure chamber via a membrane pump. Just as in the sidestream model, mice were exposed to CS of 250 and 500 mg/m^3 TPM for 50 min twice per day for 3 consecutive days as described by Eltom et al. (Eltom et al. 2011). For chronic CS exposure the mainstream model was used. Mice were exposed to a TPM of 500mg/m^3 for 50 min twice per day, 5 days a week, for up to 6 months. Mice were analyzed after 2, 4 and 6 months of CS exposure, 24h after the last exposure.
To determine TPM concentrations sample air from the exposure chamber was collected on quartz fiber filters and the total air volume was measured. Via gravimetric analysis of the filters prior and after

exposure TPM mass concentration was obtained (estimated accuracy of approximately 5%). A GCO 100 CO Meter (Greisinger Electronic, Regenstauf, Germany) was used to constantly monitor CO concentrations in the exposure chamber. To measure levels of arterial blood carboxyhemoglobin (CO-Hb) in mice 30 min after CS exposure retro-orbital blood samples were analyzed in an ABL80 FLEX blood gas analyzer (Radiometer, Willich, Germany). All acute CS exposure experiments were performed with n=6, chronic CS exposure experiments were performed with n=4 animals per group and all experiments were repeated twice.

1.9.2 Lung function measurement

For lung function testing anesthetized mice were tracheostomized and connected to the FlexiVent system (Emka, France). The mice were ventilated with a tidal volume of around 10mg/kg at a frequency of 150 breaths/min to reach a mean lung volume similar to that of spontaneous breathing. Measurement of lung mechanical properties was started by a computer generated program to measure dynamic lung compliance and resistance. These measurements were repeated four times for each animal.

1.9.3 Quantitative morphometry and immunohistochemistry

By default two histopathological aspects of COPD have been analyzed using the right mouse lung: 1) airway inflammation with infiltration of neutrophils, macrophages and lymphocytes, 2) development of emphysema with increased mean chord length. Design-based stereology was used to analyze the lung sections. In this connection, samples have to be treated in a standardized way (‚systematic uniform random sampling') to ensure that tissue samples, slides and finally the microscopic view fields which are included in the analysis are representative for the entire organ independent of the properties of the investigated structures.
Quantitative determination of lymphocyte subsets and other immune cells was performed by immunohistochemical staining of paraffin slides. Therefore, the so-called ‚physical-dissector' method (sections with a known distance from each other) has to be used to allow serial sections. The localization and total number of lymphocytes or macrophages was determined by staining with the particular cell-specific antibody, CD45R for B cells, CD3 for T cells and MMP12 for macrophages. The quantitative analyses were performed using an Olympus BX51 light microscope equipped with the computer-assisted stereological toolbox newCAST of Visiopharm.

1.9.4 Molecular biology

The aim of the molecular studies was to carry out a screening for differentially expressed pro- and anti-inflammatory genes in CS exposed Wt vs. CS exposed µMT mice and in control mice. Furthermore, the time-dependent appearance of certain cellular mediators in various lung compartments during COPD development should be determined. For this purpose, the left lung was shock-frozen in liquid nitrogen for protein and RNA analysis. Expression analysis of the target parameters was performed at the mRNA level by quantitative real-time RT-PCR and on protein level by Western Blot.

1.9.5 **Analysis of immunological parameters**

To monitor immunological parameters in different compartments, a variety of techniques was established. These include: the analysis of lymphocyte subsets and their activation status, the detection of inflammatory mediators as well as differential cell analysis of BAL. Using flow cytometry analysis, lymphocyte subsets in mouse lung tissue have been characterized during the duration of CS exposure. Concentrations of inflammatory mediators were quantified by magnetic bead-based multiplex protein assays. These allow the simultaneous determination of multiple analytes in a small sample volume of cell supernatant or BAL using specific capture antibodies, which are coupled to dual-color labeled beads. The analysis of the beads is carried out by a dual-laser flow-based detection instrument (Luminex® 100/200™ System). One laser excites the internal dyes defining the bead sets and a second laser excites PE, the fluorescent dye on the reporter molecule.

2 Zusammenfassung

Die chronisch obstruktiven Lungenerkrankungen (COPD) stellen ein globales Gesundheitsproblem mit steigender Prävalenz, Morbidität und Mortalität dar. Die WHO prognostiziert für COPD im Jahr 2020 Rang drei der häufigsten Todesursachen weltweit. COPD ist charakterisiert durch eine progressive, nicht vollständig reversible Verschlechterung der Lungenfunktion welche durch die Entstehung des Emphysems und den Umbau der Atemwege bedingt ist. Anormale entzündliche Reaktionen der Lunge auf gesundheitsschädliche Partikel oder Gase werden mit diesen pathologischen Veränderungen assoziiert. Der Hauptrisikofaktor in den Industrieländern stellt das Rauchen dar. Gegenwärtig existiert keine heilende Therapie für COPD, die Behandlung zielt lediglich auf die Linderung der Symptome ab.

Chronischer Zigarettenrauch führt in der Lunge zu einer anormalen Entzündungsantwort, welche sowohl Zellen des angeborenen Immunsystems wie Neutrophile und Makrophagen als auch Zellen der adaptiven Immunität wie B- und T-Lymphozyten einschließt. Interessanterweise konnten wir in unserer ersten Arbeit zeigen dass die Dynamik der Rekrutierung von Entzündungszellen in die Lunge stark von der Zusammensetzung des Zigarettenrauchs abhängt. Es wurden hierbei die Entzündungsreaktionen als Antwort auf Zigarettenrauch unter Aktiv- und Passivrauchbedingungen verglichen. Wildtyp Mäuse wurden zwei Konzentrationen (250 und 500mg/m3 Rohkondensat) Aktiv- oder Passivrauch für 3 Tage ausgesetzt. Wir beobachteten eine starke Entzündungsreaktion, gekennzeichnet durch einen Neutrophileneinstrom, einer vermehrten Zytokinsezernierung (KC, MIP1a, MCP1, TNFa, MIP2), einer erhöhten proinflammatorischen Genexpression (KC, MIP2, MMP12) und einer hochregulierten GM-CSF-Produktion im Aktivrauchmodell. Das Passivrauchmodell erzeugte hingegen eine verminderte Entzündungsantwort, gekennzeichnet durch das dominierende Auftreten von Makrophagen und dem Fehlen von Neutrophilen sowie der verringerten GM-CSF-Produktion, höchstwahrscheinlich verursacht durch erhöhte CO-Konzentrationen unter Passivrauchbedingungen. Um für die chronische Zigarettenrauchexposition von Mäusen einen negativen Effekt der höheren CO-Konzentrationen auszuschließen, wurden für das chronische Modell Aktivrauchbedingungen verwendet. Chronische Zigarettenrauchexposition führt in Mäusen besonders zu einer Akkumulation von B-Zellen, organisiert in iBALT Strukturen, und Makrophagen in der Lunge. Die Frage nach deren möglicher Beteiligung an der Entstehung des Emphysems war Inhalt unserer chronischen Studie. Wir haben gezeigt, dass bis zu sechs Monate Zigarettenrauch exponierte B-Zell defiziente Mäuse gegenüber Wildtyp (Wt) Mäusen vor der Entwicklung COPD-ähnlicher Veränderungen geschützt sind. Verglichen mit µMT Mäusen wiesen Wt Mäuse nach chronischer Zigarettenrauchexposition deutliche lymphoide Strukturen (iBALT) auf, sowie eine signifikante Verschlechterung der Lungenfunktion und einen signifikanten Verlust alveolärer Septen. Die erhöhte Akkumulation von lungenansässigen Makrophagen um die iBALT Strukturen herum und in den alveolären, emphysematösen Bereichen in zigarettenrauchexponierten Wt Mäusen war assoziiert mit einer signifikant stärkeren MMP12 Expression. Anschließende in vitro - Co-Kultur- Experimente unter Verwendung von B -Zellen und Makrophagen zeigten, dass von B-Zellen sezerniertes IL-10 die Makrophagenaktivierung und MMP12 Expression induziert. Zusammenfassend konnte gezeigt werden dass Antikörper-unabhängige Funktionen von B-Zellen in der iBALT Formation von Bedeutung für die Makrophagen-induzierte Gewebezerstörung in Zigarettenrauch-vermittelter Emphysementstehung sind. Daraus ergibt sich möglicherweise ein Angriffsziel für neue therapeutische Ansätze.

3 Summary

Chronic obstructive pulmonary disease (COPD) represents a global health problem with increasing prevalence, morbidity and mortality. The WHO ranked COPD the third common cause of death worldwide by 2020. COPD is characterized by a progressive and not fully reversible impairment of lung function which is caused by the development of emphysema and remodeling of the airways. Abnormal inflammatory responses of the lungs to noxious particles or gases are associated with these pathological changes. In developed countries the main risk factor is smoking. Currently there is no curative therapy for COPD; treatment may only aim to alleviate symptoms.

Chronic cigarette smoke leads to an abnormal inflammatory response in the lungs, which includes cells of both the innate immune system such as neutrophils and macrophages, as well as cells of the adaptive immunity, such as B- and T-lymphocytes. Interestingly, we have shown in our first study that the dynamics of the inflammatory cell recruitment to the lung strongly depends on the composition of cigarette smoke. In this connection, inflammatory responses to either mainstream smoke or sidestream smoke were compared. Mice were exposed to two concentrations (250 and 500 mg/m3 total particulate matter) sidestream and mainstream cigarette smoke for 3 days. We observed a strong inflammatory response characterized by a neutrophilic influx, an increased cytokine secretion (KC, TNFa, MIP1a, MCP1, MIP2), elevated pro-inflammatory gene expression (KC, MIP2, MMP12) and an up-regulated GM-CSF production in the mainstream model. However, the sidestream CS model induced a dampened immune reaction lacking neutrophils and consisting only of macrophages and impaired GM-CSF production, most likely caused by higher CO levels under sidestream CS conditions. In order to exclude negative effects of high CO concentrations in chronically CS exposed mice, mainstream smoke conditions were used for the chronic exposure model. Chronic CS exposure of mice leads to the accumulation of B cells organized in iBALT structures, as well as macrophages in the lungs. This might contribute to CS-induced emphysema, but the mechanisms thereof remain unclear. We have shown that up to six months cigarette smoke-exposed B-cell deficient mice compared to Wt mice are protected against the development of COPD-like changes. In contrast to µMT mice chronically CS exposed Wt mice exhibited significant lymphoid structures (iBALT), a significant decline of lung function and a significant loss of alveolar septa. The increased accumulation of lung resident macrophages surrounding the iBALT structures and in the alveolar, emphysematous areas in CS exposed Wt mice was associated with a significantly increase of MMP12 expression. In following in vitro experiments, it could be shown that cigarette smoke extract stimulated B cells to secrete IL-10 and IL-10 containing B-cell supernatants in turn induced MMP12 expression in macrophages. This up-regulated MMP12 expression was inhibited by the addition of an IL-10-neutralizing antibody. In summary, our data highlight that CS exposure leads to B cell-dependent iBALT formation, which contributes to the pathogenesis of COPD via IL-10-induced macrophage activation and MMP12 up-regulation. This mechanism maintains the severe inflammatory response causing subsequent emphysema development in COPD. The link between innate and adaptive immune cell responses to CS in COPD is of great clinical relevance and could be explored as a target for therapeutic intervention in COPD patients.

4 The composition of cigarette smoke determines inflammatory cell recruitment to the lung in COPD mouse models

Gerrit John

Katrin Kohse

Jürgen Orasche

Ahmed Reda

Jürgen Schnelle-Kreis

Ralf Zimmermann

Otmar Schmid

Oliver Eickelberg

Ali Önder Yildirim

Published first in “Clinical Science”

John G, Kohse K, Orasche J, Reda A, Schnelle-Kreis J, Zimmermann R, Schmid O, Eickelberg O, Yildirim AÖ

The composition of cigarette smoke determines inflammatory cell recruitment to the lung in COPD mouse models.

Clin Sci (Lond). 2014 Feb; 126(3):207-21. doi: 10.1042/CS20130117

Clinical Science (2014) **126**, 207–221 (Printed in Great Britain) doi: 10.1042/CS20130117

The composition of cigarette smoke determines inflammatory cell recruitment to the lung in COPD mouse models

Gerrit JOHN*, Katrin KOHSE*, Jürgen ORASCHE†, Ahmed REDA†, Jürgen SCHNELLE-KREIS†, Ralf ZIMMERMANN†§, Otmar SCHMID*, Oliver EICKELBERG*‡ and Ali Önder YILDIRIM*§

*Comprehensive Pneumology Center, Institute of Lung Biology and Disease, Helmholtz Zentrum München, Member of the German Center for Lung Research, Ingolstädter Landstr. 1, 85764 Neuherberg, Germany
†Joint Mass Spectrometry Centre of Helmholtz Zentrum München and University of Rostock, Comprehensive Molecular Analytics, Helmholtz Zentrum München, Ingolstädter Landstr. 1, 85764 Neuherberg, Germany
‡Klinikum der Universität München, Max-Lebsche-Platz 31, 81377 München, Germany
§HICE–Helmholtz Virtual Institute of Complex Molecular Systems in Environmental Health-Aerosols and Health

Abstract

COPD (chronic obstructive pulmonary disease) is caused by exposure to toxic gases and particles, most often CS (cigarette smoke), leading to emphysema, chronic bronchitis, mucus production and a subsequent decline in lung function. The disease pathogenesis is related to an abnormal CS-induced inflammatory response of the lungs. Similar to active (mainstream) smoking, second hand (sidestream) smoke exposure severely affects respiratory health. These processes can be studied *in vivo* in models of CS exposure of mice. We compared the acute inflammatory response of female C57BL/6 mice exposed to two concentrations [250 and 500 mg/m^3 TPM (total particulate matter)] of sidestream and mainstream CS for 3 days and interpreted the biological effects based on physico-chemical differences in the gas and particulate phase composition of CS. BAL (bronchoalveolar lavage fluid) was obtained to perform differential cell counts and to measure cytokine release. Lung tissue was used to determine mRNA and protein expression of proinflammatory genes and to assess tissue inflammation. A strong acute inflammatory response characterized by neutrophilic influx, increased cytokine secretion [KC (keratinocyte chemoattractant), TNF-α (tumour necrosis factor α), MIP-2 (macrophage inflammatory protein 2), MIP-1α and MCP-1 (monocyte chemoattractant protein-1)], pro-inflammatory gene expression [KC, MIP-2 and MMP12 (matrix metalloproteinase 12)] and up-regulated GM-CSF (granulocyte macrophage colony-stimulating factor) production was observed in the mainstream model. After sidestream exposure there was a dampened inflammatory reaction consisting only of macrophages and diminished GM-CSF levels, most likely caused by elevated CO concentrations. These results demonstrate that the composition of CS determines the dynamics of inflammatory cell recruitment in COPD mouse models. Different initial inflammatory processes might contribute to COPD pathogenesis in significantly varying ways, thereby determining the outcome of the studies.

Key words: chronic obstructive pulmonary disease (COPD), inflammation, mainstream, neutrophil, sidestream, smoke

INTRODUCTION

COPD (chronic obstructive pulmonary disease) is a major public health problem and its morbidity and mortality are still rising [1]. Patients suffering from COPD exhibit a constant and accelerated decline in lung function leading to airflow limitation. The pathogenesis of COPD is characterized by severe pathophysiological changes including chronic bronchitis, small airway remodelling, mucus production and the development of emphysaema [2]. However, the exact processes involved in disease pathogenesis are so far not fully understood and treatment can only aim at alleviating symptoms.

Abbreviations: BAL, bronchoalveolar lavage; CC, carbonyl compounds; CMD, count median diameter; CO-Hb, carboxyhaemoglobin; COPD, chronic obstructive pulmonary disease; CS, cigarette smoke; DNPH, 2,4-dinitrophenylhydrazine; GC-SIM-MS, gas-chromatography with selective ion monitoring MS; GM-CSF, granulocyte macrophage colony-stimulating factor; HO, haem oxygenase; H&E, haematoxylin and eosin; HPRT-1, hypoxanthine–guanine phosphoribosyltransferase; IFNβ, interferon β; IL-1β, interleukin 1β; KC, keratinocyte chemoattractant; LPS, lipopolysaccharide; MCP-1, monocyte chemoattractant protein-1; MIP, macrophage inflammatory protein; MMD, mass median diameter; MMP12, matrix metalloproteinase 12; NE, neutrophil elastase; NF-κB, nuclear factor κB; PAH, polycyclic aromatic hydrocarbons; PM, particulate matter; TNF-α, tumour necrosis factor α; TPM, total particulate matter.

Correspondence: Dr Ali Önder Yildirim (email oender.yildirim@helmholtz-muenchen.de).

CS (cigarette smoke) is a major etiologic factor in the pathogenesis of COPD and other diseases [3]. The health impact of environmental CS is under critical evaluation, due to the risk for non-smokers. Environmental CS is mainly composed of exhaled mainstream CS and sidestream CS, whereby the impact of sidestream CS with respect to environmental CS surpasses that of exhaled mainstream CS [4]. Chronic CS exposure results in severe lung inflammation by initiating a complex inflammatory cascade accompanied by the activation and influx of various inflammatory cells and by the secretion of disease-specific mediators such as cytokines and growth factors [5]. The smoke-induced increase in inflammatory cell influx and responses involves both innate immune cells, with macrophages and neutrophils predominating, and adaptive immune cells, specifically T and B lymphocytes. The numbers of neutrophils, macrophages and lymphocytes are increased in both airways and parenchyma of patients with COPD [6–9]. The progression and severity of COPD are also associated with increasing infiltration of the airways by innate and adaptive immune cells, leading to obstruction of small airways and thickening of the airway wall [10]. Nevertheless, it still remains unclear that inflammatory events and cell types involved in this complex cascade are central for the development of COPD.

In order to elucidate these processes *in vivo*, CS exposure of rodents/mice is a commonly used model. Chronic exposure, that is, up to 4 months or longer, recapitulates most features of COPD by inducing pathophysiological changes in mice similar to those observed in COPD patients, such as small airway remodelling and septal tissue damage/emphysaema. On the other hand, acute CS exposure is mostly useful and employed to study early and more direct effects of smoking on inflammatory responses and cell recruitment in the lung, specifically innate immune cells [11].

Several animal studies have analysed the contribution of neutrophils and macrophages to CS-induced lung inflammation and subsequent emphysema development. It is now generally accepted that in CS models the inflammatory response driving the pathophysiological changes is characterized by two phases: the acute reaction during the first week of CS exposure, which shows a strong neutrophilic influx, and the progressive inflammation after 1 month of exposure consisting of neutrophils, macrophages and lymphocytes [12–14]. Interestingly, it was shown that in CS-exposed mice innate immune cells were sufficient for driving inflammatory processes in the lung thereby initiating COPD development [15,16]. Innate immune cell-specific factors MMP (matrix metalloproteinase) 12 and NE (neutrophil elastase) were even necessary for inducing experimental emphysema after prolonged exposure [17,18]. Although CS-exposed MMP12-knockout mice failed to recruit macrophages and did not develop lung destruction [17], NE was required for neutrophil and monocyte recruitment as well as for the activation of MMP12 after CS exposure [18]. These studies highlight the importance of prompt CS-induced inflammatory mechanisms and innate immune cell activation that potentially contribute to COPD pathogenesis at an early stage of smoke exposure.

However, different smoke exposure models with regards to machines and setups using either mainstream smoke only or a mixture of side- and main-stream smoke (usually consisting of about 90 % sidestream smoke and 10 % mainstream smoke) have been established and might generate varying results, especially when comparing the degree of CS-induced changes [19]. The dynamics of early lung immune cell reactions to CS was characterized using the mainstream model in acute settings of smoke exposure for a few days [20–22]. But even though sidestream CS is more toxic than mainstream CS [23], data on acute lung inflammation from this model are missing. The only acute sidestream study investigated oxidative DNA damage in mouse heart, liver and lung tissue after a single CS exposure [24].

Interestingly, time- and dose-dependent inflammatory responses after acute mainstream CS exposure have already been described [20–22]. However until now, no study has ever performed a comprehensive comparison of the dynamics of acute lung inflammation between the main- and side-stream CS model with regards to physico-chemical characteristics of CS, specifically concentration, size distribution and chemical composition of TPM (total particulate matter) as well as composition of the gas phase.

Therefore using two different experimental models of smoke exposure (mainstream and sidestream CS) with two TPM concentrations, the present study aimed at investigating the effect of the physico-chemical characteristics of CS on the acute inflammatory response in the lungs of mice after 3 days of CS exposure. We hypothesized that early signs of inflammation would be apparent, but significantly different between the two types of CS. The results were interpreted based on detailed information on concentration, size distribution and chemical composition of TPM as well as on CO concentration.

Interestingly, a strong acute inflammatory response characterized by neutrophilic influx, accompanied by increased cytokine secretion and pro-inflammatory gene expression, and upregulated GM-CSF (granulocyte macrophage colony-stimulating factor) production was only observed in the mainstream CS model, whereas there was a dampened inflammatory reaction after sidestream exposure, most probably caused by elevated CO concentrations.

MATERIALS AND METHODS

Animals and maintenance

Pathogen-free female C57BL/6 mice (8–10-weeks old) were obtained from Charles River and housed in rooms maintained at constant temperature and humidity with a 12 h light cycle. Animals were allowed food and water *ad libitum*. All animal experiments were conducted under strict governmental and international guidelines and were approved by the local government for the administrative region of Upper Bavaria.

CS exposure and CO monitoring

For both exposure models, smoke was generated from 3R4F Research Cigarettes (Tobacco Research Institute, University of Kentucky, Lexington, KY, U.S.A.). Control mice for all experiments were kept in a filtered air environment.

For sidestream CS exposure, mice were placed in an exposure chamber connected to a TE-10 smoking machine (Teague Enterprises). The machine is adjusted to produce 89 % sidestream and 11 % mainstream smoke. The chamber atmosphere was monitored to maintain TPM at 250 and 500 mg/m^3 and mice were exposed to CS for 50 min twice per day for 3 consecutive days.

In the mainstream CS model, mice were exposed to active smoke (100 % mainstream smoke) in a manner mimicking natural human smoking habits. The smoke was drawn into the exposure chamber via a membrane pump. Mice were exposed to CS of 250 and 500 mg/m^3 TPM for 50 min twice per day for 3 consecutive days as described by Eltom et al. [25].

TPM concentrations were monitored by drawing sample air from the exposure chamber through a quartz fibre filter and measuring the total air volume. The TPM mass concentration was obtained via gravimetric analysis of the filters prior to and after exposure (estimated accuracy of approximately 5 %). CO concentrations in the exposure chamber were constantly monitored by using a GCO 100 CO Meter (Greisinger Electronic). Levels of arterial blood CO-Hb (carboxyhaemoglobin) in mice 30 min after CS exposure were determined by retro-orbital blood sampling and analysed in an ABL80 FLEX blood gas analyser (Radiometer). All CS exposure experiments were performed with $n = 6$ animals per group and were repeated twice.

CS particle size measurements

The size distribution of the PM (particulate matter) of CS was measured during exposure experiments according to the same protocol as described above, but without mice in the exposure chamber. Sample air was drawn from the sampling port of the exposure chamber (located in the centre near the top of the chamber) and delivered at 0.75 l/min through 3 m of tubing to a scanning mobility particle sizer (SMPS, TSI, Model 3080, TSI) in combination with a CPC (condensation particle counter; Model 3025, TSI). The excess air was resupplied into the exposure system downstream of the exposure chamber. The SMPS is a standard aerosol sizer with a sizing accuracy of up to 2 % (here approximately 5 %), which measures the size of aerosol particles based on their velocity (mobility) in an electric field [26]. To avoid potential measurement biases because of high particle concentration and high CO/CO_2 concentrations, the sample air was diluted by a factor of 650 and 400 for the mainstream and sidestream conditions respectively [27]. The SMPS was operated at a sample and sheath flow rate of 0.3 and 1.5 l/min respectively, and the inertial impactor at the inlet of the SMPS was removed to obtain an upper sizing limit of 1000 nm (lower sizing limit, 23 nm). An entire size distribution was obtained within 3 min. For quality assurance, the particle sizing accuracy of the SMPS was verified with size-certified reference particles (230 and 506 nm) and filtre samples were taken for gravimetric analysis of aerosol mass concentrations. For each of the four investigated cases (sidestream and mainstream at 250 and 500 mg/m^3) 3–5 size distributions were recorded and averaged, since no significant trends were observed after a short equilibration phase of a few minutes. The measured number size distributions between 23 and 1000 nm were converted into length, surface area and mass-weighted size distributions (density of 1 g/cm^3) and the data were fitted simultaneously on all four moments (number, length, surface area and mass) assuming a lognormal shape with constant geometric standard deviation. Since the median diameters of these moments are directly related by the Hatch–Choate moment conversion equations, this procedure enhances measurement accuracy especially near the upper size range, where a part of the size distribution was outside of the detection limit of the SMPS [28].

Analysis of organic PM compounds in mainstream and sidestream CS

For organic analyses of the PM of CS, approximately 25 litres of sample air were drawn from the exposure chamber and PM was collected on quartz fibre filters (T293, 25 mm diameter; Munktell). Prior to sampling, the filters were tempered at 500 °C for at least 12 h.

The samples were analysed by using a newly developed *in-situ* derivatization and thermal desorption method, which is coupled to GC-MS (gas-chromatography with mass selective detection) [29]. An internal standard mixture (isotope labelled compounds) was spiked on a filter punch (3 mm diameter) prior to analysis for quantification.

Gas phase analysis of CC (carbonyl compounds) in mainstream and sidestream CS

Carbonyl emissions in the gas phase of CS were sampled using high sample volume DNPH (2,4-dinitrophenylhydrazine) cartridges (Sigma–Aldrich). Parallel samples were collected for each CS type with different flow rates starting form 0.16 to 1.2 l/min using critical nozzles connected to a vacuum pump.

CCs were assessed by GC-SIM-MS (gas-chromatography with selective ion monitoring MS) using DNPH derivatization. Prior to analysis, the cartridges were eluted with 1 ml of acetonitrile and samples were injected into the GC-SIM-MS system for quantitative measurements.

Animal preparation

At 24 h after the last CS exposure, mice were killed with an overdose of ketamine/xylazine followed by exsanguination. Mice were dissected and BAL (bronchoalveolar lavage) was obtained to perform total and differential cell counts for inflammatory cell recruitment of neutrophils, macrophages and lymphocytes. BAL fluid was used to evaluate cytokine secretion via multiplex analysis. Lung tissue was either shock-frozen in liquid nitrogen to determine tissue mRNA expression or fixed by intratracheal instillation of PBS-buffered 6 % (v/v) PFA (paraformaldehyde) and embedded into paraffin for H&E (haematoxylin and eosin) staining.

Preparation of BAL

The lungs were lavaged by using a cannula inserted into the trachea and instilling the lungs with 4×0.5 ml aliquots of sterile PBS (Gibco). For cytospins, cells were spun down at 400 ***g*** and resuspended in RPMI 1640 medium containing 10 % (v/v) FBS (both from Gibco). Total cell counts were determined in a hemocytometer via Trypan Blue exclusion. Maximally 1–2 % Trypan Blue-positive cells were detected in both filtered air and CS-exposed animals from the two CS models. Differential cell counts

Table 1 Primers used for quantitative real-time PCR of lung tissue

Gene	Forward primer (5′→3′)	Reverse primer (5′→3′)
HPRT-1	CCTAAGATGAGCGCAAGTTGAA	CCACAGGACTAGAACACCTGCTAA
KC (CXCL1)	CCGAGTCATAGCCACAC	GTGCCATCAGAGCAGTCT
TNF-α	CACCACGCTCTTCTGTCT	GGCTACAGGCTTGTCACTC
MIP-2 (CXCL2)	CTGTTGTGGCCAGTGAAC	GCCCTTGAGAGTGGCTAT
MMP12	TGTACCCCACCTACAGATACCTTA	CCATAGAGGGACTGAATGTTACGT
CD68	CCTCCACCCTCGCCTAGT C	TTGGGTATAGGATTCGGATTTGA
GM-CSF	GCCATCAAAGAAGCCCTG	GCGGGTCTGCACACATGTTA

were performed using morphological criteria on May–Grünwald–Giemsa-stained cytospins (200 cells/sample).

Quantitative real-time RT (reverse transcription)-PCR

Total RNA from lung tissue homogenate was isolated using a peqGOLD Total RNA Kit (Peqlab) according to the manufacturer's instructions. cDNA was synthesized using Random Hexamers and MuLV Reverse Transcriptase (Applied Biosystems). mRNA expression of target genes KC (keratinocyte chemoattractant; CXCL1), TNF-α (tumour necrosis factor α), MIP-2 (macrophage inflammatory protein 2) (CXCL2), MMP12, CD68 and GM-CSF in comparison with housekeeping control HPRT-1 (hypoxanthine–guanine phosphoribosyltransferase 1) was determined using Platinum SYBR Green qPCR SuperMix (Applied Biosystems) on a StepOnePlus^{TM} 96 well Real-Time PCR System (Applied Biosystems). The primers used are listed in Table 1. Relative transcript expression of a gene is given as $2^{-\Delta C_t}$ ($\Delta C_t = C_{t_{target}} - C_{t_{reference}}$), relative changes compared with control are $2^{-\Delta\Delta C_t}$ values ($\Delta\Delta C_t = \Delta C_{t_{treated}} - \Delta C_{t_{control}}$). Primers were generated using Primer-BLAST software [30].

Multiplex cytokine analysis

Concentrations of secreted cytokines and chemokines IL-1β (interleukin 1β), IL-2, IL-4, IL-5, IL-6, IL-7, IL-9, IL-10, IL-13, IL-17A, GM-CSF, KC (CXCL1), TNF-α, IFNβ (interferon β), MCP-1 (monocyte chemoattractant protein-1; CCL2), MIG (monokine induced by interferon-γ; CXCL9), MIP2 (CXCL2) and MIP-1α (CCL3) in BAL were determined using a magnetic bead-based MILLIPLEX *MAG* multiplex assay (Millipore) and analysed on a Luminex^{100} (Bio-Rad Laboratories). For this assay, BAL fluid was concentrated (10×) by ultrafiltration in Amicon Ultra-0.5 centrifugal filter devices (Millipore).

Statistics

Results are given as mean values ± S.D. One-way ANOVA following Bonferroni post-hoc test was used for all studies with more than two groups, if equal variances and normal distribution was given. Student's unpaired *t* test was performed to compare the concentration of particulate organic compounds [PAHs (polycyclic aromatic hydrocarbons) and alkanes] between two different TPMs. Analyses were conducted using GraphPad Prism 6 software (GraphPad Software).

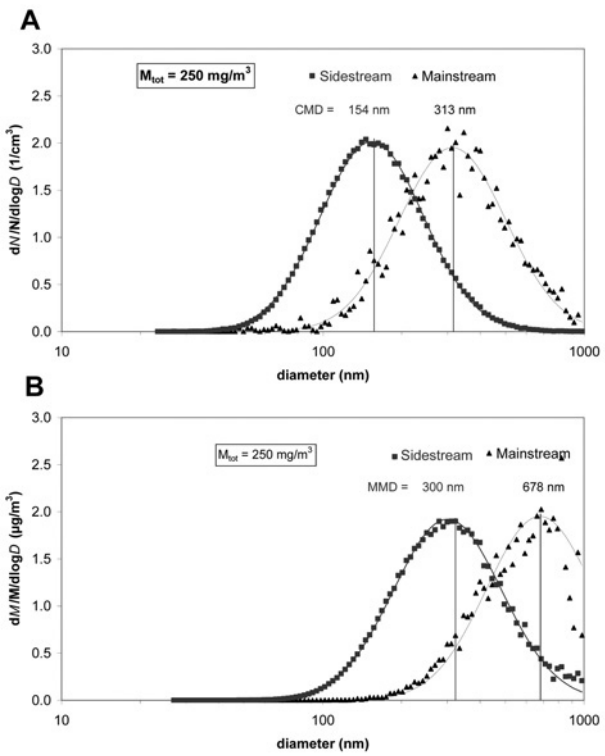

Figure 1 Measured number (A) and mass-based size distribution (B) of CS particles in the exposure chamber at a TPM of 250 mg/m^3 for both sidestream (square) and mainstream CS (triangle)

The symbols represent the measured values and the solid lines represent the corresponding lognormal curve fit of the data. CMD and MMD of the size distributions are also depicted. The size distributions were normalized to their respective total number and total mass concentration.

RESULTS

Sidestream CS particles are smaller in size than mainstream CS particles

The size distribution of the PM of CS was determined using an SMPS. Figure 1 depicts the number- and mass-weighted particle size distribution for sidestream and mainstream conditions for a mass concentration of 250 mg/m^3. A summary of all size distribution data is presented in Table 2.

Sidestream CS particles exhibited a CMD (count median diameter) of 154 nm and were therefore significantly smaller than mainstream CS particles (CMD = 313 nm) (Figure 1A). The geometric standard deviation (width of the size distribution) was

Table 2 Overview of characteristic parameters of the cigarette smoke size distributions for sidestream and mainstream conditions

M_{tot}, mass concentration of total particulate matter in the smoke chamber; σ_g, geometric S.D. *The reported alveolar lung deposited fraction refers to the specific MMD and is based on *in silico* lung deposition data for mice published by Nadithe et al. [31]. **A breathing frequency of 150/min and a tidal volume of 200 μl were assumed, resulting in an inhaled air volume of 1.8 l/h.

		Sidestream		Mainstream	
Parameter	**M_{tot} (mg/m^3) . . .**	**250**	**500**	**250**	**500**
CMD (nm)		154	189	313	338
σ_g		1.60	1.56	1.60	1.62
MMD (nm)		300	373	678	756
Lung-deposited particle fraction*		0.11	0.11	0.05	0.05
Lung-deposited particle dose per h (μg/h)**		49.5	99	22.5	45

about 1.60 for all cases (Table 2). Multiplication of each size bin of the number size distribution with the respective (spherical) particle volume ($\pi d^3/6$, d = particle diameter) and density (1 g/cm^3) provided the corresponding mass-weighted size distribution. As depicted in Figure 1(B), the mass-weighted size distribution showed an MMD (mass median diameter) of 300 and 678 nm for sidestream and mainstream CS particles respectively, confirming that mainstream CS particles were approximately two times larger than sidestream CS particles. The increased size of mainstream particles was observed for both concentration settings (250 and 500 mg/m^3), with 10–20 % larger diameters for the 500 mg/m^3 case (Table 2). It is important to note that even though a significant fraction of the mass-based mainstream size distribution was beyond the upper sizing limit of the SMPS (1000 nm), the reported MMD were still reliable, since the curve fit was performed simultaneously on all moments (number, length, surface area and mass) as described in the Materials and methods section.

From the size distribution parameters provided in Table 2, the biologically relevant lung deposited dose was calculated by multiplying the aerosol mass concentration by the inhaled air volume (1.8 l/h) and the lung-deposited particle fraction (at the MMD) provided by Nadithe et al. [31]. The lung deposited particle dose ranged from 22.5 to 99 μg/h, depending on the aerosol mass concentration and sidestream or mainstream smoke conditions. Although there are several *in silico* models of particle deposition in the lungs of mice, their general trend predicted elevated deposition of 300 nm relative to 700 nm particles, due to enhanced diffusional deposition of 300 nm particles [31].

In summary, mainstream CS particles were approximately two times larger than sidestream CS particles for a given TPM level. Enhancing the TPM level from 250 to 500 mg/m^3 increased the particle size only moderately (10–20 %). This indicates that the type of CS generation (mainstream/sidestream) was more relevant for the observed particle size than the TPM level. Interestingly, the biologically relevant, i.e. lung deposited particle dose for 250 mg/m^3 TPM sidestream conditions corresponded closely to the pulmonary dose delivered for 500 mg/m^3 TPM mainstream conditions (Table 2).

Organic composition of CS particles

A total of 14 relevant PAHs in the PM CS were analysed (Table 3). Sidestream CS showed extremely high concentrations of PAH. The most toxic Benz[a]pyrene [$LD_{50\ (rat)} = 50$ mg/kg] within the compound class of PAHs were found in potentially harmful concentrations in sidestream CS (1.4 μg/m^3 at 250 mg/m^3 TPM and 2.7 μg/m^3 at 500 mg/m^3 TPM, with corresponding lung delivered doses of 0.069 and 0.13 μg/kg respectively), whereas the levels below the LOQ (limit of quantification; 1 ng/m^3) were measured in mainstream CS. The composition of mainstream CS showed no significant differences in concentrations of PAHs with regards to different TPM levels.

The *n*-alkanes and the branched alkanes (Table 4) showed the typical pattern of CS as already described [32]. Alkanes with odd carbon numbers are mainly formed, in particular with C-numbers C27–C33. For branched alkanes, an alternation can be observed between odd-C-numbered iso-alkanes and even-C-numbered anteiso-alkanes. The most abundant iso-alkanes were isononacosane (i-C29), isohentriacontane (i-C31) and isotritriacontane (i-C33), whereas the most abundant anteiso-alkanes were anteisotriacontane (a-C30) and anteisodotriacontane (a-C32). In contrast with the PAHs, significantly higher amounts of alkanes in sidestream CS were only found at 500 mg/m^3 TPM.

CC in the gas phase of CS

A total of 12 relevant CCs were identified in gas phase emissions from CS. Among those, acetaldehyde dominated in both sidestream and mainstream CS emissions with 250 and 500 mg/m^3 TPM (Table 5). This predominance of acetaldehyde was already described in previous studies [33,34]. Unsaturated CCs such as acrolein, methacrolein and crotonaldehyde were also found in relevant concentrations in both types of CS.

For most of the identified CCs the concentrations in sidestream CS were generally higher compared with mainstream CS and also showed greater than 2-fold increases with increasing TPM concentrations.

BAL inflammation after sidestream CS exposure lacks neutrophilic influx

To determine inflammatory cell recruitment in BALs, differential cell counts on May–Grünwald–Giemsa-stained cytospins were performed.

The 3 days of mainstream CS exposure significantly increased total cell numbers from control levels (44 167 $\pm$ 9601) to 83 000 $\pm$ 21 389 for 250 mg/m^3 TPM and 149 750 $\pm$ 38 756 for

Table 3 **Sidestream and mainstream yields of PAH from two different cigarette smoke concentrations**
P values were calculated using Student's unpaired *t* test. Values in bold are significant. <DL, below detection limit; na, not analysed.

	Sidestream			Mainstream		
Substance (μg/m^3)	**250 mg/m^3**	**500 mg/m^3**	***P* value**	**250 mg/m^3**	**500 mg/m^3**	***P* value**
Phenanthrene	28.6	55.0	**0.01**	8.6	8.4	0.7
Anthracene	6.1	14.3	**0.01**	1.7	1.5	0.5
Pyrene	11.1	18.2	**0.02**	3.1	2.6	0.1
Fluoranthene	4.7	7.1	**0.01**	2.5	2.4	0.6
Benzo[a]anthracene	2.2	4.0	**0.00**	0.5	<DL	na
Chrysene	7.7	15.0	**0.01**	0.9	<DL	na
Sum Benzofluoranthenes	2.0	4.1	**0.00**	<DL	<DL	na
Benzo[e]pyrene	0.7	1.3	0.35	<DL	<DL	na
Benzo[a]pyrene	1.4	2.7	**0.01**	<DL	<DL	na
Perylene	1.2	2.8	0.11	<DL	<DL	na
Dibenzo[ah]anthracene	<DL	<DL	na	<DL	<DL	na
Indeno[1,2,3-cd]pyrene	1.3	1.8	0.08	2.6	2.5	0.6
Benzo[ghj]perylene	<DL	1.1	na	<DL	<DL	na
Coronene	<DL	<DL	na	<DL	<DL	na
Sum PAH	67.0	126.9	**0.00**	19.4	17.3	0.1

Table 4 **Summary of *n*-alkanes and iso- and anteiso-alkanes in sidestream and mainstream CS**
P values were calculated using Student's unpaired *t* test. Values in bold are significant. na, not analysed.

	Sidestream			Mainstream		
Substance (μg/m^3)	**250 mg/m^3**	**500 mg/m^3**	***P* value**	**250 mg/m^3**	**500 mg/m^3**	***P* value**
Nonadecane	90.3	97.9	0.52	193.5	60.1	na
Eicosane	82.7	163.5	**0.01**	43.1	59.3	0.14
Heneicosane	105.1	224.0	**0.01**	65.0	149.2	0.09
Docosane	111.7	269.5	0.10	75.8	64.1	0.29
Tricosane	86.8	237.6	**0.01**	73.1	57.5	0.15
Tetracosane	103.9	174.3	**0.03**	64.3	61.7	0.55
Pentacosane	189.4	379.9	**0.01**	147.8	117.3	**0.00**
Heptacosane	1006.2	2181.8	**0.00**	1040.6	825.1	**0.04**
Nonacosane	874.0	2170.7	**0.00**	1084.1	861.9	0.06
Triacontane	259.7	632.9	**0.00**	326.3	240.9	**0.02**
Hentriacontane	2966.9	7756.1	**0.00**	3677.9	2738.7	**0.03**
Dotriacontane	495.3	1199.4	**0.02**	695.3	513.9	**0.03**
Tritriacontane	1358.2	3609.9	**0.00**	2151.3	1515.5	**0.03**
Tetratriacontane	70.6	138.5	**0.01**	118.8	172.3	0.19
Pentatriacontane	41.5	78.7	0.06	57.2	48.5	0.13
Iso-nonacosane	169.4	452.3	**0.00**	222.7	192.4	0.34
Anteiso-triacontane	686.5	1749.8	**0.02**	838.4	837.7	1.00
Iso-hentriacontane	1069.2	3194.0	**0.00**	1578.0	1415.0	0.21
Anteiso-dotriacontane	1510.2	3639.7	**0.03**	2016.3	1918.0	0.71
Iso-tritriacontane	547.5	1440.8	**0.00**	735.6	650.8	0.22

500 mg/m^3 TPM respectively (Figure 2A). These mice showed BAL inflammation predominantly consisting of neutrophils and macrophages that were significantly elevated after exposure to 500 mg/m^3 TPM (Figures 2B and 2C). Neutrophil numbers increased from 152 ± 203 in filtered air controls to $16\,238 \pm 5878$ at 250 mg/m^3 TPM and to $45\,158 \pm 29\,315$ at 500 mg/m^3. Macrophages increased from $48\,967 \pm 12\,636$ in filtered air controls to $69\,080 \pm 18\,357$ for 250 mg/m^3 TPM and to $103\,523 \pm 33\,576$ for 500 mg/m^3 TPM.

In contrast, BAL inflammation in the sidestream model was dominated by macrophages, leading to significantly elevated total cell and macrophage numbers after CS exposure to 500 mg/m^3 TPM compared with control animals (Figures 2A and 2B). Total cell counts increased from

Table 5 **Carbonyl compounds in the gas phase of sidestream and mainstream CS**
P values were calculated using Student's unpaired *t* test.

	Sidestream			Mainstream		
Compound ($\mu g/m^3$)	**250 mg/m³**	**500 mg/m³**	***P* value**	**250 mg/m³**	**500 mg/m³**	***P* value**
Formaldehyde	207.6	318.7	**0.02**	477.8	1027.5	**0.00**
Acetaldehyde	8000.0	11000.0	**0.00**	11900.0	32300.0	**0.00**
Propanal	330.5	492.2	**0.00**	415.4	1229.9	**0.00**
Acetone	2290.0	3120.0	**0.00**	2860.0	9700.0	**0.00**
Acrolein	139.7	263.6	**0.00**	336.1	746.6	**0.01**
Methacrolein	108.1	204.5	**0.00**	243.7	711.3	**0.00**
Crotonaldehyde	144.0	279.9	**0.00**	152.0	317.9	**0.00**
Isobutanal	128.3	228.2	**0.00**	131.2	318.2	**0.00**
Butanal	312.0	521.2	**0.01**	220.4	816.8	**0.00**
Butan-2-one	629.5	823.0	**0.02**	329.3	934.3	**0.00**
Isopentanal	241.1	432.2	**0.00**	221.5	548.9	**0.00**
Butan-2,3-dione	310.8	635.4	**0.00**	312.9	753.9	**0.00**

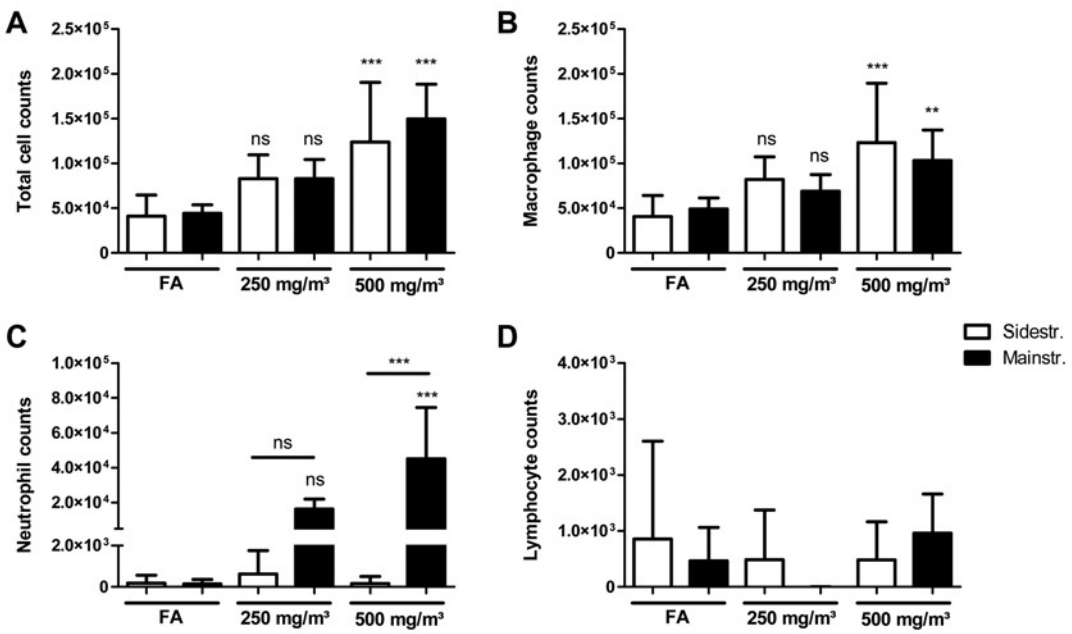

Figure 2 **Characterization of BAL inflammation after acute smoke exposure reveals lack of neutrophilic influx in sidestream CS-exposed mice**
The lungs of mice exposed to CS for 3 days were lavaged with 4×0.5 ml aliquots of sterile PBS. Total cell counts were determined in a haemocytometer via Trypan Blue exclusion. Differential cell counts were performed using morphological criteria on May–Grünwald-Giemsa–stained cytospins (200 cells/sample). (**A**) Total cell counts. (**B**) Macrophages. (**C**) Neutrophils. (**D**) Lymphocytes. Results are means ± S.D., one-way ANOVA following Bonferroni post-hoc test. $^{**}P < 0.01$ and $^{***}P < 0.001$; FA, filter air; $n = 12$. ns, not significant.

41 071 ± 23 579 in controls to 83 000 ± 26 609 in 250 mg/m³ TPM and to 123 889 ± 66 628 in 500 mg/m³ TPM respectively. Macrophage numbers increased from 40 657 ± 23 659 in controls to 81 881 ± 25 488 in 250 mg/m³ TPM and to 123 240 ± 66 195 in 500 mg/m³ TPM. BAL neutrophils remained unchanged after exposure to both sidestream CS concentrations (Figure 2C), leading to a significant difference in neutrophil cell counts between animals exposed to 500 mg/m³ mainstream CS compared with 500 mg/m³ sidestream CS.

As expected, lymphocyte numbers did not show any increase in both models compared with filtered air control animals (Figure 2D), confirming previous findings of two phases of inflammatory responses, with elevated lymphocyte levels starting after 1 month of CS exposure [12–14].

In sum, these results demonstrate that: (i) the CS concentration in the exposure chamber determines inflammatory cell recruitment to the alveolar lumen; and (ii) after sidestream CS exposure, a neutrophilic influx is not detectable.

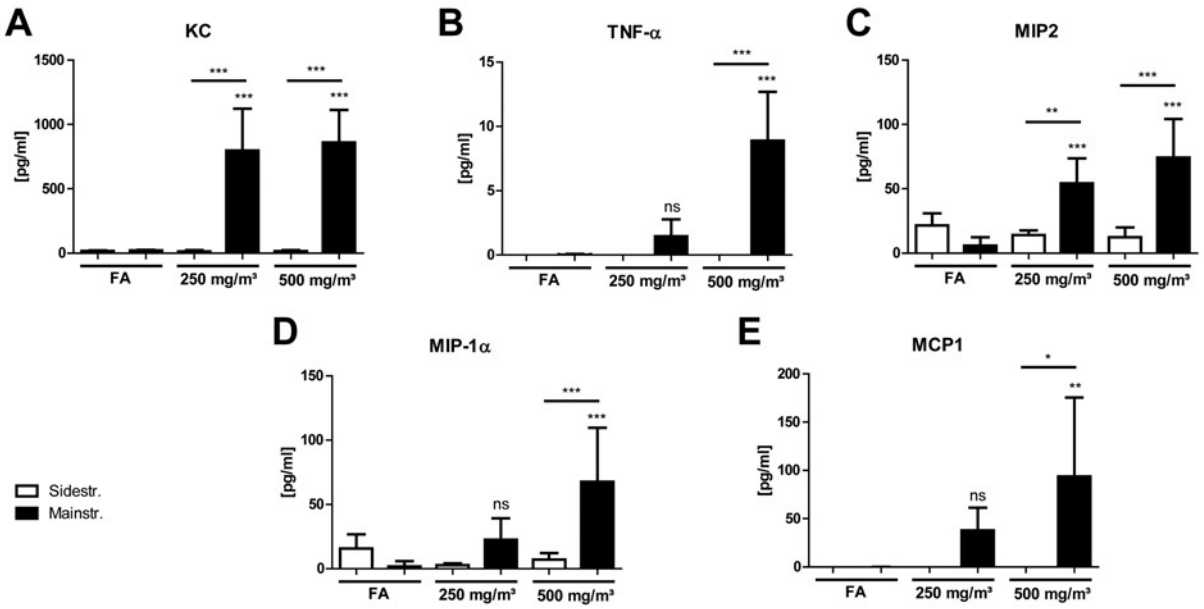

Figure 3 BAL inflammatory cytokine secretion after acute smoke exposure is only increased in mainstream CS-exposed mice

Concentrations of secreted cytokines KC (**A**), TNF-α (**B**), MIP-2 (**C**), MIP-1α (**D**) and MCP1 (**E**) in BAL after 3 days of CS exposure were determined using a magnetic bead-based multiplex assay. For this assay, BAL fluid was concentrated (10×) by ultrafiltration in centrifugal filter devices. Results are means ± S.D., one-way ANOVA following Bonferroni post-hoc test. $*P < 0.05$, $**P < 0.01$ and $***P < 0.001$; FA, filter air; $n = 12$. ns, not significant.

BAL inflammatory cytokines and chemokines are only increased after mainstream CS exposure

The secretion of a broad variety of inflammatory cytokines and chemokines into the airway lumen was analysed by sampling BAL fluid via a magnetic bead-based multiplex assay.

Significantly up-regulated inflammatory mediators were only observed in BAL of mice exposed to mainstream CS compared with filtered air controls (Figure 3). Specifically, KC (CXCL1), TNF-α, MCP-1 (CCL2), MIP2 (CXCL2) and MIP-1α (CCL3), all of which are involved in innate immune cell activation and recruitment, were detected and found to be induced predominantly by the higher CS concentration of 500 mg/m^3 TPM. In the sidestream model, no up-regulation was seen for any of the cytokines analysed in BAL as well as in the lung tissue homogenates (results not shown) of CS-exposed mice, explaining the significant differences in cell recruitment observed between animals exposed to mainstream CS compared with sidestream CS.

These results indicate a strong acute inflammatory response in the mainstream CS model, whereas there is no increased cytokine secretion after sidestream exposure for the markers analysed.

Lung tissue inflammation is more prominent in mainstream CS-exposed mice

Lung tissue inflammation was further investigated by analysing mRNA expression levels of inflammatory target genes KC (CXCL1), TNF-α, MIP2 (CXCL2), MMP12 and CD68 in homogenized lung tissue.

In the mainstream CS model, mRNA levels for KC (CXCL1), MIP2 (CXCL2) and MMP12 were significantly increased after exposure of mice to CS concentrations of 250 and 500 mg/m^3 TPM compared with control animals (Figures 4A, 4C and 4D). Interestingly, CD68 only showed elevated mRNA expression after CS exposure to 250 mg/m^3 TPM (Figure 4E), whereas TNF-α did not increase at both concentrations (Figure 4B).

Mice exposed to sidestream CS also exhibited higher KC mRNA levels for both CS concentrations compared with control animals (Figure 4A). In contrast with the mainstream model, TNF-α showed elevated mRNA expression after CS exposure to 500 mg/m^3 TPM (Figure 4B). However, MIP2 (CXCL2), MMP12 and CD68 did not increase at both concentrations (Figures 4C–4E). Significant differences in mRNA levels between animals exposed to mainstream CS compared with sidestream CS were observed for KC, MIP2 (CXCL2), MMP12 and CD68, mostly at higher CS concentrations of 500 mg/m^3 TPM.

These results demonstrate that the strong acute inflammation observed in BAL (with increases in inflammatory cell recruitment and cytokine/chemokine secretion) after mainstream CS exposure was concomitant with increases in mRNA expression levels of inflammatory marker genes in lung tissue.

Despite the findings of elevated mRNA expression of several proinflammatory genes, H&E staining of lung tissue from both models revealed only marginal inflammatory cell infiltrates after sidestream exposure to a CS concentration of 500 mg/m^3 TPM (Figure 5). Furthermore, we did not observe any differences in lung function between control animals and CS-exposed mice from both exposure models (results not shown).

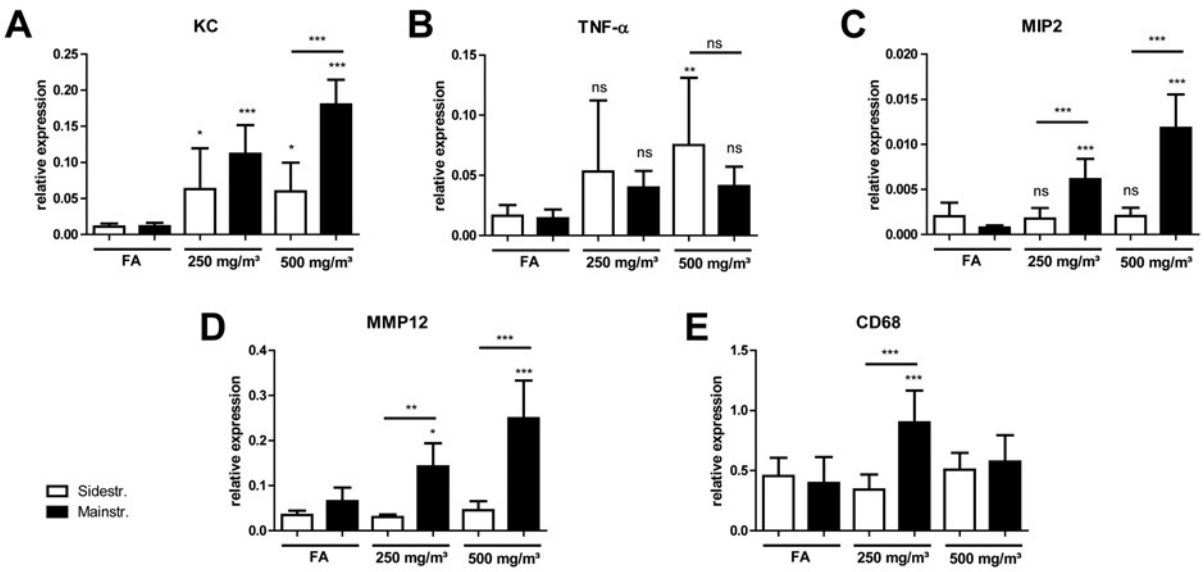

Figure 4 **Gene expression profile in lung tissue after acute smoke exposure shows more prominent inflammation in mainstream CS-exposed mice**

mRNA expression levels of target genes KC (**A**), TNF-α (**B**), MIP-2 (**C**), MMP12 (**D**) and CD68 (**E**) in comparison with housekeeping control HPRT-1 were determined via quantitative real-time PCR using cDNA synthesized from lung tissue homogenate. Primers used are listed in Table 1. Relative mRNA expression of a gene is given as $2^{-\Delta C_t}$ ($\Delta C_t = C_{t_{target}} - C_{t_{reference}}$), relative changes compared with control are $2^{-\Delta\Delta C_t}$ values ($\Delta\Delta C_t = \Delta C_{t_{treated}} - \Delta C_{t_{control}}$). Results are means $\pm$ S.D., one-way ANOVA following Bonferroni post-hoc test. $^*P < 0.05$, $^{**}P < 0.01$ and $^{***}P < 0.001$; $n = 12$. FA, filter air; $n = 12$. ns, not significant.

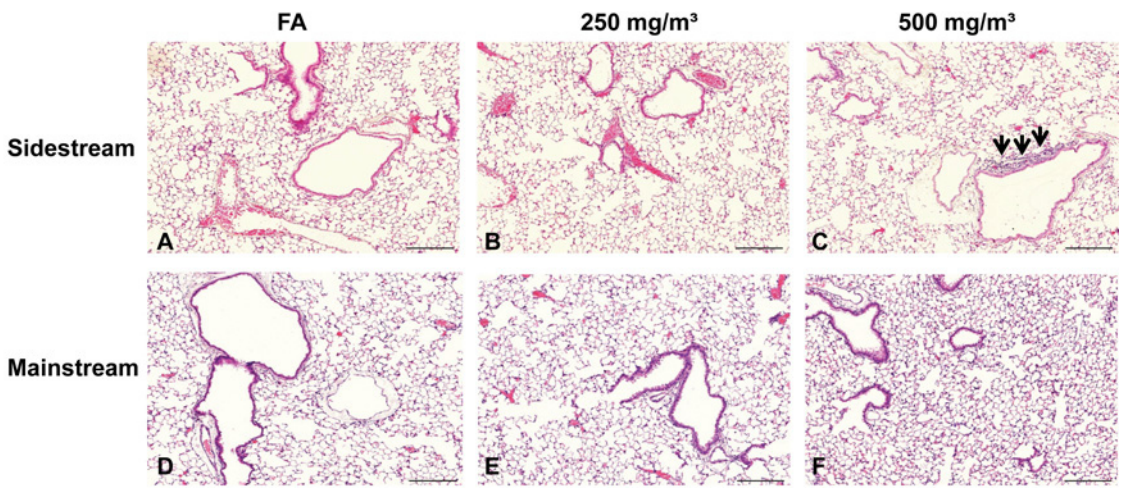

Figure 5 **HE staining of lung tissue slides from mice exposed to filter air (A and D), sidestream (B and C) and mainstream (E and F) CS**

Exemplary micrographs revealed marginal inflammatory cell infiltrates after sidestream exposure to a CS concentration of 500 mg/m^3 TPM (black arrows). Magnification 20×, scale bar 200 μm. FA, filter air.

Sidestream CS exposure leads to higher CO concentrations in the exposure chamber

CO, a gas derived from partial, i.e. incomplete, oxidation of carbon-containing compounds, is not only known to have toxic effects [35], but has revealed an important biological activity as a signalling molecule with protective actions against apoptosis and endothelial oxidative damage [36]. Therefore CO concentrations in the exposure chamber were constantly monitored during smoke exposure using a CO meter.

Mainstream CS of 250 and 500 mg/m^3 TPM caused CO concentrations of 266 ± 42 and 288 ± 74 ppm, respectively (Figure 6A). On the other hand, sidestream CS exposure led to significantly higher CO levels in the exposure chamber compared with mainstream CS, with 563 ± 119 ppm for 250 mg/m^3 TPM and 1008 ± 49 ppm for 500 mg/m^3 TPM.

To determine the effects of CO levels on mice in the exposure chamber, arterial blood CO-Hb was measured in a subgroup of mice ($n = 4$), 30 min after the last exposure. All mice tolerated

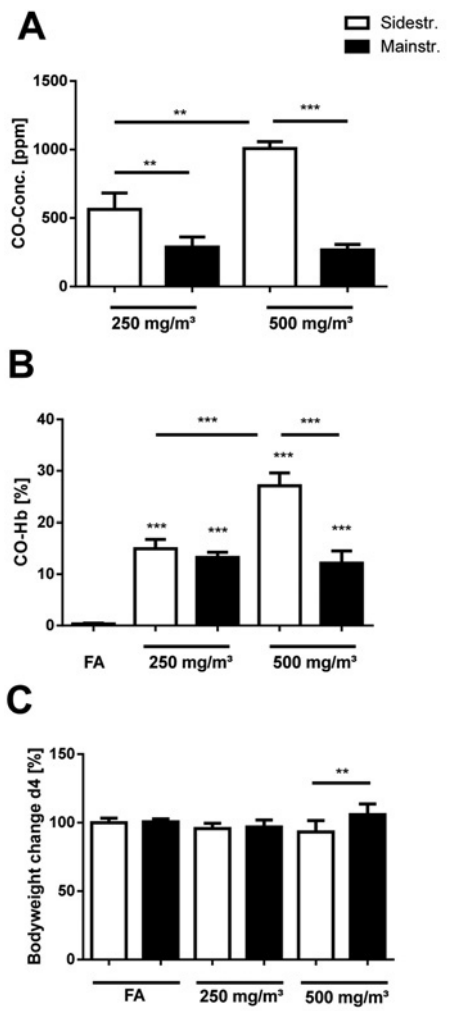

Figure 6 CO concentrations in the exposure chamber, levels of arterial blood CO–Hb and body weight changes in mice after acute smoke exposure

(**A**) CO concentrations in the exposure chamber were monitored by using a GCO 100 CO Meter ($n = 4$ measurements during one exposure cycle). (**B**) Levels of arterial blood CO-Hb in a subgroup of mice ($n = 4$) 30 min after CS exposure were determined by retro-orbital blood sampling and analysed in an ABL80 FLEX blood gas analyser. (**C**) Body weight changes of CS-exposed mice on day of analysis (day 4); $n = 12$. Results are means $\pm$ S.D., one-way ANOVA following Bonferroni post-hoc test. $^{**}P < 0.01$ and $^{***}P < 0.001$. FA, filter air; $n = 12$. ns, not significant.

CS-mediated CO concentrations without any sign of toxicity. In the mainstream model, arterial blood CO-Hb levels in mice exposed to 250 and 500 mg/m^3 TPM increased from control values (0.3 ± 0.2 %) in filtered air animals to 13.2 ± 1.1 and 12.2 ± 2.4 % respectively (Figure 6B). This is consistent with the similar levels of CO observed in the exposure chamber for both concentration levels of mainstream CS. Sidestream CS exposure to 250 mg/m^3 TPM showed 15.0 ± 1.8 % at similar increases in CO-Hb compared with mainstream CS, in spite of almost 2-fold higher CO levels. In contrast, sidestream CS of 500 mg/m^3 TPM was associated with significantly higher CO-Hb levels (27.1 ± 2.5 %) in mice compared with 500 mg/m^3 mainstream CS (12.2 ± 2.4 %).

During the 3 days of smoke exposure, the body weight of all animals was monitored. Compared with controls, mice exposed to either main- or side-stream CS did not show any significant body weight changes during the whole exposure period (results not shown). However, a significant body weight difference (normalized to weight of each group on day 1) between animals exposed to 500 mg/m^3 TPM of mainstream and sidestream CS was observed on the day of animal preparation (day 4), 24 h after the last CS exposure (Figure 6C), at 105.9 ± 7.7 % (mainstream) compared with 93.2 ± 8.4 % (sidestream).

These results demonstrate that sidestream CS exposure is associated with increased CO concentrations in the exposure chamber, thereby inducing elevated CO-Hb levels and body weight changes in mice especially for the CS concentration of 500 mg/m^3.

GM-CSF is only up-regulated in BAL and lung tissue of mainstream CS-exposed mice

Previous studies have described a role for GM-CSF in CS-induced pulmonary inflammation [37], and decreased GM-CSF production following CO exposure was observed in LPS (lipopolysaccharide)-stimulated macrophages [38]. Therefore mRNA and protein levels of GM-CSF in lung tissue and BALs were determined in the present study.

mRNA expression levels of GM-CSF did not increase in sidestream CS-exposed mice, whereas the mainstream model shows a significant up-regulation for both CS concentrations (Figure 7A). The same was observed for secreted GM-CSF analysed in BAL of CS-exposed mice (Figure 7B), confirming the important role for GM-CSF in inflammatory cell recruitment in response to CS and its potential inhibition by CO.

DISCUSSION

The present study aimed at investigating the composition of CS and the acute inflammatory response in the lungs of mice using two different experimental models of CS exposure for 3 days. The results presented here demonstrate that the composition of CS (TPM and CO concentration, chemical composition and size distribution of PM) determines the dynamics of inflammatory cell recruitment to the mouse lung.

CS is a toxic collection of more than 4800 chemicals and exceptionally rich in oxidants both in the gaseous and particle phases [39,40]. It is the major risk factor for cardiovascular diseases, atherosclerosis and lung diseases such as COPD and cancer. COPD is a disease characterized by airflow limitation caused by severe pathophysiological changes including chronic bronchitis, small airway remodelling, mucus production and the development of emphysaema [2]. In order to recapitulate these changes observed in patients suffering from COPD, CS-induced animal models are commonly used in laboratories around the world. Acute CS exposure has enabled researchers to study early and direct effects of smoking on inflammatory responses and cell recruitment, specifically innate immune cells and oxidative stress in the lung [20–22,24].

It is now generally accepted that the inflammatory response plays a major role in driving the pathophysiological changes

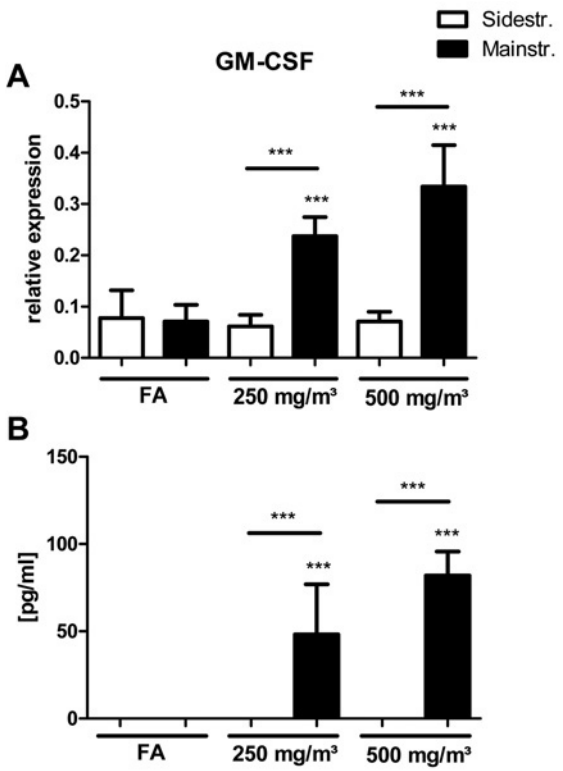

Figure 7 GM-CSF expression and secretion after acute smoke exposure is only up-regulated in lung tissue and BAL of mainstream CS-exposed mice

(**A**) mRNA expression levels of GM-CSF in comparison with housekeeping control HPRT-1 were determined via quantitative real-time PCR using cDNA synthesized from lung tissue homogenate. Primers used are listed in Table 1. Relative mRNA expression is given as $2^{-\Delta C_t}$ ($\Delta C_t = C_{t_{target}} - C_{t_{reference}}$), relative changes compared with control are $2^{-\Delta\Delta C_t}$ values ($\Delta\Delta C_t = \Delta C_{t_{treated}} - \Delta C_{t_{control}}$). (**B**) Concentrations of secreted GM-CSF in BAL after 3 days of CS exposure were determined using a magnetic bead-based multiplex assay. For this assay, BAL fluid was concentrated (10×) by ultrafiltration in centrifugal filter devices. Results are means ± S.D., one-way ANOVA following Bonferroni post-hoc test. ***$P < 0.001$. FA, filter air; $n = 12$. ns, not significant.

observed in COPD [15,16]. Identical to observations in humans, CS constantly induces a neutrophil and macrophage inflammatory response in the lower respiratory tract of exposed animals (reviewed in [11,41]), and the acute reaction during the first week of CS exposure is dominated by a strong neutrophilic influx [12–14].

All studies looking at the dynamics of early lung immune cell reactions to CS used the mainstream model in acute settings of smoke exposure for a few days. In accordance with these studies, a strong acute inflammatory response characterized by neutrophilic influx, increased cytokine secretion (KC, TNF-α, MIP-2, MIP-1α and MCP1), proinflammatory gene expression (KC, MIP-2 and MMP12) and up-regulated GM-CSF production was observed in the mainstream CS model.

In contrast, only one study ever utilized the sidestream model in an acute setting, but did not focus on lung inflammation [24]. Howard et al. [24] investigated oxidative DNA damage via analysis of 8-OHdG (8-hydroxy-2′-deoxyguanosine) in mouse heart, liver and lung tissue and detected increased levels already after a single CS exposure for 30 min. In a chronic setting, Wooduff et al. [42] did not even observe neutrophil recruitment after exposures for 1, 2 and 3 months using the sidestream model, whereas macrophages were increased. Interestingly, the results of the present study show that there was a dampened inflammatory reaction after sidestream exposure, characterized by macrophages and slight increases in TNF-α mRNA expression.

In response to CS, neutrophils and macrophages release cytokines and proteolytic enzymes and generate oxidants, thereby causing tissue damage and perpetuating inflammation and immune reactions [41]. Gene expression profiling also revealed an early up-regulation of stress response and inflammation markers after acute CS exposure [13]. The proteolytic enzymes MMP12 and NE were even required for inducing experimental emphysaema after prolonged exposure [17,18]. CS-exposed MMP12-knockout mice failed to recruit macrophages and did not develop lung destruction [17], whereas NE was necessary for neutrophil and monocyte recruitment as well as for the activation of MMP12 after CS exposure [18].

Several studies characterized the inflammatory response after gradually increasing the exposure time and dose in the acute mainstream model [20–22]. Stevenson et al. [20] described a time- and dose-dependent increase in neutrophil chemokines, specifically CXCR2 ligands in the rat lung, which was mirrored by neutrophil infiltration. The work by Vlahos et al. [21] detected mRNA up-regulation of chemokines such as MIP-2 and MCP1, inflammatory mediators such as TNF-α, the leucocyte growth and survival factor GM-CSF and matrix degrading MMPs 9 and 12. Morris et al [22] confirmed time- and dose-dependent neutrophil increases in four different mouse strains, with highly up-regulated KC and MMP12 levels. The results of the present study also showed an mRNA up-regulation of CXCR2 ligands KC and MIP-2 as well as MMP12 after mainstream CS exposure. An increase in cytokine secretion was observed for KC, TNF-α, MIP-2, MIP-1α and MCP1.

The differences seen between sidestream and mainstream CS could be related to the biologically relevant, i.e. lung deposited PM dose. The observed smaller particle size in sidestream relative to mainstream CS was translated into a difference in the lung deposited dose using *in silico* models for particle deposition in the murine lung [31]. For a given TPM level, the lung-delivered PM dose of sidestream CS was approximately two times higher than for mainstream CS (see Table 2). Despite the enhanced biologically effective dose for sidestream CS conditions, the biological response for a given TPM level was less pronounced compared with the mainstream model. Thus, the pulmonary dose of PM cannot account for the inhibited inflammatory response in the sidestream CS model.

Besides the lung-delivered dose, the chemical composition of CS might influence the observed biological reactions. Mainstream and sidestream CS exhibit differences in the chemical profile, which is particularly related to the different combustion conditions during puffing and smoldering. Therefore the toxicological impact of mainstream and sidestream CS most probably differs as well. Sidestream CS is formed under more oxygen-deficient conditions at lower temperatures compared with mainstream CS. Large differences are obtained for the yields of toxic gaseous compounds such as acrolein, butadiene or benzene and

CO, which are much higher for sidestream CS [43,44]. In addition, sidestream CS is characterized by significantly higher relative concentrations of nitrogen-containing compounds (e.g. ammonia or aniline- and pyridine-derivatives) [44], whereas mainstream CS exhibits higher concentrations of nitric oxide.

In the present study, CS-associated PAHs and alkanes were analysed. PAHs are a product of incomplete combustion as well as pyrolysis processes. Humans are mainly exposed to PAHs via inhalation of aerosols, such as CS particles. Animal testing has shown that many PAHs are potentially carcinogenic as PAH molecules bind to the AH (aromatic hydrocarbon) receptors. The enzymatic degradation yields in phenols and epoxides are caused by cytochrome P-450 dependent oxidases. The epoxy metabolites are partially transferred to dihydrodiol epoxides before excretion. Owing to ring-opening reactions, these epoxy derivatives can bind to DNA bases [45]. The knowledge of acute toxicity is sparse, but chronic health effects are to be expected, including lung, immune and reproduction toxicity. Furthermore, the total amount of alkanes far beyond 1 mg/m^3 can cause irritations of the respiratory tract. The concentrations of *n*-alkanes and iso- and anteiso-alkanes in the 500 mg/m^3 sidestream CS samples (0.75–8.53 ng/m^3) were higher than those measured in 250 mg/m^3 sidestream CS samples (0.77–1.51 ng/m^3). Therefore differences in PM composition depending on the TPM level are expected. However, alkane as well as PAH concentrations only increased with higher TPM levels of sidestream CS, indicating the typically lower combustion temperatures and subsequently less complete combustion in sidestream CS conditions [44].

Sidestream CS of 250 mg/m^3 and 500 mg/m^3 TPM contained 3.4-fold and 7.2-fold higher PAH levels than mainstream CS respectively. The observed high concentrations of PAHs in sidestream CS indicate that high amounts of PAHs are formed during the smoldering phase of cigarette smoking when no puff is made [44]. In contrast with sidestream CS, the availability of oxygen and high temperatures during a puff of mainstream CS results in a more complete combustion of organic compounds yielding lower concentrations of PAHs. These results show the importance of sidestream CS for public health implications. However, the higher concentrations of PAHs and alkanes in sidestream CS were not reflected in enhanced biological responses in our model, suggesting a significant role of gas-phase components especially for sidestream CS.

CCs are important gaseous constituents of CS and some are toxic and carcinogenic or mutagenic to humans. They are highly reactive towards nucleophilic molecules in the cell such as DNA, proteins, aminophospholipids and glutathione and thereby contribute to the development of smoking related diseases [46,47]. The findings of the present study are in line with previous observations that higher concentrations for CCs such as acetaldehyde, acrolein, methacrolein and crotonaldehyde in the sidestream model might be caused by the incomplete combustion of sidestream CS as already described above.

Acrolein was described as effective in eliciting IL-8 release in pulmonary cells thereby contributing to neutrophil chemotaxis and activation [48,49]. Despite the higher production of acrolein in sidestream CS, we did not detect any appreciable level of neutrophils. Notably, this unresponsiveness needs further analysis. However, the dampened inflammatory response observed in the sidestream model might be related to elevated CO concentrations in the exposure chamber resulting in significantly higher levels of arterial blood CO-Hb in CS-exposed mice at 500 mg/m^3 TPM compared with mainstream CS. Recent reviews pointed out the anti-inflammatory effects of CO in a multitude of *in vitro* studies and animal models of inflammation, indicating a therapeutic potential [36,50]. Besides its known toxic effects, CO has revealed an important biological function by protecting against apoptosis and endothelial oxidative damage. Recently, CO was shown to mediate anti-apoptotic effects of HO (haem oxygenase)-1, an isoform of the enzyme HO involved in the oxidative degradation of haem [51]. Moreover, CO as one of the three main byproducts of the catabolism of haem by HO altered iron homoeostasis in the lung thereby reducing oxidative stress and proliferation of bronchial epithelial cells [52].

An important study recently showed a protective effect of inhaled CO during pulmonary inflammation after LPS challenge [53]. CO administered to mice both before and after intratracheal instillation of LPS was effective in reducing neutrophil recruitment to the lung due to decreased bone marrow mobilization of leucocytes. The authors speculated that the effect on neutrophil mobilization occurred via decreased production of GM-CSF following CO exposure. This mechanism was already described in LPS-stimulated murine macrophages [38]. HO-1 overexpression as well as CO exposure inhibited LPS-induced GM-CSF production in macrophages via NF-κB (nuclear factor κB) inhibition, with NF-κB as the transcriptional regulator of GM-CSF.

As shown in Figure 7 GM-CSF levels for the sidestream CS model are significantly lower than for the mainstream model. GM-CSF might have an important role in CS-related lung diseases because it functions as a leucocyte growth, activation and survival factor [54]. It promotes proliferation and differentiation of haematopoietic progenitors into neutrophils and macrophages and is produced by many structural and inflammatory cells. Furthermore, GM-CSF acts as a direct neutrophil chemotactic factor and may increase neutrophil survival in the respiratory tract [55,56]. Vlahos et al. [37] demonstrated that neutralizing GM-CSF inhibited CS-induced lung inflammation by reducing BAL neutrophils and macrophages as well as TNF-α, MIP-2 and MMP12 mRNA expression. Possible mechanisms in this context were increased apoptosis of neutrophils and macrophages, because it was already shown that GM-CSF inhibits neutrophil apoptosis [57]. Furthermore, the effects of anti-GM-CSF treatment on MIP-2, another potent neutrophil chemotactic factor, could also account for the inhibited inflammation. The contribution of CXCR2-mediated signalling to CS-induced lung inflammation characterized by neutrophil influx was determined by treatment of mice with an inhibitor of CXCR2 [58]. A further study blocking GM-CSF receptor also described attenuated neutrophil influx in CS-exposed mice [59], confirming the major role of GM-CSF in CS-induced pulmonary inflammation.

Thus, the results of the present study are consistent with the hypothesis that in the sidestream CS model, high levels of CO and subsequently higher levels of arterial blood CO-Hb led to inhibited production and release of GM-CSF and CXCR2

ligands KC and MIP-2. However, despite the lack of difference in CO-Hb at 250 mg/m^3 between the two models a largely different inflammatory response was observed. This might also point to effects of other gas phase components aside from CO that could significantly alter the inflammatory response in the lung. However, despite the findings of a dampened inflammatory response, it must be noted that inhaled fresh sidestream CS is approximately four times more toxic per gram TPM than mainstream CS [23]. In animals exposed to whole sidestream CS, sensory irritation and respiratory tract epithelium damage increases with longer exposures. However, the results of the present study show that the enhanced toxicity of TPM from sidestream CS was rather repressed by the gas-phase effects.

In summary, we demonstrated that significant differences exist between two mouse models of acute smoke exposure. Mainstream CS induced a strong acute inflammatory response and led to increased levels of neutrophils and related proinflammatory markers. In contrast, sidestream CS exposure only caused a dampened inflammatory reaction, with slightly elevated macrophage numbers. The different responses between the two models were most probably related to elevated CO concentrations, which inhibited early inflammatory responses in the sidestream CS model. The COPD mouse models for acute mainstream and sidestream CS exposure (i.e. also environmental CS) described in the present study are potentially interesting for evaluating the toxicological and health effects of other aerosol sources, such as emissions from house heating (e.g. wood stoves) or traffic-sources (e.g. trucks, cars or ships).

We conclude that a detailed analysis of physico-chemical and biological data generated from acute CS models can provide important information for potential therapeutic interventions at early stages of smoke exposure.

CLINICAL PERSPECTIVES

- Initial inflammatory processes might contribute to COPD pathogenesis at an early stage of smoke exposure, but different animal CS exposure systems have been established and employed in acute and chronic COPD studies. In order to elucidate potential differences between mainstream and sidestream CS exposure, we investigated the CS composition and the acute inflammatory response in the lungs of mice after 3 days of CS exposure.
- We observed a strong acute inflammatory response characterized by neutrophilic influx, increased cytokine secretion and proinflammatory gene expression, and up-regulated GM-CSF production in the mainstream CS model, whereas there was a dampened inflammatory reaction after sidestream exposure, most probably caused by elevated CO concentrations.
- This comparison might be useful for the interpretation of data from the various CS mouse models and will potentially impact on therapeutic intervention studies starting at the early stages of smoke exposure.

AUTHOR CONTRIBUTION

Gerrit John, Katrin Kohse, Oliver Eickelberg and Ali Önder Yildirim designed experiments; Gerrit John, Katrin Kohse, Jürgen Orasche, Ahmed Reda, Jürgen Schnelle-Kreis, Ralf Zimmermann and Otmar Schmid conducted experiments; Gerrit John, Otmar Schmid and Ali Önder Yildirim wrote the paper; and all authors contributed to scientific discussions and read the paper.

ACKNOWLEDGEMENTS

We acknowledge the help of Bernd Lentner, Gunter Eder, Andreas Schröppel, Christine Hollauer, Theodora Astalaki and Marina Fischer.

FUNDING

This work was supported by a European Respiratory Society Fellowship [grant number LTRF MC1520-2010 (to G.J.)].

REFERENCES

1 Vestbo, J., Hurd, S. S., Agusti, A. G., Jones, P. W., Vogelmeier, C., Anzueto, A., Barnes, P. J., Fabbri, L. M., Martinez, F. J., Nishimura, M. et al. (2012) Global strategy for the diagnosis, management and prevention of chronic obstructive pulmonary disease, GOLD executive summary. Am. J. Respir. Crit. Care Med. **187**, 347–365

2 Pauwels, R. A., Buist, A. S., Calverley, P. M., Jenkins, C. R. and Hurd, S. S. (2001) Global strategy for the diagnosis, management, and prevention of chronic obstructive pulmonary disease. NHLBI/WHO Global Initiative for Chronic Obstructive Lung Disease (GOLD) Workshop summary. Am. J. Respir. Crit. Care Med. **163**, 1256–1276

3 Thun, M. J., Carter, B. D., Feskanich, D., Freedman, N. D., Prentice, R., Lopez, A. D., Hartge, P. and Gapstur, S. M. (2013) 50-Year Trends in Smoking-Related Mortality in the United States. N. Engl. J. Med. **368**, 351–364

4 Baker, R. R. and Proctor, C. J. (1990) The origins and properties of environmental tobacco smoke. Environ. Int. **16**, 231–245

5 Hogg, J. C. (2004) Pathophysiology of airflow limitation in chronic obstructive pulmonary disease. Lancet **364**, 709–721

6 Saetta, M., Turato, G., Facchini, F. M., Corbino, L., Lucchini, R. E., Casoni, G., Maestrelli, P., Mapp, C. E., Ciaccia, A. and Fabbri, L. M. (1997) Inflammatory cells in the bronchial glands of smokers with chronic bronchitis. Am. J. Respir. Crit. Care Med. **156**, 1633–1639

7 Saetta, M., Di Stefano, A., Turato, G., Facchini, F. M., Corbino, L., Mapp, C. E., Maestrelli, P., Ciaccia, A. and Fabbri, L. M. (1998) CD8$^+$ T-lymphocytes in peripheral airways of smokers with chronic obstructive pulmonary disease. Am. J. Respir. Crit. Care Med. **157**, 822–826

8 van der Strate, B. W., Postma, D. S., Brandsma, C. A., Melgert, B. N., Luinge, M. A., Geerlings, M., Hylkema, M. N., van den Berg, A., Timens, W. and Kerstjens, H. A. (2006) Cigarette smoke-induced emphysema: a role for the B cell? Am. J. Respir. Crit. Care Med. **173**, 751–758

9 Gosman, M. M., Willemse, B. W., Jansen, D. F., Lapperre, T. S., van Schadewijk, A., Hiemstra, P. S., Postma, D. S., Timens, W., Kerstjens, H. A., Groningen and Leiden Universities Corticosteroids in Obstructive Lung Disease Study (2006) Increased number of B-cells in bronchial biopsies in COPD. Eur. Respir. J. (2006) **27** 60–64

10 Hogg, J. C., Chu, F., Utokaparch, S., Woods, R., Elliott, W. M., Buzatu, L., Cherniack, R. M., Rogers, R. M., Sciurba, F. C., Coxson, H. O. and Pare, P. D. (2004) The nature of small-airway obstruction in chronic obstructive pulmonary disease. N. Engl. J. Med. **350**, 2645–2653

11 Churg, A., Cosio, M. and Wright, J. L. (2008) Mechanisms of cigarette smoke-induced COPD: insights from animal models. Am. J. Physiol. Lung Cell. Mol. Physiol. **294**, L612–L631
12 D'Hulst A, I., Vermaelen, K. Y., Brusselle, G. G., Joos, G. F. and Pauwels, R. A. (2005) Time course of cigarette smoke-induced pulmonary inflammation in mice. Eur. Respir. J. **26**, 204–213
13 Stevenson, C. S., Docx, C., Webster, R., Battram, C., Hynx, D., Giddings, J., Cooper, P. R., Chakravarty, P., Rahman, I., Marwick, J. A. et al. (2007) Comprehensive gene expression profiling of rat lung reveals distinct acute and chronic responses to cigarette smoke inhalation. Am. J. Physiol. Lung Cell. Mol. Physiol. **293**, L1183–L1193
14 Wan, W. Y., Morris, A., Kinnear, G., Pearce, W., Mok, J., Wyss, D. and Stevenson, C. S. (2010) Pharmacological characterisation of anti-inflammatory compounds in acute and chronic mouse models of cigarette smoke-induced inflammation. Respir. Res. **11**, 126
15 Botelho, F. M., Gaschler, G. J., Kianpour, S., Zavitz, C. C., Trimble, N. J., Nikota, J. K., Bauer, C. M. and Stampfli, M. R. (2010) Innate immune processes are sufficient for driving cigarette smoke-induced inflammation in mice. Am. J. Respir. Cell Mol. Biol. **42**, 394–403
16 D'Hulst A, I., Maes, T., Bracke, K. R., Demedts, I. K., Tournoy, K. G., Joos, G. F. and Brusselle, G. G. (2005) Cigarette smoke-induced pulmonary emphysema in scid-mice. Is the acquired immune system required? Respir. Res. **6**, 147
17 Hautamaki, R. D., Kobayashi, D. K., Senior, R. M. and Shapiro, S. D. (1997) Requirement for macrophage elastase for cigarette smoke-induced emphysema in mice. Science **277**, 2002–2004
18 Shapiro, S. D., Goldstein, N. M., Houghton, A. M., Kobayashi, D. K., Kelley, D. and Belaaouaj, A. (2003) Neutrophil elastase contributes to cigarette smoke-induced emphysema in mice. Am. J. Pathol. **163**, 2329–2335
19 Stevenson, C. S. and Birrell, M. A. (2011) Moving towards a new generation of animal models for asthma and COPD with improved clinical relevance. Pharmacol. Therap. **130**, 93–105
20 Stevenson, C. S., Coote, K., Webster, R., Johnston, H., Atherton, H. C., Nicholls, A., Giddings, J., Sugar, R., Jackson, A., Press, N. J. et al. (2005) Characterization of cigarette smoke-induced inflammatory and mucus hypersecretory changes in rat lung and the role of CXCR2 ligands in mediating this effect. Am. J. Physiol. Lung Cell. Mol. Physiol. **288**, L514–L522
21 Vlahos, R., Bozinovski, S., Jones, J. E., Powell, J., Gras, J., Lilja, A., Hansen, M. J., Gualano, R. C., Irving, L. and Anderson, G. P. (2006) Differential protease, innate immunity, and NF-κB induction profiles during lung inflammation induced by subchronic cigarette smoke exposure in mice. Am. J. Physiol. Lung Cell. Mol. Physiol. **290**, L931–L945
22 Morris, A., Kinnear, G., Wan, W. Y., Wyss, D., Bahra, P. and Stevenson, C. S. (2008) Comparison of cigarette smoke-induced acute inflammation in multiple strains of mice and the effect of a matrix metalloproteinase inhibitor on these responses. J. Pharmacol. Exp. Ther. **327**, 851–862
23 Schick, S. and Glantz, S. (2005) Philip Morris toxicological experiments with fresh sidestream smoke: more toxic than mainstream smoke. Tob. Control **14**, 396–404
24 Howard, D. J., Briggs, L. A. and Pritsos, C. A. (1998) Oxidative DNA damage in mouse heart, liver, and lung tissue due to acute side-stream tobacco smoke exposure. Arch. Biochem. Biophys. **352**, 293–297
25 Eltom, S., Stevenson, C. S., Rastrick, J., Dale, N., Raemdonck, K., Wong, S., Catley, M. C., Belvisi, M. G. and Birrell, M. A. (2011) P2$\times$7 receptor and caspase 1 activation are central to airway inflammation observed after exposure to tobacco smoke. PLoS ONE **6**, e24097
26 Kinney, P. D., Pui, D. Y. H., Mulholland, G. W. and Bryner, N. P. (1991) Use of the electrostatic classification method to size 0.1 μm SRM particles. J. Res.Natl. Inst. Stand. Technol. **96**, 147–176
27 Schmid, O., Trueblood, M. B., Gregg, N., Hagen, D. E. and Whitefield, P. D. (2002) Sizing of aerosol in gases other than air using a differential mobility analyzer. Aerosol. Sci. Tech. **36**, 351–360
28 Hinds, W. C. (1999) Aerosol Technology, Wiley-Interscience Publications, New York
29 Orasche, J., Schnelle-Kreis, J., Abbaszade, G. and Zimmermann, R. (2011) Technical note: *in-situ* derivatization thermal desorption GC-TOFMS for direct analysis of particle-bound non-polar and polar organic species. Atmos. Chem. Phys. **11**, 8977–8993
30 Ye, J., Coulouris, G., Zaretskaya, I., Cutcutache, I., Rozen, S. and Madden, T. L. (2012) Primer-BLAST: a tool to design target-specific primers for polymerase chain reaction. BMC Bioinf. **13**, 134
31 Nadithe, V., Rahamatalla, M., Finlay, W. H., Mercer, J. R. and Samuel, J. (2003) Evaluation of nose-only aerosol inhalation chamber and comparison of experimental results with mathematical simulation of aerosol deposition in mouse lungs. J. Pharmaceutical Sci. **92**, 1066–1076
32 Rogge, W. F., Hildemann, L. M., Mazurek, M. A., Cass, G. R. and Simoneit, B. R. (1994) Sources of fine organic aerosol. 6. Cigaret smoke in the urban atmosphere. Environ. Sci. Technol. **28**, 1375–1388
33 Talhout, R., Opperhuizen, A. and van Amsterdam, J. G. (2007) Role of acetaldehyde in tobacco smoke addiction. Eur. Neuropsychopharmacol. **17**, 627–636
34 Seeman, J. I., Dixon, M. and Haussmann, H. J. (2002) Acetaldehyde in mainstream tobacco smoke: formation and occurrence in smoke and bioavailability in the smoker. Chem. Res. Toxicol. **15**, 1331–1350
35 Prockop, L. D. and Chichkova, R. I. (2007) Carbon monoxide intoxication: an updated review. J. Neurol. Sci. **262**, 122–130
36 Rochette, L., Cottin, Y., Zeller, M. and Vergely, C. (2013) Carbon monoxide: mechanisms of action and potential clinical implications. Pharmacol. Therap. **137**, 133–152
37 Vlahos, R., Bozinovski, S., Chan, S. P., Ivanov, S., Linden, A., Hamilton, J. A. and Anderson, G. P. (2010) Neutralizing granulocyte/macrophage colony-stimulating factor inhibits cigarette smoke-induced lung inflammation. Am. J. Respir. Crit. Care Med. **182**, 34–40
38 Sarady, J. K., Otterbein, S. L., Liu, F., Otterbein, L. E. and Choi, A. M. (2002) Carbon monoxide modulates endotoxin-induced production of granulocyte macrophage colony-stimulating factor in macrophages. Am. J. Respir. Cell Mol. Biol. **27**, 739–745
39 Takahashi, Y., Horiyama, S., Honda, C., Suwa, K., Nakamura, K., Kunitomo, M., Shimma, S., Toyoda, M., Sato, H., Shizuma, M. and Takayama, M. (2013) A chemical approach to searching for bioactive ingredients in cigarette smoke. Chem. Pharm. Bull. **61**, 85–89
40 Cantin, A. M. (2010) Cellular response to cigarette smoke and oxidants: adapting to survive. Proc. Am. Thorac. Soc. **7**, 368–375
41 Tetley, T. D. (2005) Inflammatory cells and chronic obstructive pulmonary disease. Curr. Drug Targets: Inflammation Allergy **4**, 607–618
42 Woodruff, P. G., Ellwanger, A., Solon, M., Cambier, C. J., Pinkerton, K. E. and Koth, L. L. (2009) Alveolar macrophage recruitment and activation by chronic second hand smoke exposure in mice. COPD **6**, 86–94
43 Brunnemann, K. D., Kagan, M. R., Cox, J. E. and Hoffmann, D. (1990) Analysis of 1,3–butadiene and other selected gas-phase components in cigarette mainstream and sidestream smoke by gas chromatography-mass selective detection. Carcinogenesis **11**, 1863–1868

44 Streibel, T., Mitschke, S., Adam, T. and Zimmermann, R. (2013) Time-resolved analysis of the emission of sidestream smoke (SSS) from cigarettes during smoking by photo ionisation/time-of-flight mass spectrometry (PI-TOFMS): towards a better description of environmental tobacco smoke. Anal. Bioanal. Chem. **405**, 7071–7082

45 Weis, L. M., Rummel, A. M., Masten, S. J., Trosko, J. E. and Upham, B. L. (1998) Bay or baylike regions of polycyclic aromatic hydrocarbons were potent inhibitors of Gap junctional intercellular communication. Environ. Health Perspect. **106**, 17–22

46 Freeman, T. L., Haver, A., Duryee, M. J., Tuma, D. J., Klassen, L. W., Hamel, F. G., White, R. L., Rennard, S. I. and Thiele, G. M. (2005) Aldehydes in cigarette smoke react with the lipid peroxidation product malonaldehyde to form fluorescent protein adducts on lysines. Chem. Res. Toxicol. **18**, 817–824

47 Berry, K. A., Henson, P. M. and Murphy, R. C. (2008) Effects of acrolein on leukotriene biosynthesis in human neutrophils. Chem. Res. Toxicol. **21**, 2424–2432

48 Moretto, N., Facchinetti, F., Southworth, T., Civelli, M., Singh, D. and Patacchini, R. (2009) α,β-Unsaturated aldehydes contained in cigarette smoke elicit IL-8 release in pulmonary cells through mitogen-activated protein kinases. Am. J. Physiol. Lung Cell. Mol. Physiol. **296**, L839–L848

49 Moretto, N., Bertolini, S., Iadicicco, C., Marchini, G., Kaur, M., Volpi, G., Patacchini, R., Singh, D. and Facchinetti, F. (2012) Cigarette smoke and its component acrolein augment IL-8/CXCL8 mRNA stability via p38 MAPK/MK2 signaling in human pulmonary cells. Am. J. Physiol. Lung Cell. Mol. Physiol. **303**, L929–L938

50 Naito, Y., Uchiyama, K., Takagi, T. and Yoshikawa, T. (2012) Therapeutic potential of carbon monoxide (CO) for intestinal inflammation. Curr. Med. Chem. **19**, 70–76

51 Al-Owais, M. M., Scragg, J. L., Dallas, M. L., Boycott, H. E., Warburton, P., Chakrabarty, A., Boyle, J. P. and Peers, C. (2012) Carbon monoxide mediates the anti-apoptotic effects of heme oxygenase-1 in medulloblastoma DAOY cells via K^+ channel inhibition. J. Biol. Chem. **287**, 24754–24764

52 Ghio, A. J., Stonehuerner, J. G., Dailey, L. A., Richards, J. H., Madden, M. D., Deng, Z., Nguyen, N. B., Callaghan, K. D., Yang, F. and Piantadosi, C. A. (2008) Carbon monoxide reversibly alters iron homeostasis and respiratory epithelial cell function. Am. J. Respir. Cell Mol. Biol. **38**, 715–723

53 Wilson, M. R., O'Dea, K. P., Dorr, A. D., Yamamoto, H., Goddard, M. E. and Takata, M. (2010) Efficacy and safety of inhaled carbon monoxide during pulmonary inflammation in mice. PLoS ONE **5**, e11565

54 Vlahos, R., Bozinovski, S., Hamilton, J. A. and Anderson, G. P. (2006) Therapeutic potential of treating chronic obstructive pulmonary disease (COPD) by neutralising granulocyte macrophage-colony stimulating factor (GM-CSF). Pharmacol. Therap. **112**, 106–115

55 Gomez-Cambronero, J., Horn, J., Paul, C. C. and Baumann, M. A. (2003) Granulocyte-macrophage colony-stimulating factor is a chemoattractant cytokine for human neutrophils: involvement of the ribosomal p70 S6 kinase signaling pathway. J. Immunol. **171**, 6846–6855

56 Barnes, P. J., Shapiro, S. D. and Pauwels, R. A. (2003) Chronic obstructive pulmonary disease: molecular and cellular mechanisms. Eur. Respir. J. **22**, 672–688

57 Coxon, A., Tang, T. and Mayadas, T. N. (1999) Cytokine-activated endothelial cells delay neutrophil apoptosis *in vitro* and *in vivo*. A role for granulocyte/macrophage colony-stimulating factor. J. Exp. Med. **190**, 923–934

58 Thatcher, T. H., McHugh, N. A., Egan, R. W., Chapman, R. W., Hey, J. A., Turner, C. K., Redonnet, M. R., Seweryniak, K. E., Sime, P. J. and Phipps, R. P. (2005) Role of CXCR2 in cigarette smoke-induced lung inflammation. Am. J. Physiol. Lung Cell. Mol. Physiol. **289**, L322–L328

59 Botelho, F. M., Nikota, J. K., Bauer, C., Davis, N. H., Cohen, E. S., Anderson, I. K., Coyle, A. J., Kolbeck, R., Humbles, A. A., Stampfli, M. R. and Sleeman, M. A. (2011) A mouse GM-CSF receptor antibody attenuates neutrophilia in mice exposed to cigarette smoke. Eur. Respir. J. **38**, 285–294

Received 28 March 2013/18 July 2013; accepted 23 July 2013

Published as Immediate Publication 23 July 2013, doi: 10.1042/CS20130117

5 Cigarette smoke-induced iBALT mediates macrophage activation in a B cell-dependent manner in COPD

Gerrit John-Schuster*

Katrin Hager*

Thomas Conlon

Martin Irmler

Johannes Beckers

Oliver Eickelberg

Ali Önder Yildirim

*authors contributed equally to this publication

Published first in American Journal of Physiology - Lung Cellular and Molecular Physiology

John-Schuster G, Hager K, Conlon TM, Irmler M, Beckers J, Eickelberg O, Yildirim AÖ

Cigarette smoke-induced iBALT mediates macrophage activation in a B cell-dependent manner in COPD.

Am J Physiol Lung Cell Mol Physiol. 2014 Nov 1;307(9):L692-706. doi: 10.1152/ajplung.00092.2014. Epub 2014 Aug 15

Am J Physiol Lung Cell Mol Physiol 307: L692–L706, 2014.
First published August 15, 2014; doi:10.1152/ajplung.00092.2014.

CALL FOR PAPERS: | *Translational Research in Acute Lung Injury and Pulmonary Fibrosis*

Cigarette smoke-induced iBALT mediates macrophage activation in a B cell-dependent manner in COPD

Gerrit John-Schuster,[1]* Katrin Hager,[1]* Thomas M. Conlon,[1] Martin Irmler,[2] Johannes Beckers,[2,3] Oliver Eickelberg,[1,4] and Ali Önder Yildirim[1]

[1]*Comprehensive Pneumology Center, Institute of Lung Biology and Disease, Helmholtz Zentrum München, Member of the German Center for Lung Research, Neuherberg, Germany;* [2]*Institute of Experimental Genetics, Helmholtz Zentrum Muenchen, Neuherberg, Germany;* [3]*Experimental Genetics, Technical University Munich, Freising-Weihenstephan, Germany; and* [4]*Klinikum der Universität München, Munich, Germany*

Submitted 10 April 2014; accepted in final form 6 August 2014

John-Schuster G, Hager K, Conlon TM, Irmler M, Beckers J, Eickelberg O, Yildirim AÖ. Cigarette smoke-induced iBALT mediates macrophage activation in a B cell-dependent manner in COPD. *Am J Physiol Lung Cell Mol Physiol* 307: L692–L706, 2014. First published August 15, 2014; doi:10.1152/ajplung.00092.2014.—Chronic obstructive pulmonary disease (COPD) is characterized by a progressive decline in lung function, caused by exposure to exogenous particles, mainly cigarette smoke (CS). COPD is initiated and perpetuated by an abnormal CS-induced inflammatory response of the lungs, involving both innate and adaptive immunity. Specifically, B cells organized in iBALT structures and macrophages accumulate in the lungs and contribute to CS-induced emphysema, but the mechanisms thereof remain unclear. Here, we demonstrate that B cell-deficient mice are significantly protected against CS-induced emphysema. Chronic CS exposure led to an increased size and number of iBALT structures, and increased lung compliance and mean linear chord length in wild-type (WT) but not in B cell-deficient mice. The increased accumulation of lung resident macrophages around iBALT and in emphysematous alveolar areas in CS-exposed WT mice coincided with upregulated MMP12 expression. In vitro coculture experiments using B cells and macrophages demonstrated that B cell-derived IL-10 drives macrophage activation and MMP12 upregulation, which could be inhibited by an anti-IL-10 antibody. In summary, B cell function in iBALT formation seems necessary for macrophage activation and tissue destruction in CS-induced emphysema and possibly provides a new target for therapeutic intervention in COPD.

COPD; B cells; iBALT; IL-10; macrophages

CHRONIC OBSTRUCTIVE PULMONARY DISEASE (COPD) is a major public health problem and its prevalence as well as morbidity and mortality are still rising worldwide (50, 53). The stimulus of long-term exposure to toxic gases and particles, most often cigarette smoke (CS), induces mucus production, remodeling of small airways, septal tissue damage, and chronic bronchitis (36). These severe pathophysiological changes are the cause for the constant and accelerated decline in lung function observed in patients suffering from COPD. Currently, there is no therapy for COPD and treatment can only aim at alleviating symptoms.

In the lung, chronic CS exposure causes activation and influx of various inflammatory cells, including both innate immune cells, with macrophages and neutrophils predominating, and adaptive immune cells, specifically T and B lymphocytes (2, 20). Their numbers are increased in both airways and parenchyma of patients with COPD (4, 44, 45). Moreover, the progression and severity of COPD are associated with increasing infiltration of the airways by innate and adaptive immune cells, which form ectopic lymphoid follicles (LFs) consisting of B cells surrounded mainly by CD4 T cells (21). Further studies have confirmed that increased B cell numbers are observed in the mucosa of large airways in COPD patients compared with controls (16) and the number of B cell follicles present in the lung also increases with disease severity (52).

Highly organized ectopic LFs are referred to as tertiary lymphoid organs (TLOs) because of their structural similarity to secondary lymphoid organs, which include distinct B and T cell areas, germinal centers, and high endothelial venules (1, 10, 33). TLOs form in various tissues targeted by chronic inflammation and have an important role in maintaining immune responses that can either be harmful or beneficial. They have been associated with local pathogenic autoantibody production (37, 42) or, in respiratory infections and lung cancer, with favorable outcome (14, 17, 34). However, it is still under critical debate whether TLOs in COPD are beneficial or harmful because their role in COPD pathogenesis remains unknown (8, 57).

Lung TLOs, preferentially termed inducible bronchus-associated lymphoid tissue (iBALT), have also been described in in vivo models of COPD. Mice develop LFs after chronic CS exposure (12, 52). Recently, Litsiou et al. (29) discovered that CXCL13 is involved in lymphoid neogenesis in COPD by promoting B cell migration to ectopic sites of lymphoid tissue formation and by upregulating lymphotoxin on B cells, which in turn further induces CXCL13 required for follicle expansion. In CS-exposed mice, administration of an anti-CXCL13 antibody prevents the formation of pulmonary LFs, thereby

* G. John-Schuster and K. Hager made equal contribution to this work.

Address for reprint requests and other correspondence: A. Ö. Yildirim, Comprehensive Pneumology Center, Institute of Lung Biology and Disease, Helmholtz Zentrum München, Member of the German Center for Lung Research, Ingolstädter Landstr. 1, 85764 Neuherberg, Germany (e-mail: oender.yildirim@helmholtz-muenchen.de).

attenuating the destruction of alveolar walls and bronchoalveolar lavage (BAL) inflammation (6).

Aside from their involvement in lymphoid neogenesis and their antibody-producing capacity, B cells can also function as antigen-presenting cells and provide costimulatory signals to T cells (15). Furthermore, the secretion of a variety of cytokines including IL-6 and IL-10 may enable B cells to influence and modulate differentiation and polarization of macrophages, T cells, and dendritic cells during the development of the immune response, thereby regulating immune reactions (23). B cell-mediated modulation of macrophage effector functions via cytokine secretion has been described to be important for the outcome of various models of infection, inflammation, and cancer (3, 32, 56).

In COPD, the role of innate immune cells in CS-induced lung inflammation and subsequent emphysema development has been addressed in several animal studies (5, 12). Macrophage-derived matrix metalloproteinase (MMP) 12 was described as being required for the induction of experimental emphysema after prolonged CS exposure because CS-exposed MMP12 knockout mice failed to recruit macrophages and did not develop lung destruction (7, 18). This finding points to a primary role for macrophages and derived factors in the development of emphysema both in patients and CS-exposed animals. We hypothesized that B cell-dependent iBALT formation is involved in macrophage activation and polarization, thereby inducing and maintaining a severe inflammatory response that drives the pathophysiological changes in COPD. Therefore, we monitored the development of COPD in wild-type (WT) and B cell-deficient knockout mice exposed to CS. We characterized structural and functional changes, iBALT formation, and the inflammatory response occurring in lung tissue. Interestingly, we identified B cell-derived IL-10 as one of the possible key regulators of MMP12 production in macrophages. Thus the responsiveness of B cells to CS induces iBALT formation in the lung, thereby leading to accumulation and activation of matrix-degrading macrophages. This finding could lead to the development of new therapeutic targets for the treatment of COPD patients.

MATERIALS AND METHODS

Animals and maintenance. B cell-deficient B6.129S2-Igh-6^{tm1Cgn} mice (27), also known as μMT mice, and their respective 8- to 10-wk-old pathogen-free female C57BL/6 WT control mice were purchased from Charles River (Sulzfeld, Germany). Animals were housed in rooms maintained at constant temperature and humidity with a 12-h light cycle and were allowed food and water ad libitum. All experiments were conducted under strict governmental and international guidelines and were approved by the local government for the administrative region of Upper Bavaria.

Cigarette smoke exposure. CS was generated from 3R4F Research Cigarettes (Tobacco Research Institute, University of Kentucky, Lexington, KY). Mice were whole body exposed to 100% mainstream CS of 500 mg/m^3 total particulate matter (TPM) for 50 min twice per day for 1, 4, and 6 mo in a manner mimicking natural human smoking habits (24). Control mice were kept in a filtered air (FA) environment, but exposed to the same stress as CS-exposed animals. At 24 h after the last CS exposure, mice were euthanized.

The TPM level was monitored via gravimetric analysis of quartz fiber filters prior and after sampling air from the exposure chamber and measuring the total air volume. CO concentrations in the exposure chamber were constantly monitored by using a GCO 100 CO Meter (Greisinger Electronic, Regenstauf, Germany) and reached values of 288 ± 74 ppm. All mice tolerated CS-mediated CO concentrations without any sign of toxicity, with CO-Hb levels of 12.2 ± 2.4%. Experiments were performed with $n = 8$ animals per group and were repeated twice. All animals were subjected to lung function analysis. Afterward, $n = 4$ animals per group were lavaged, the right lung was shock-frozen in liquid nitrogen, and the left lung was fixed in paraformaldehyde (PFA; see below). The remaining $n = 4$ animals per group were used for FACS analysis of whole lung single-cell suspensions.

Elastase application. Emphysema was induced in mice by oropharyngeal application of porcine pancreatic elastase (PPE, 80 U/kg body wt in 80 μl volume) as previously described (59). Control mice received 80 μl of sterile PBS. Mice were killed on *day 28*. Experiments were performed with $n = 8$ animals per group and were repeated twice.

Lung function measurement. Pulmonary function in mice was measured by use of a flexiVent system (Scireq, Montréal, Canada). Mice were anesthetized with ketamine-xylazine, tracheostomized, and connected to the flexiVent system. Mice were ventilated with a tidal volume of 10 ml/kg at a frequency of 150 breaths/min to reach a mean lung volume similar to that of spontaneous breathing. Testing of lung mechanical properties including dynamic lung compliance and resistance was carried out by a software-generated script. Measurements were repeated four times per animal.

Preparation of BAL. BAL was obtained to perform total and differential cell counts for inflammatory cell recruitment of neutrophils, macrophages, and lymphocytes. The lungs were lavaged by instilling the lungs with 4 × 0.5 ml aliquots of sterile PBS (GIBCO, Life Technologies, Darmstadt, Germany). For cytospins, cells were spun down at 400 *g* and resuspended in RPMI-1640 medium containing 10% FCS (both from GIBCO). Total cell counts were determined in a hemocytometer. Differential cell counts were performed by using morphological criteria on May-Grünwald-Giemsa-stained cytospins (200 cells/sample). BAL fluid was used to evaluate cytokine secretion via multiplex analysis.

Lung tissue processing. Lung tissue was either shock-frozen in liquid nitrogen to isolate mRNA for gene expression analysis or fixed at a constant pressure (20 cm fluid column) by intratracheal instillation of PBS buffered 6% PFA and embedded into paraffin for histological analysis of hematoxylin-eosin (HE)-stained slides and for immunohistochemistry.

For analysis of lymphocyte infiltration, single-cell suspensions of whole lung tissue were used. Lungs were perfused with sterile PBS via the right ventricle to clear leukocytes and erythrocytes from the pulmonary circulation. Lung homogenization was performed via enzymatic digestion and mechanical dissociation steps using a lung dissociation buffer and the gentleMACS Dissociator (both from Miltenyi Biotec, Bergisch Gladbach, Germany). After dissociation, samples were applied to a filter to remove any remaining larger particles from the single-cell suspensions.

FACS analysis of whole lung lymphocyte infiltration. For FACS analysis of single-cell suspensions, one part of the sample was directly labeled with FACS antibodies against T and B cell surface antigens. Staining of activated T lymphocytes was performed with antibodies against CD4, CD8 (both from eBioscience, San Diego, CA), and B lymphocytes were stained with an antibody against CD20 (eBioscience). Remaining lung cells were subjected to density gradient centrifugation using Pancoll (PAN Biotech, Aidenbach, Germany) to isolate mononuclear cells. Isolated cells were cultured overnight in anti-CD3/anti-CD28-coated plates to perform intracellular cytokine staining. On the following day, cultivated cells were restimulated with leukocyte activation cocktail with Golgi Plug (BD Pharmingen) for 4 h. Afterward, cells were stained with anti-CD4, fixed in 2% formaldehyde, permeabilized in 0.3% saponin buffer, and stained with antibodies against IL-17A, IFN-γ (both from eBioscience), and IL-4 (Biozol) to distinguish between different T helper cell subpopulations.

Multicolor analysis of stained cells was conducted with a BD FACSCanto II flow cytometer (BD Biosciences, Heidelberg, Germany) and BD FACSDiva software.

Quantitative morphometry. Design-based stereology was used to analyze sections via an Olympus BX51 light microscope equipped with a computer-assisted stereological toolbox (newCAST, Visiopharm, Hoersholm, Denmark) on HE-stained lung tissue slides as previously described (59). Air space enlargement was assessed by quantifying mean linear chord length (MLI) on 30 fields of view per lung. Briefly, a line grid was superimposed on lung section images. Intercepts of lines with alveolar septa and points hitting air space were counted to calculate MLI by applying the formula $MLI = \sum P_{air} \times L(p)/\sum I_{septa} \times 0.5$. P_{air} are the points of the grid hitting air spaces, $L(p)$ is the line length per point, and I_{septa} is the sum of intercepts of alveolar septa with grid lines.

Volume of iBALT normalized to the basal membrane was quantified on 50 fields of view per lung by counting points hitting iBALT (P_{iBALT}) and intercepts of lines with vessels and airways ($I_{airway+vessel}$). The volume was calculated by applying the formula $V/S = \sum P_{iBALT.} \times L(p)/\sum I_{airway+vessel}$.

The frequency of macrophages expressing MMP12 in lung tissue was quantified on 30 fields of view per lung. A frame grid was superimposed on lung section images. Within the frame, macrophages either positive or negative for MMP12 staining were counted and the percentage of MMP12-positive macrophages was calculated.

Immunohistochemistry. For immunohistochemistry, lungs were fixed in paraformaldehyde and embedded into paraffin. After deparaffinizing in xylene and rehydrating in alcohol, the tissue was treated with 1.8% (vol/vol) H_2O_2 solution (Sigma-Aldrich, St. Louis, MO) to block endogenous peroxidase. Heat-induced epitope retrieval was performed in HIER citrate buffer (pH 6.0, Zytomed Systems) in a Decloaking chamber (Biocare Medical, Concord, CA). To inhibit nonspecific binding of antibodies, tissue slides were treated with a rodent blocking antibody (Biocare Medical). After overnight incubation with primary antibodies against MMP12 (Abcam, Cambridge, UK), CD45R (BD Pharmingen), CD3 (Sigma Aldrich), or IL-10 (Santa Cruz Biotechnology, Dallas, TX), tissue slides were incubated with an alkaline phosphatase-labeled secondary antibody (Biocare Medical). Signals were amplified by adding chromogen substrate Vulcan fast red (Biocare Medical). Slides were counterstained with hematoxylin (Sigma-Aldrich) and dehydrated in xylene. Afterward, coverslips were mounted.

Quantitative real-time RT-PCR. Total RNA from lung tissue homogenate was isolated by using a peqGOLD Total RNA Kit (Peqlab, Erlangen, Germany) according to the manufacturer's instructions. cDNA was synthesized by using Random Hexamers and MuLV Reverse Transcriptase (Applied Biosystems, Darmstadt, Germany). mRNA expression of target genes KC (CXCL1), TNF-α, MCP1, MMP12, TIMP1, F4/80, IL-17A, CXCL13, IL-10, IL-6, and GM-CSF compared with housekeeping control hypoxanthine-guanine phosphoribosyltransferase (HPRT)-1 was determined by using Platinum SYBR Green qPCR SuperMix (Applied Biosystems) on a StepOnePlus 96-well Real-Time PCR System (Applied Biosystems, Carlsbad, CA). Relative transcript expression of a gene is given as $2^{-\Delta Ct}$ ($\Delta Ct = Ct_{target} - Ct_{reference}$); relative changes compared with control are $2^{-\Delta\Delta Ct}$ values ($\Delta\Delta Ct = \Delta Ct_{treated} - \Delta Ct_{control}$). Primers were generated by use of Primer-BLAST software (58) and according to published mRNA sequences.

Western blot. Protein (20 μg) was separated by SDS-PAGE, transferred onto a polyvinylidene difluoride membrane (Bio-Rad, Munich, Germany), blocked by 5% nonfat milk, and immunoblotted with anti-MMP12 (Millipore, Schwalbach, Germany) antibody. Upon developing with Amersham ECL Prime reagent (GE Healthcare, Freiburg, Germany), the bands were detected and quantified by use of the Chemidoc XRS system (Bio-Rad).

Multiplex cytokine analysis. Concentrations of secreted cytokines and chemokines KC (CXCL1), TNF-α, and MCP1 in BAL were determined by a magnetic bead-based MILLIPLEX *MAG* multiplex assay (Millipore, Schwalbach, Germany) and analyzed on a Luminex^{100} (Bio-Rad). For this assay, BAL fluid was concentrated (10×) by ultrafiltration in Amicon Ultra-0.5 centrifugal filter devices (Millipore).

In vitro cell culture experiments. In vitro experiments were performed with the B cell lymphoma line A20 and the macrophage cell line MH-S, both maintained at 37°C in 5% CO_2 atmosphere. A20 cells were cultured in RPMI-1640 supplemented with 10% FCS, 0.1 mM 2-mercaptoethanol, 100 U/ml penicillin-streptomycin, 10 mM HEPES, 2 mM L-glutamine, 1 mM sodium-pyruvate, 0.1 mM nonessential amino acids, and 1 × MEM vitamin solution. MH-S cells were maintained in RPMI-1640 supplemented with 10% FCS and 0.05 mM 2-mercaptoethanol.

CS extract for stimulation of cells was prepared by bubbling smoke from three research cigarettes (3R4F; see above) through 30 ml of RPMI-1640 cell culture medium at puffing speed in a closed environment with limited air flow. This stock was considered as 100% CS extract.

For testing the influence of B cell secreted cytokines on macrophages, A20 cells were stimulated either with LPS or with CS extract for 24 h, and afterward supernatants were used for stimulation of MH-S cells. In brief, A20 cells were seeded at a density of 4×10^5 cells per well in a 24-well plate. The following day, A20 cells were stimulated either with LPS (20 μg/ml) as positive control or with CS extract (1%) and (4%) for 24 h. Pure cell culture medium served as negative control. After 24 h, supernatants from A20 cells were removed, centrifuged, and used for stimulation of MH-S cells that had been seeded the day before at a density of 2×10^5 cells per well in a 24-well plate. Stimulation was performed for 6 h; afterward, cells were lysed for subsequent RNA isolation. Blockade of IL-10 signaling was performed by adding a blocking anti-IL-10 antibody (Santa Cruz Biotechnology) to the supernatants 30 min before stimulation of MH-S cells. All treatments did not significantly affect cell viability (data not shown).

Determination of IL-10 secretion by ELISA. Concentrations of IL-10 in the cell culture supernatants were determined by a commercially available kit for enzyme-linked immunosorbent assay (eBioscience) and normalized to the protein concentration of the lysed cells (as measured by BCA Protein Assay).

Th17 cell differentiation. Naive CD4 T cells were purified from total murine splenocytes by use of the CD4+CD62L+ T cell Isolation Kit II (Miltenyi Biotec). These were then stimulated for 72 h with anti-CD3/anti-CD28 coupled beads (Life Technologies, Darmstadt, Germany), along with recombinant human TGF-β (10 ng/ml, R&D Systems, Wiesbaden, Germany), IL-6 (60 ng/ml, R&D Systems), anti-IL-4 (10 ng/ml, BioLegend, San Diego, CA), anti-IL-12 (10 ng/ml, BioLegend), anti-IFN-γ (5 ng/ml, BioLegend) and anti-IL-2 (2.5 ng/ml, Miltenyi Biotec). Th0 control cells were stimulated with anti-CD3/anti-CD28 coupled beads alone for 72 h.

Cells were restimulated with PMA (20 nM) and Ionomycin (1 μM, both from Merck, Darmstadt, Germany) for 5 h with the addition of brefeldin A (10 μg/ml, Sigma-Aldrich) for the last 2.5 h. Cells were stained with anti-mouse CD4 and Fixable Viability Dye eFluor 450 (both from eBioscience) before fixation with 4% PFA and permeabilization in PBS/0.5% saponin/1% BSA. Cells were then stained with anti-IL-17A (eBioscience) before being analyzed on a BD FACSCanto II flow cytometer (BD Biosciences).

Microarray analysis. Lung tissue was obtained from CS-treated C57BL/6 mice ($n = 3$) and FA-treated control animals ($n = 3$) as described above. Total RNA was isolated employing the RNeasy Mini Kit (Qiagen) including digestion of remaining genomic DNA. The Agilent 2100 Bioanalyzer was used to assess RNA quality, and only high-quality RNA (RIN>7) was used for microarray analysis; 300 ng of total RNA were amplified using the Illumina TotalPrep RNA Amplification kit (Ambion). Amplified cRNA was hybridized to Mouse Ref-8 v2.0 Expression BeadChips (Illumina, San Diego, CA).

Staining and scanning were done according to the Illumina expression protocol. Data was processed by using the GenomeStudioV2010.1 software (gene expression module version 1.6.0) in combination with the MouseRef-8_V2_0_R3_11278551_A.bgx annotation file. The background subtraction option was used and an offset to remove remaining negative expression values was introduced. CARMAweb was used for quantile normalization (40). Statistical analyses were performed by utilizing the statistical programming environment R [R Development Core Team (39a)] implemented in CARMAweb. Gene-wise testing for differential expression was done by employing the limma *t*-test and Benjamini-Hochberg multiple testing correction (false discovery rate $< 10\%$). Pathway enrichment analyses were done with Ingenuity Pathway Software and significant terms ($P < 0.05$) were determined. Microarray data was submitted to GEO and link for review was generated: http://www.ncbi.nlm.nih.gov/geo/query/acc.cgi?token=etknuseghzkfvkn&acc=GSE52509.

Statistics. Results are given as mean values ± SD. One-way ANOVA following Bonferroni posttest was used for all studies with more than two groups. Analyses were conducted by use of GraphPad Prism 6 software (GraphPad Software, La Jolla, CA).

RESULTS

B cells are required for iBALT formation after CS exposure. In the lungs of severe COPD patients, increased T and B cell numbers and LF-like structures have been described (21, 29). To investigate the role of B cells in a CS-induced COPD mouse model, B cell-deficient (μMT) and WT mice were exposed to CS for 1–6 mo. We found that in WT animals marginal inflammatory cell infiltrates could be seen after 1 mo of CS exposure compared with FA control mice. After 4 and 6 mo of CS exposure, these infiltrates forming in WT mice, which we termed iBALT, showed significant increases in volume as shown by quantitative morphological assessment (Fig. 1, *A* and *B*). Interestingly, the formation of iBALTs did not proceed in the lungs of μMT mice exposed to CS. Previously, Litsiou et al. (29) have shown that CXCL13 plays an important role in LF formation. Therefore, we investigated whether B cell deficiency in vivo leads to altered CXCL13 expression. Using qPCR analysis we found a significant induction of CXCL13 mRNA expression in WT mice compared with μMT mice, supporting the finding of iBALT formation in WT mouse lungs only (Fig. 1*C*).

We further investigated the immune cell composition of iBALT structures by staining for B and T lymphocytes. CS-induced follicles in WT mice contained an abundance of CD45R-positive B cells and CD3-positive T cells compared with FA control and μMT mice (Fig. 1, *D* and *E*). Nevertheless, we observed slightly increased numbers of CD3-positive T cells in μMT lungs after CS exposure.

These expected results demonstrate that in our clinically relevant COPD mouse model B cells play crucial roles in CS-induced formation of iBALT structures, which predominantly consist of B and T cells in WT mice.

B cell-deficient mice show different lymphocyte infiltration in lung tissue after chronic CS exposure. Given the clear differences in lung tissue inflammation and iBALT formation in WT mice after CS exposure (Fig. 1), we aimed at confirming our lung tissue results by using flow cytometric quantification of B cells and CD4-positive T cell subsets in single-cell suspensions of whole lungs from WT and μMT mice. Compared with FA animals, lungs from CS-exposed WT mice revealed increased numbers of CD20-positive B cells starting from 1 mo of exposure (Fig. 2*A*). Numbers of CD4-positive T cell subtypes Th1 and Th2 increased during the whole time course, but, except for lower Th1 cell numbers at 6 mo in CS-exposed μMT compared with WT mice, no significant differences were observed for CS exposure and between WT and μMT mice, respectively (Fig. 2, *C* and *D*). Th17 cell numbers were significantly different after 6 mo of CS exposure in WT mice compared with CS-exposed μMT and FA mice (Fig. 2*E*). This was supported by significantly elevated IL-17 mRNA levels at the later time point of 6 mo (Fig. 2*F*). Recently, T helper cell subsets have been further characterized by dual expression of the prototypic cytokines. Therefore, we undertook a more detailed analysis of the subsets found in our CS-exposed mice. We did not observe an increase in IFN-γ^+ Th17, IL-17^+ Th2, and IFN-γ^+IL-17^+IL-4^+ cells after CS exposure for 1 and 4 mo. After CS exposure for 6 mo, these subsets were significantly increased in WT compared with FA- and CS-exposed μMT mice (IFN-γ^+ Th17: 2.8 ± 1.3% in WT vs. 1.4 ± 1.0% in μMT mice; IL17^+ Th2: 0.6 ± 0.2% in WT vs. 0.2 ± 0.1% in μMT mice; IFN-γ^+IL-17^+IL-4^+: 0.5 ± 0.3% in WT vs. 0.1 ± 0.1% in μMT mice).

Because we did not observe increases in Th17 cells after CS exposure of μMT mice, we investigated whether B cell deficiency alters the ability of CD4 T cells to differentiate into Th17 cells in these animals. We found that there was no differentiation defect in μMT mice as indicated by comparable Th17 levels after ex vivo stimulation of naive CD4 T cells from WT and μMT mice (12.5 ± 2.0 vs. 14.1 ± 3.0% Th17 cells).

These results demonstrate that chronic CS exposure is associated with early increases in B cells and later increases of Th17 cells in lung tissue of WT mice.

B cells play a critical role in CS-induced emphysema development. CS-induced lung damage was assessed by lung function analysis and by determining MLI with the computer-assisted stereological toolbox. After 1 mo of chronic CS exposure, significant changes in lung architecture and lung compliance could be detected neither for WT nor for μMT mice compared with the respective FA control animals (Fig. 3). However, there was a significant increase in emphysema development after 4 mo of exposure to CS in the lungs of WT mice compared with CS-exposed μMT and FA mice. We further exposed WT and μMT animals to CS for another 2 mo to enhance the CS-induced emphysema response. Interestingly, there were no changes in MLI in μMT animals even after 6 mo of exposure to CS compared with FA control groups (Fig. 3, *A* and *B*). Lung compliance was further augmented in WT compared with μMT mice exposed to CS for 4 and 6 mo (Fig. 3*C*). In contrast, slight age-dependent increases in lung compliance and MLI were observed for both WT and μMT mice during the whole time course. These data were confirmed by a reduction of body weight in CS-exposed WT mice, whereas both μMT groups showed comparable body weight levels (Fig. 3*D*). These results indicate that μMT mice were protected against CS-induced air space enlargement.

To rule out the possibility that μMT mouse lungs are generally protected against air space enlargement as shown by Lucey et al. (30) for combined TNF-α- and IL-1βR-deficient mice, as well as to clarify the role of immune cells, specifically B cells in emphysema development, we treated μMT mice with PPE. In the elastase mouse model, emphysema develops independent of immune cell (re)actions. Interestingly, oropharyngeal administration of elastase resulted in severe pulmonary

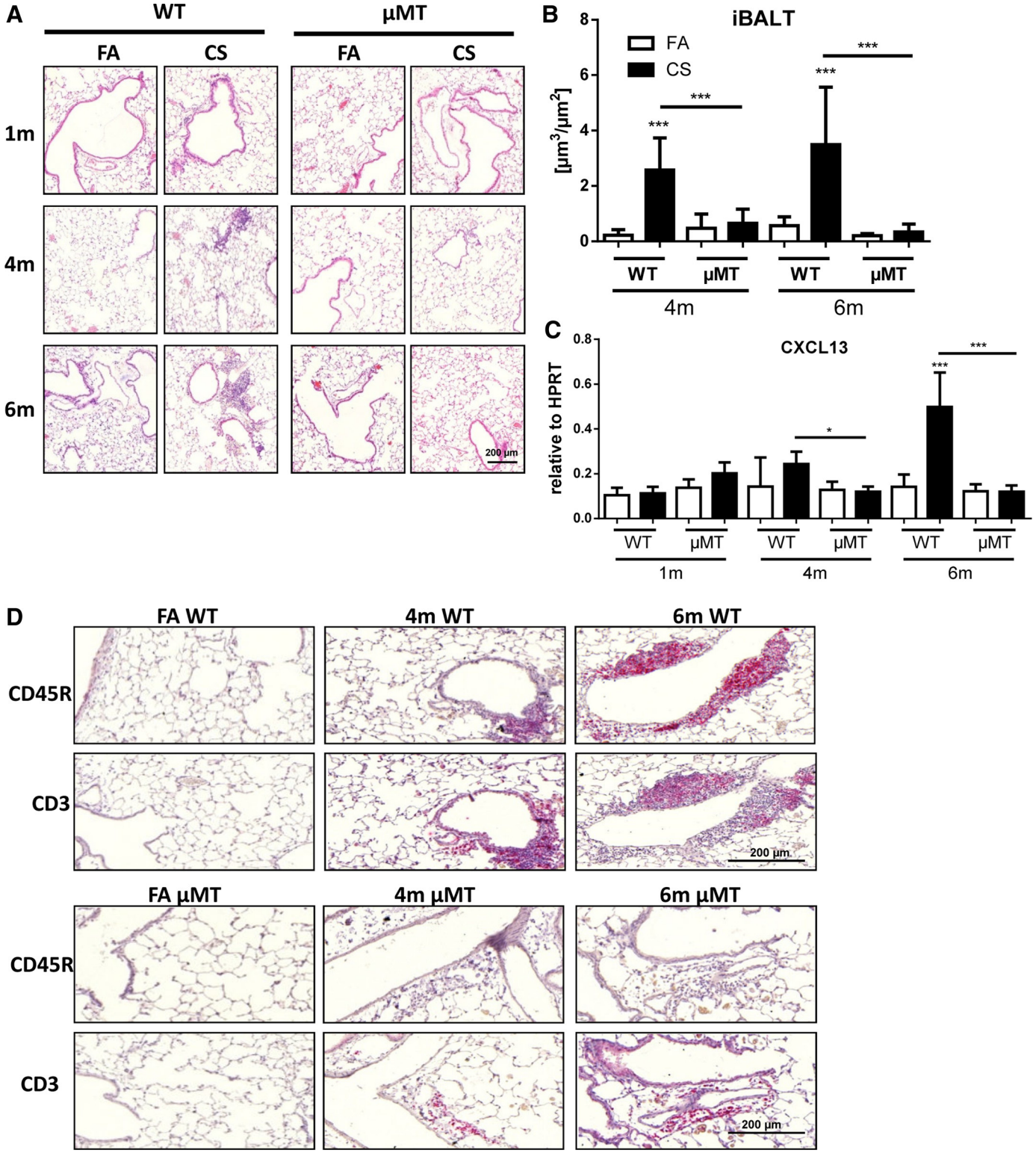

Fig. 1. Chronic cigarette smoke (CS) exposure leads to inflammatory cell recruitment and inducible bronchus-associated lymphoid tissue (iBALT) formation in lungs of wild-type (WT) mice. Data were combined from 2 independent experiments (8 mice per group and per time point) and are given as mean values ± SD; 1-way ANOVA following Bonferroni posttest with $*P < 0.05$, $**P < 0.01$, $***P < 0.001$. *A*: representative micrographs of hematoxylin and eosin (HE)-stained lung tissue sections from filtered air (FA)- and CS-exposed WT mice vs. FA- and CS-exposed µMT mice at indicated time points; scale bar 200 µm. *B*: volume of iBALT per basal membrane was determined via quantitative morphological assessment. *C*: mRNA expression of CXCL13 in lung tissue was measured by qPCR and data are presented as relative expression to housekeeping control HPRT-1. *D* and *E*: immunohistochemistry for CD45R and CD3 in lung tissue from FA- and CS-exposed WT mice (*D*) vs. FA- and CS-exposed µMT mice (*E*) at indicated time points.

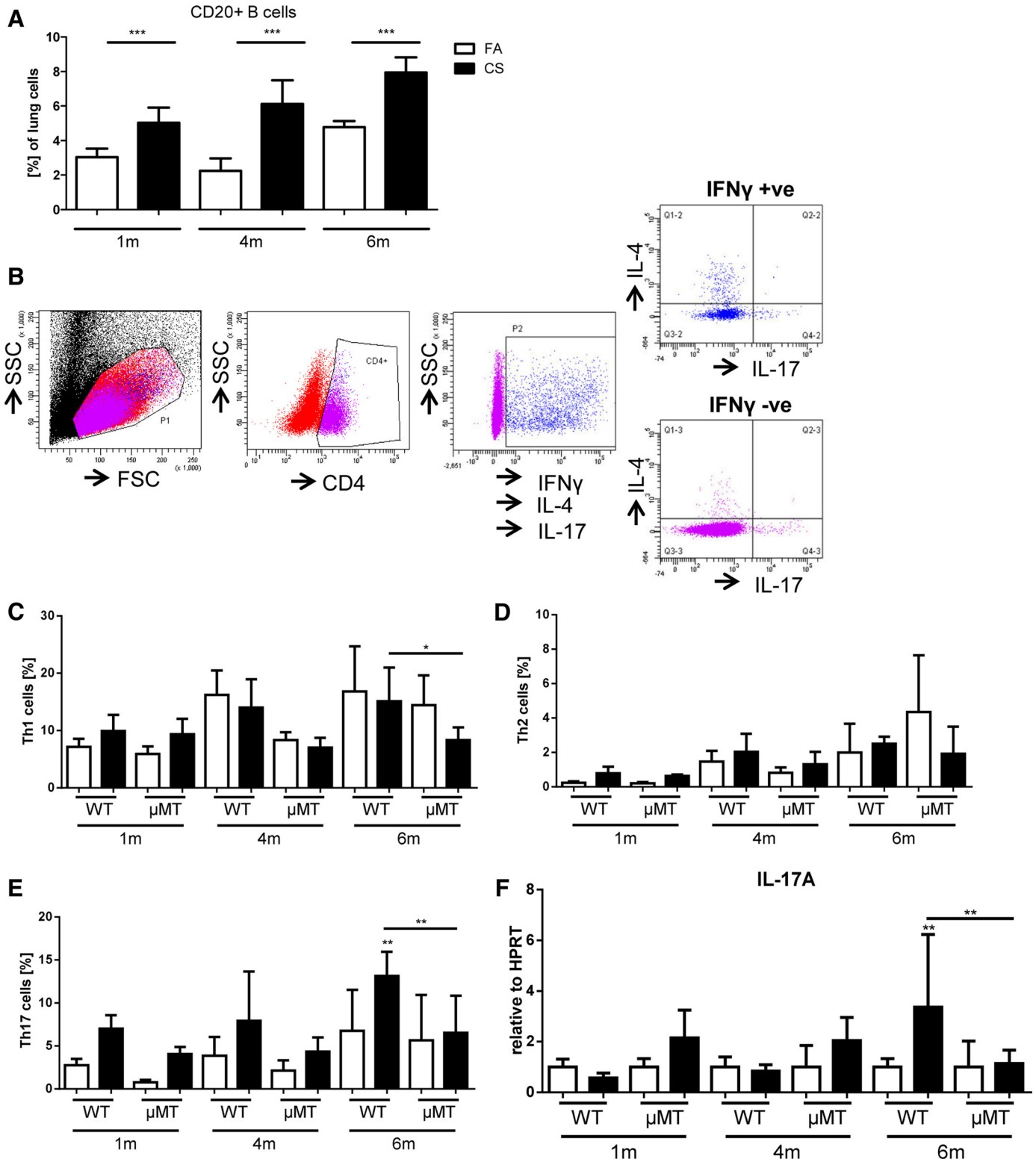

Fig. 2. Staining for B cells and CD4 positive Th subsets in lung tissue after chronic CS exposure reveals increases in B cells and Th17 cells in WT mice. For flow cytometric analysis single-cell suspensions were prepared from lung tissue. Surface marker stainings were directly performed with single-cell suspensions. For intracellular cytokine stainings, mononuclear cells were isolated from total lung cells by density gradient purification, stimulated overnight and restimulated for 4 h prior to fixation, permeabilization, and intracellular staining (see representative FACS plots for each staining performed). Data were combined from 2 independent experiments (4–6 mice per group and per time point) and are given as mean values ± SD; 1-way ANOVA following Bonferroni posttest with $^{*}P < 0.05$, $^{**}P < 0.01$, $^{***}P < 0.001$. *A*: mature B cells defined by expression of CD20 in FA- and CS-exposed WT mice. *B*: gating strategy for lung CD4+ T cells expressing either IFN-γ (Th1), IL-4 (Th2), or IL-17 (Th17) or different combinations thereof. FSC, forward scatter; SSC, side scatter. *C–E*: Th1 cells (*C*), Th2 cells (*D*), and Th17 cells (*E*) in FA- and CS-exposed WT mice vs. FA- and CS-exposed μMT mice. *F*: lung mRNA expression levels of target gene IL17A in comparison to housekeeping control HPRT-1 were determined via qPCR using cDNA synthesized from lung tissue homogenate.

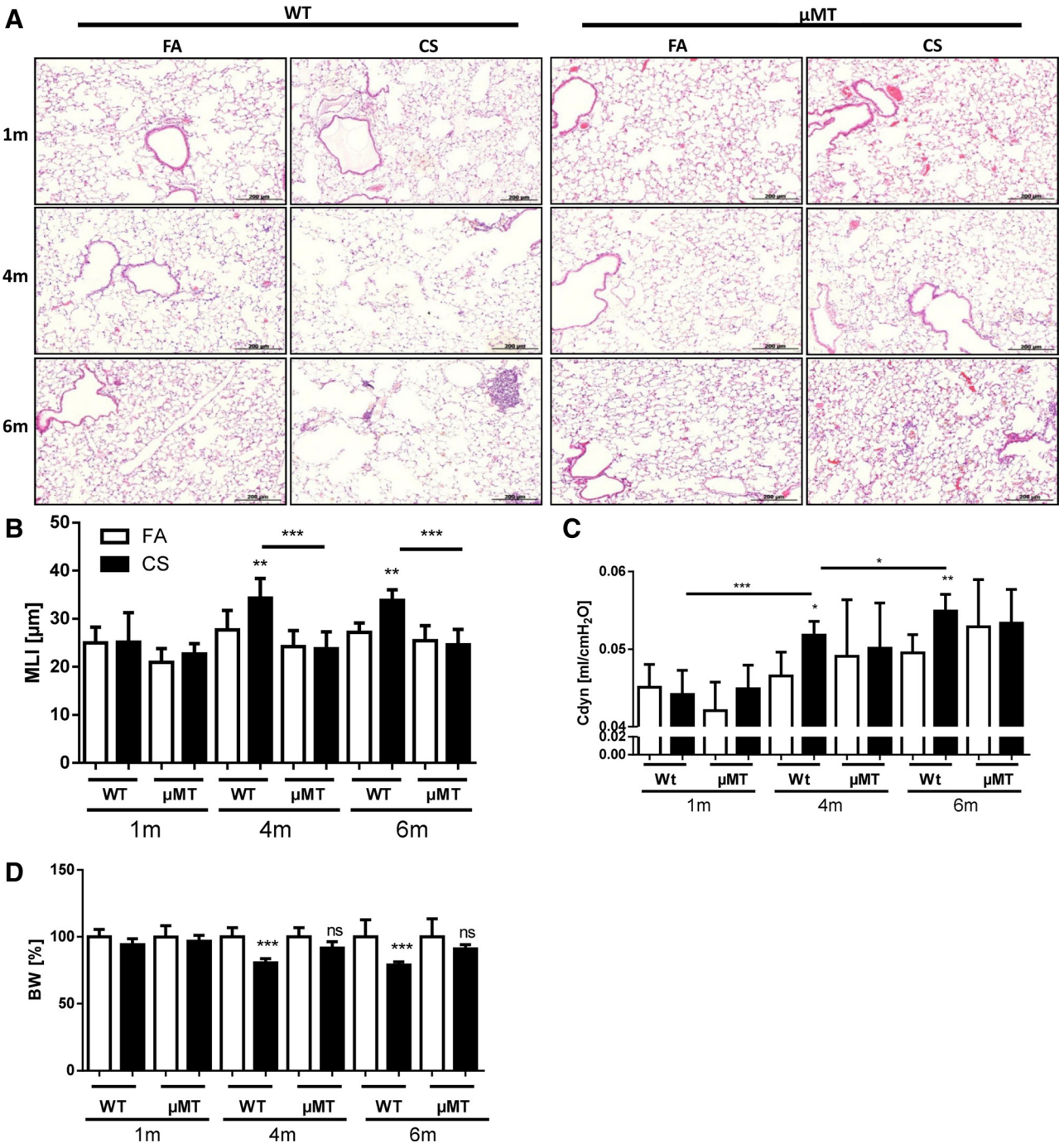

Fig. 3. B cell deficiency protects against air space enlargement and lung dysfunction after chronic CS exposure. Data were combined from 2 independent experiments (8 mice per group and per time point) and are given as mean values ± SD; 1-way ANOVA following Bonferroni posttest with $*P < 0.05$, $**P < 0.01$, $***P < 0.001$. *A*: representative micrographs of FA- and CS-exposed WT mice vs. FA- and CS-exposed µMT mice at indicated time points; scale bar 200 µm. *B*: quantitative measurement of emphysema was determined by design-based stereology of HE-stained lung tissue sections by use of an Olympus BX51 light microscope equipped with the computer-assisted stereological toolbox newCAST. MLI, mean linear intercept. *C*: lung function measurements for dynamic compliance (Cdyn) were performed in chronic CS-exposed WT and µMT mice after 1, 4, and 6 mo. *D*: body weight (BW) changes are given in % compared with respective FA controls.

emphysema after 28 days in both WT and µMT mice as demonstrated by HE-stained lung tissue slides (Fig. 4*A*). Quantitative morphological assessment confirmed air space enlargement as indicated by significant increases in MLI for both groups (Fig. 4*B*). The emphysematous changes in WT and µMT animals were associated with significantly increased lung compliance (Fig. 4*C*). As expected, HE-stained lung sections did not show any significant tissue inflammation in the lungs of elastase-exposed WT and µMT mice (Fig. 4*A*).

Our observations indicate that time-dependent iBALT formation and expansion in WT mice after CS exposure are also associated with the development of COPD.

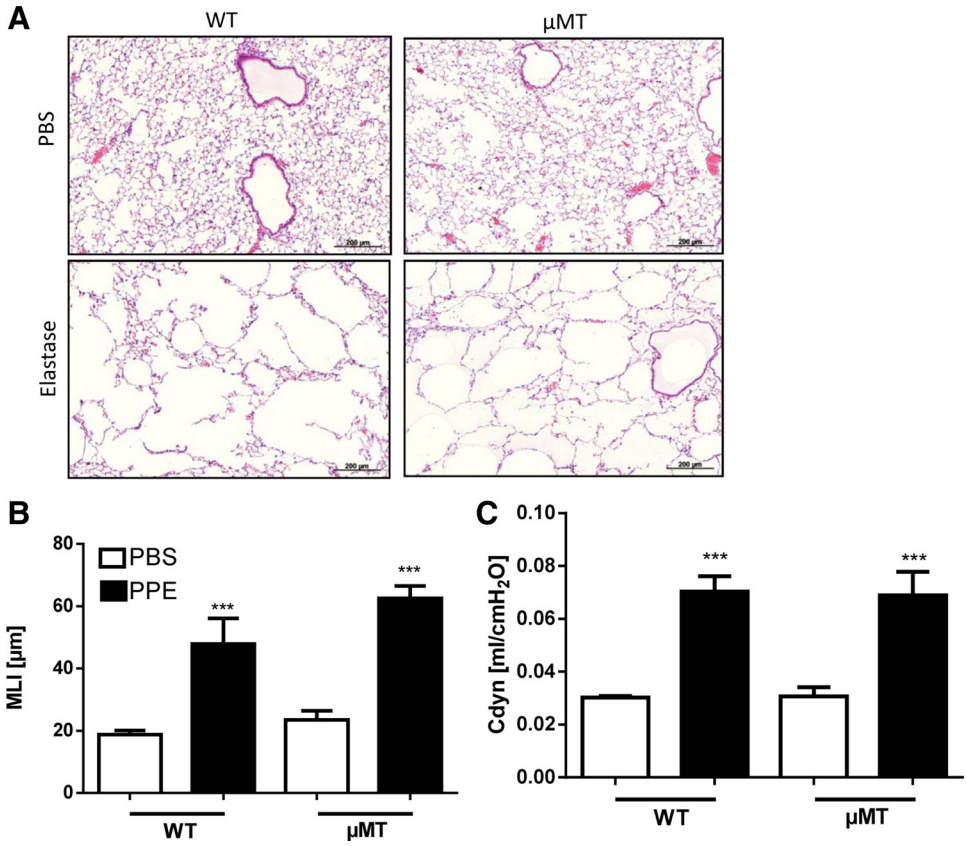

Fig. 4. Elastase treatment results in severe pulmonary emphysema after 28 days in both WT and μMT mice. Data were combined from 2 independent experiments (8 mice per group) and are given as mean values ± SD; 1-way ANOVA following Bonferroni post-test with $*P < 0.05$, $**P < 0.01$, $***P < 0.001$. *A*: C57BL/6 mice were treated with porcine pancreatic elastase to induce emphysema. Representative micrographs of HE-stained lung tissue slides reveal emphysema development after 28 days; scale bar 200 μm. *B*: quantitative morphological assessment demonstrated air space enlargement as indicated by significant increases in MLI for both groups. *C*: lung function measurements revealed significantly increased lung compliance.

iBALT induces macrophage activation and polarization. Since B cells and iBALT appear to be crucial for the development of CS-induced emphysema, and macrophage-derived MMP12 was described as being required for the induction of experimental emphysema after prolonged CS exposure (18), the role of B cells in accumulation and activation of tissue macrophages in the chronic model was investigated. Despite the lack of iBALT formation in μMT mice after chronic CS exposure (Fig. 1) we did not observe any differences in secreted BAL cytokine and tissue mRNA expression levels for TNF-α, KC, and MCP1 in both CS-exposed groups (Fig. 5, *A* and *B*). This was possibly due to similar CS-induced inflammatory reactions by lung epithelial cells. The comparable levels of BAL cytokines and tissue mRNA expression were confirmed by similar increases in total BAL inflammatory cell counts in CS-exposed WT and μMT mice. For both groups, a significant and comparable increase in total cells counts in CS-exposed mice compared with FA controls was observed at all time points (fold increase compared with FA after 6-mo CS exposure: 5.0 ± 1.0 in WT vs. 4.2 ± 1.3 in μMT mice).

However, in the lung tissue of WT animals, we observed significantly increased numbers of MMP12-stained macrophages located especially in iBALT as well as in the emphysematous alveolar lumen (Fig. 6*A*). μMT mice on the other hand showed significantly lower staining for MMP12, which is consistent with the data obtained for reduced iBALT formation after CS exposure in these animals. Interestingly, we observed staining for MMP12 in airway epithelial cells in μMT mice. Quantitative analysis of MMP12-expressing macrophage numbers in lung tissue also revealed significantly higher values for CS-exposed WT compared with μMT mice (Fig. 6*B*).

We further investigated mRNA expression levels for the macrophage marker F4/80. We noticed increases in F4/80 mRNA expression after CS exposure for both WT and μMT mice, but levels were significantly higher in WT mice at 4 and 6 mo of exposure (Fig. 6*C*), indicating higher macrophage accumulation in WT lung tissue. This was confirmed by qPCR for MMP12, which showed strong CS-induced increases for WT and μMT mice, but also significantly higher expression for WT animals at 4 and 6 mo of exposure (Fig. 6*D*). The stronger increase in MMP12 expression in WT mice further led to a higher MMP12-to-TIMP1 ratio in those animals, indicating a disturbed balance of MMP12 and its inhibitor TIMP1 (Fig. 6*E*). Furthermore, Western blot analysis for MMP12 using whole lung tissue lysates from WT and μMT mice after 6 mo of CS revealed a significant increase in active protein in CS-exposed WT compared with μMT mice (Fig. 6*F*). Because MMP12 is considered a marker for M2 macrophage polarization, we also analyzed the gene expression profile of several M1 and M2 markers. We did not observe increases in gene expression for the M1 markers iNOS and IL-6 after CS exposure in both WT and μMT animals (Fig. 6*G*). In contrast, besides MMP12, M2 markers FIZZ1 and Mrc1 were elevated in WT mice starting from 4 mo of CS exposure. These data strongly indicate that CS-induced iBALT is involved in macrophage activation and positioning.

B cell-derived IL-10 activates macrophages. To decipher the genes and pathways that might be involved in COPD development in WT animals we examined the lung mRNA expression profile of 4- and 6-mo CS-exposed vs. FA-exposed mice by microarray analysis using the Illumina Mouse Ref-8 v2.0 BeadChip. CS exposure induced a strong activation of two

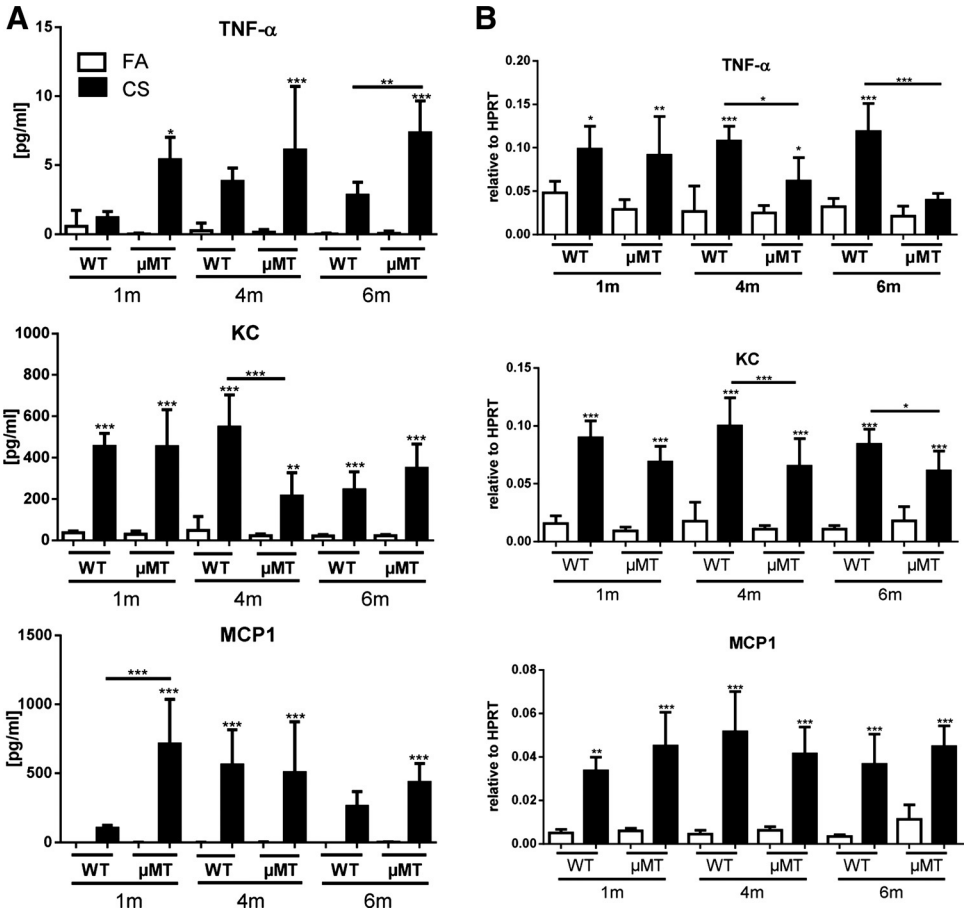

Fig. 5. Bronchoalveolar lavage (BAL) and lung tissue inflammation is similar in WT and μMT mice after chronic CS exposure. Data were combined from 2 independent experiments (8 mice per group) and are given as mean values ± SD; 1-way ANOVA following Bonferroni posttest with $*P < 0.05$, $**P < 0.01$, $***P < 0.001$. *A*: lungs of WT and μMT mice were lavaged with 4 × 0.5-ml aliquots of sterile PBS. BAL cytokine secretion of TNF-α, KC, and MCP1 was determined by a magnetic bead-based multiplex assay. For this assay, BAL fluid was concentrated (10×) by ultrafiltration in centrifugal filter devices. *B*: lung mRNA expression levels of target genes TNF-α, KC, and MCP1 compared with housekeeping control HPRT-1 were determined via qPCR using cDNA synthesized from lung tissue homogenate.

pathways: "innate and adaptive immune cell communication" and "IL-10 signaling," among others (Table 1, Fig. 7*A*). We selected two regulated genes involved in these pathways and confirmed by an independent experiment the significant increases in mRNA expression of TNF-α (Fig. 5*B*) and IL1RN (Fig. 7*B*).

Recently, it was shown that B cells are capable of polarizing macrophages to an alternatively activated phenotype via secretion of IL-10 (56). Therefore, we first investigated via qPCR whether IL-10 was upregulated in our smoke model. Though IL-10 mRNA expression levels were higher in CS-exposed μMT compared with WT mice at 1 mo, IL-10 mRNA expression increased significantly in WT animals at 6 mo of CS exposure (Fig. 8*A*). Immunohistochemistry of WT lung tissue for IL-10 demonstrated strong staining in areas of inflammatory cell accumulation consisting predominantly of CD45R-positive B cells but not in CD3-positive T cells (Fig. 8*B*).

Finally, in vitro stimulation of the murine B cell line A20 for 24 h with two concentrations of CS extract (CS 1 and 4%) showed increases in IL-10 mRNA expression and secretion after stimulation with both CS extract concentrations (Fig. 8, *C* and *D*). In contrast, increased mRNA expression of inflammatory genes such as IL-6, TNF-α, and GM-CSF was only observed in positive control (LPS)-treated cells (fold increase compared with control: 2.5 ± 0.2 for IL-6, 1.5 ± 0.1 for TNF-α, 8.5 ± 1.1 for GM-CSF).

To confirm the role for B cells in influencing macrophage activation, we treated the macrophage cell line MH-S for 6 h with LPS and CS extract as well as with supernatants obtained from A20 cells stimulated with LPS or CS extract (1 and 4%) for 24 h. qPCR analysis of MMP12 showed a strong increase in mRNA expression when MH-S cells where stimulated with supernatants from CS extract-treated A20 cells. Furthermore, to evaluate the possible role of B cell-derived IL-10, we aimed at blocking IL-10 signaling in MH-S cells treated with A20 supernatants by including an anti-IL-10 antibody. This led to a significant reduction of MMP12 expression in MH-S cells stimulated with supernatants from CS extract-treated A20 cells (Fig. 8*E*). These data indicate that B cell-derived IL-10 is involved in macrophage polarization and MMP12 upregulation after CS exposure in vivo as well as in vitro.

DISCUSSION

Our study aimed at investigating the relationship between B cell-dependent iBALT formation and the immunopathogenesis of COPD. We identified what we believe to be a major pathway that induces and maintains the severe inflammatory response causing subsequent emphysema development in COPD. The results presented here demonstrate that B cells are involved in at least two mechanisms after CS exposure: firstly, B cells are organized in iBALT, and secondly, they were found to be potent regulators of macrophage accumulation and macrophage-derived MMP12 production, thereby contributing to emphysema development.

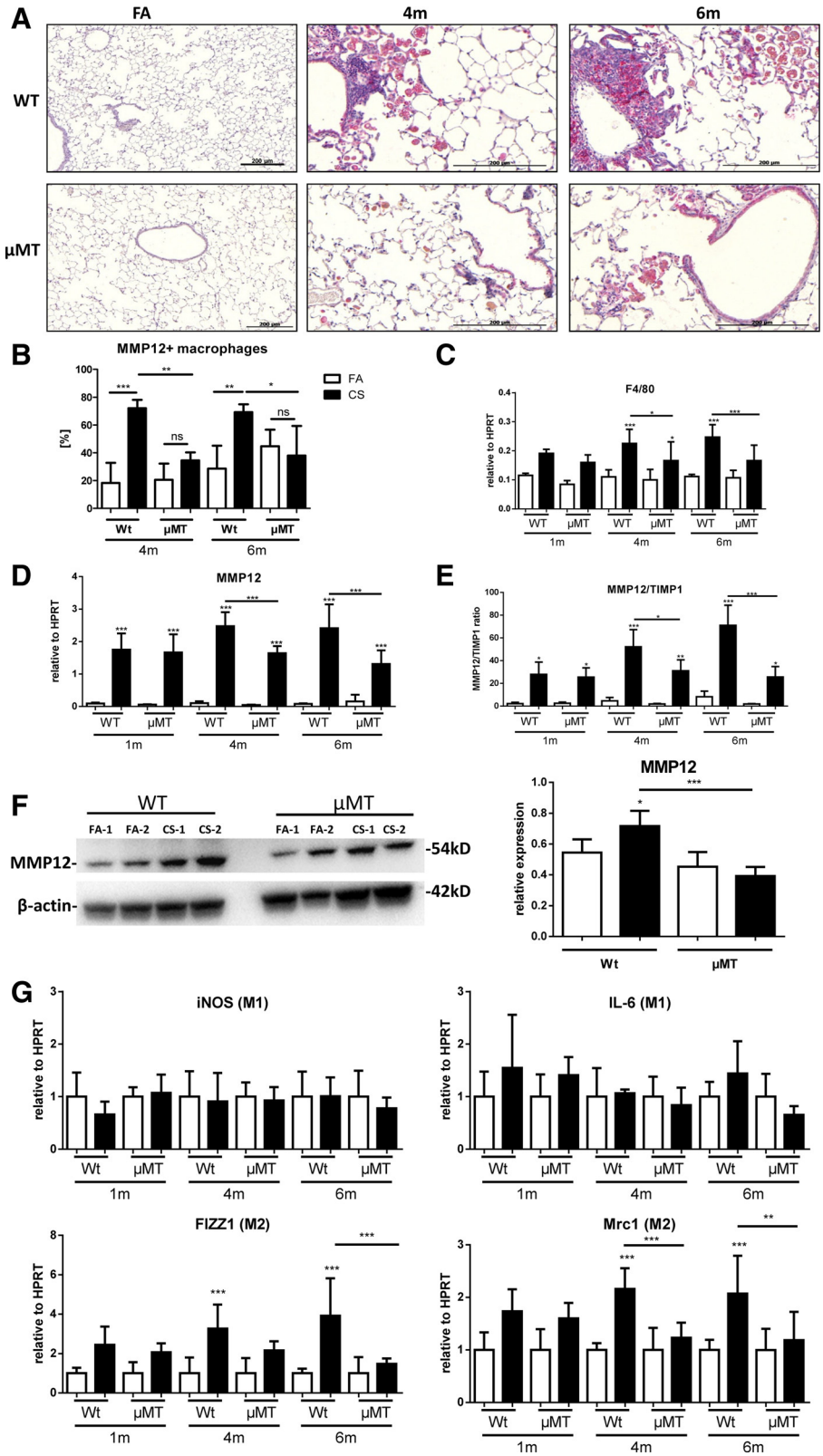

Fig. 6. Macrophage markers are increased in the lungs of CS-exposed WT mice. Data were combined from 2 independent experiments (8 mice per group and per time point) and are given as mean values ± SD; 1-way ANOVA following Bonferroni posttest with $*P < 0.05$, $**P < 0.01$, $***P < 0.001$. *A*: representative micrographs of immunohistochemical stainings for MMP12 in lung sections from FA controls and CS-exposed WT and µMT mice at indicated time points; scale bar 200 µm. *B*: quantitative analysis of MMP12-expressing macrophage numbers in lung tissue revealed significantly higher values for CS-exposed WT compared with µMT mice. *C–E*: whole lung mRNA expression levels of macrophage markers F4/80 (*C*) and MMP12 (*D*) as well as the ratio of MMP12-to-TIMP1 (*E*) were investigated compared with housekeeping control HPRT-1 by qPCR. Relative transcript expression of target genes is given as $2^{-\Delta CT}$ ($\Delta Ct = Ct_{target} - Ct_{reference}$), relative changes compared with control are $2^{-\Delta\Delta Ct}$ values ($\Delta\Delta Ct = \Delta Ct_{treated} - \Delta Ct_{control}$). Mean values ± SD; 1-way ANOVA following Bonferroni posttest with $*P < 0.05$, $**P < 0.01$, $***P < 0.001$. *F*: representative Western blot and densitometric analysis for MMP12 in lung tissue homogenate from WT and µMT mice after 6 mo of CS exposure. β-Actin was used as loading control. *G*: whole lung mRNA expression levels of M1 macrophage markers iNOS and IL-6 and M2 markers FIZZ1 and Mrc1 were investigated compared with housekeeping control HPRT-1 by qPCR.

There is considerable evidence that the CS-induced inflammatory response plays a major role in driving the pathophysiological changes observed in COPD (5, 12). Because of the high toxicity of both its gaseous and particle phases (9, 47), CS persistently induces a neutrophil and macrophage inflammatory response in the lower respiratory tract of both humans and animals exposed in experimental models (11, 24, 49). Whereas the acute reaction during the

Table 1. *Enriched canonical pathways*

Ingenuity Canonical Pathways	−log (*P* value)	Ratio	Molecules
Communication between innate and adaptive immune cells	7.81E +00	1.34E−01	IL1A, CD83, Ccl9, IL33, CXCL10, TLR2, CCL4, IL1RN, FCER1G, TLR7, CD86, CCL3L1/CCL3L3, Tlr13, CSF2, TNF
Role of hypercytokinemia/hyperchemokinemia in the pathogenesis of influenza	5.04E +00	1.74E−01	IL33, CXCL10, IL1A, CCR5, CCL4, CCL2, IL1RN, TNF
IL-10 signaling	4.95E +00	1.54E−01	IL33, HMOX1, IL1A, CCR5, JUN, FCGR2A, IL1RN, NFKBIE, IL10RB, CD14, FCGR2B, TNF
Atherosclerosis signaling	4.36E +00	1.08E−01	APOE, IL1A, MMP3, CMA1, MMP13, ALOX12, CCL11, PLA2G7, IL33, ITGB2, PLA2G2D, CCL2, IL1RN, PLA2G4F, TNF
Dendritic cell maturation	3.34E +00	7.58E−02	PLCB2, IL1A, TYROBP, FCGR2A, NFKBIE, CD83, FCGR2B, TREM2, IL33, TLR2, IL1RN, FCER1G, CD86, LY75, CSF2, TNF
Cross talk between dendritic cells and natural killer cells	2.65E +00	8.49E−02	CSF2RB, KLRD1, TYROBP, TLR7, CD86, CD83, TREM2, CSF2, TNF
NF-κB signaling	1.88E +00	7.18E−02	TLR2, IL33, TNIP1, IL1A, TGFBR1, CARD10, IL1RN, NFKBIE, TGFBR3, FCER1G, TLR7, MALT1, TNF
Nicotine degradation II	1.86E +00	7.06E−02	UGT1A6, CYP4B1, FMO1, CSGALNACT1, UGT1A9, CYP1B1
Systemic lupus erythematosus signaling	1.32E +00	4.31E−02	IL33, IL1A, JUN, FCGR2A, IL1RN, TLR7, FCER1G, CD86, C6, FCGR2B, TNF

Lung mRNA expression profiles of 4- and 6-mo cigarette smoke (CS)-exposed vs. filtered air-exposed mice were determined by microarray analysis using Illumina Mouse Ref-8 v2.0 BeadChip. CS exposure induces a strong activation of 10 pathways as analyzed with Ingenuity Pathway software.

first week of CS exposure is dominated by a strong neutrophilic and macrophage influx, the chronic phase starting from 1 mo of CS exposure is additionally characterized by infiltration of adaptive immune cells, i.e., lymphocytes, and by progressive pathophysiological changes similar to those observed in COPD patients, such as small airway remodeling and septal tissue damage/emphysema (13, 46, 54). In our present study, we found that B cell-deficient animals develop emphysematous changes in an elastase mouse model (Fig. 4); however, these animals were protected against CS-induced emphysema development (Fig. 3). In contrast, WT mice show functional and structural lung changes after 4 mo of CS exposure and this coincides with B cell accumulation.

TLOs formed in the lung belong to iBALT, which is defined as ectopic lymphoid tissue induced in response to infection or inflammation. This allows local priming and clonal expansion of B and T cells, antigen retention, somatic hypermutation, affinity maturation, and immunoglobulin (Ig) class switching (1, 28). By acquiring antigens from the airways, iBALT induces a local inflammatory response and is responsible for the maintenance of memory cells in the lungs (41). Therefore, iBALT may be beneficial for the host by providing protection against microbial colonization and infection of the lower respiratory tract. Several studies have shown a protective role for iBALT-related local immune responses in the context of influenza infection (34, 43). However, the immune response mediated by iBALTs might also be of a harmful nature in COPD patients. Two recent studies investigated lymphoid neogenesis in the COPD lung and confirmed the important role of CXCL13 (6, 29). Litsiou et al. (29) found that CXCL13 levels correlate with LF density in COPD patients and that CXCL13 promotes B cell migration to ectopic sites of lymphoid tissue formation in the lung. Bracke et al. (6) performed prophylactic and therapeutic treatment with an anti-CXCL13 antibody in mice exposed to CS for 6 mo. This inhibited the formation of pulmonary LFs and led to an attenuated BAL inflammation and a partial protection against destruction of alveolar walls. We were also able to confirm an upregulation of CXCL13 after CS exposure in WT mice. Furthermore, the prevention of iBALT formation in μMT mice inhibited COPD development in our study (Figs. 1 and 3).

This strongly points to an involvement of iBALT formation in COPD pathogenesis, but the exact contribution to disease development still remains unclear. Recent studies, mostly from the field of autoimmune diseases such as multiple sclerosis (22, 55) and rheumatoid arthritis (51), have focused their attention on the possible B cell roles that are independent of their lymphoid neogenesis and antibody secreting function. Further potent effector functions include antigen presentation, T cell activation, and regulation as well as secretion of a variety of immunmodulatory cytokines such as IL-6 and IL-10 (15, 23). Interestingly, cytokine secretion by B cells has been shown to influence and modulate differentiation and polarization of T cells, macrophages, and dendritic cells during the development of the immune response, thereby regulating immune reactions (23). Moreover, macrophage effector functions can be directly regulated by B cell-mediated cytokine secretion, which was shown to be important for the outcome of various models of infection, inflammation, and cancer. Kelly-Scumpia et al. (26) demonstrated that B cell-dependent cytokine responses are required for and enhance early innate immune responses during bacterial sepsis. During viral infection with vesicular stomatitis virus (VSV), B cells are indispensable for providing lymphotoxin and thereby maintaining an antiviral macrophage phenotype that protects against fatal CNS invasion (32).

An important role has been attributed to B cell-derived IL-10 in various disease models. Increased production of anti-inflammatory IL-10 by B cells in multiple sclerosis, lupus, and rheumatoid arthritis patients is capable of downregulating T cell responses (19, 22). IL-10-producing B cells were also shown to regulate macrophage function by decreasing their phagocytic activity and cytokine and NO production (25, 39). The modulated phagocytic activity of macrophages was described as facilitating fungal infection in mice (38). Interestingly, B1 cells, a B cell subset predominantly located in peritoneal and pleural cavities, were described as the main source of B cell-derived IL-10 (31), and IL-10 secreted by

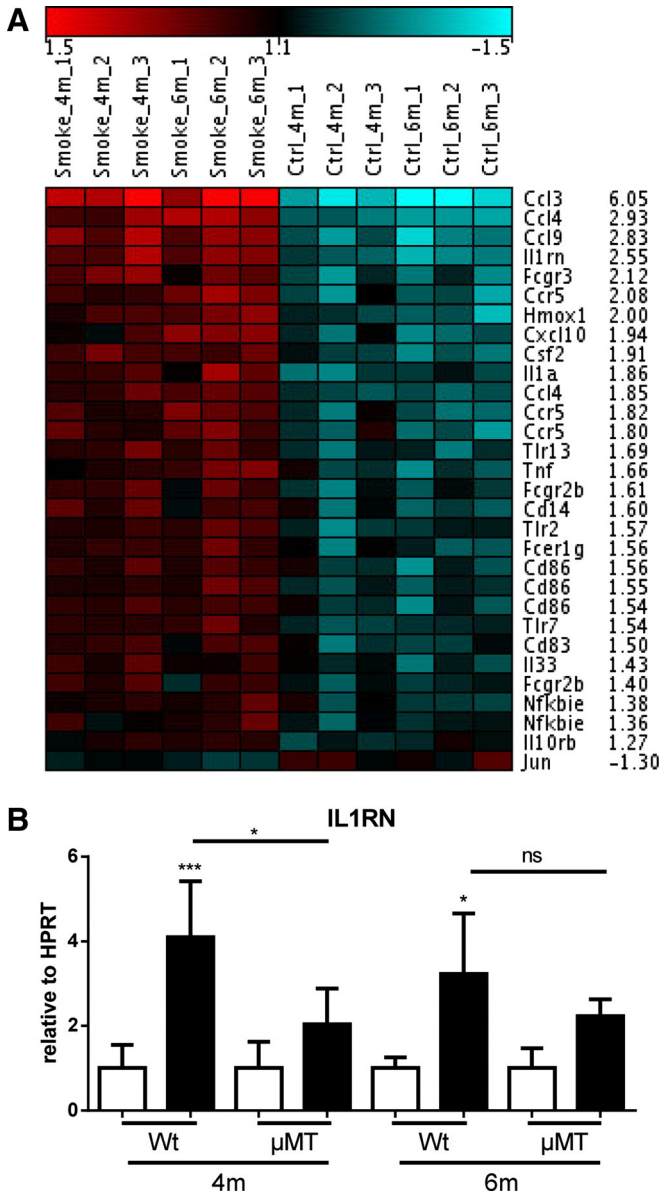

Fig. 7. Microarray analysis of 4- and 6-mo CS-exposed vs. FA-exposed mice. *A*: heat map depicting regulated genes from the 2 strongly activated pathways "innate and adaptive immune cell communication" and "IL-10 signaling." *B*: whole lung mRNA expression levels of IL1RN in WT and µMT mice after 4 and 6 mo of CS exposure were investigated compared with housekeeping control HPRT-1 by qPCR. $*P < 0.05$, $***P < 0.001$; ns, not significant.

these cells plays a role in polarizing macrophages to an M2-like phenotype that promotes tumor growth in a melanoma model (56) and modulates wound-healing processes in mice (35).

Macrophages are involved in the severe chronic lung inflammation observed in COPD. In response to CS, macrophages release cytokines and proteolytic enzymes and generate oxidants, thereby causing tissue damage and perpetuating inflammation and immune reactions (49). Because MMP12 knockout mice are protected against CS-induced macrophage recruitment and emphysema development, these cells and their derived factors seem to be required for disease onset and progression (18). Here, we showed strong differences in lung tissue inflammation between WT and µMT mice, with significant increases in tissue macrophages and upregulated MMP12 expression in CS-exposed WT mice (Fig. 6). Moreover, we identified a role for B cell-derived IL-10 in enhancing macrophage activation and MMP12 upregulation (Fig. 8). To our knowledge, our data are the first to provide a link between macrophages and B cells involved in COPD pathogenesis.

Interestingly, CXCL13 neutralization was also shown to directly affect macrophages (6). Bracke et al. (6) found reduced expression of MMP12 in macrophages of CS-exposed, anti-CXCL13-treated mice, which confirms our findings of B cell-mediated MMP12 induction in macrophages. However, because CXCL13 treatment did not significantly alter lung inflammation, alveolar enlargement, and airway remodeling in their study, the authors concluded that the innate immune system might be sufficient to induce emphysema after CS exposure, as shown by D'hulst et al. (12) using severe combined immunodeficiency (scid) mice, which lack B and T lymphocytes (12). These animals developed emphysema after CS exposure. But since scid mice are from a BALB/c background, results are difficult to compare with our study. Nevertheless, CS exposure of scid and anti-CXCL13-treated mice also revealed a marked increase in lung macrophages and MMP12 expression. On the basis of these findings, we suggest that further investigation and targeting of B cells or especially IL-10-releasing B cells in the formation of iBALT and subsequent emphysema development in a CS-induced COPD mouse model may shed further light on mechanisms that could induce reparative and regenerative processes in the COPD lung.

In conclusion, we have shown that CS exposure leads to B cell-dependent iBALT formation, which contributes to the pathogenesis of COPD via IL-10-induced macrophage activation and MMP12 upregulation. Unraveling the mechanisms that are involved in and link innate and adaptive immune cell responses to CS in COPD is of great clinical relevance. The significant role for B cells and iBALT formation in CS-induced emphysema development provides a new innovative mechanism, which could be explored as a target for therapeutic intervention in COPD patients. Targeting iBALT formation in early stages after CS exposure to inhibit subsequent macrophage upregulation could be a promising option to prevent COPD progression.

ACKNOWLEDGMENTS

The authors acknowledge the help of Bernd Lentner, Gunter Eder, Christine Hollauer, and Anke Bettenbrock.

GRANTS

This work was supported by a European Respiratory Society Fellowship awarded to Gerrit John-Schuster (LTRF MC1520-2010).

DISCLOSURES

No conflicts of interest, financial or otherwise, are declared by the author(s).

AUTHOR CONTRIBUTIONS

G.J.-S., K.H., O.E., and A.Ö.Y. conception and design of research; G.J.-S., K.H., T.M.C., and M.I. performed experiments; G.J.-S., K.H., T.M.C., M.I., J.B., O.E., and A.Ö.Y. analyzed data; G.J.-S., K.H., T.M.C., J.B., O.E., and A.Ö.Y. interpreted results of experiments; G.J.-S. and K.H. prepared figures; G.J.-S., K.H., and A.Ö.Y. drafted manuscript; G.J.-S., T.M.C., O.E., and

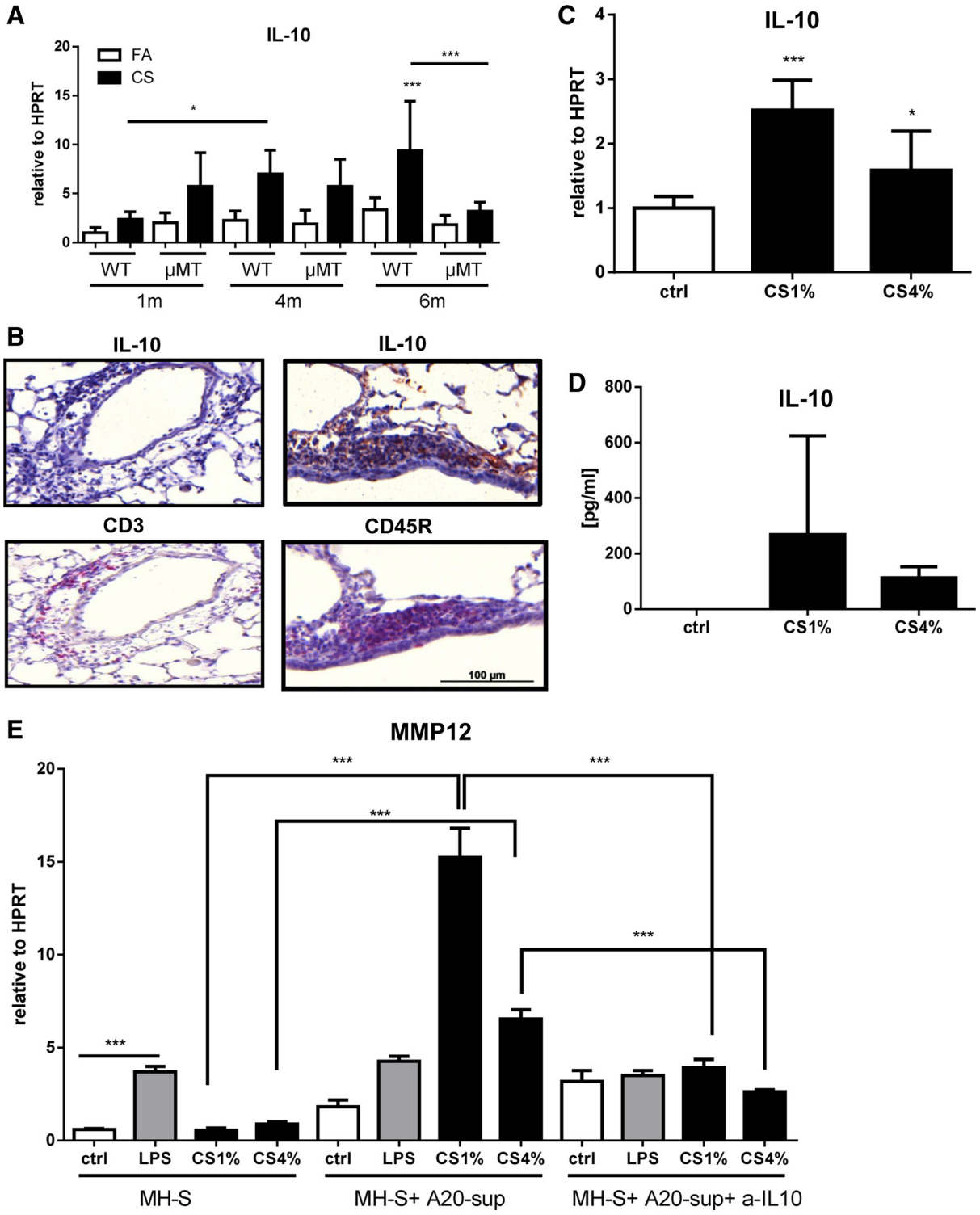

Fig. 8. B cell-derived IL-10 secretion upregulates MMP12 expression. In vivo data from 2 independent experiments (8 mice per group and per time point) and in vitro data from 3 independent experiments were combined and are given as mean values ± SD; 1-way ANOVA following Bonferroni posttest with $*P < 0.05$, $**P < 0.01$, $***P < 0.001$. A20-sup, supernatant from A20 cells; CS, cigarette smoke extract. *A*: IL-10 mRNA expression levels in lung tissue homogenates were investigated compared with housekeeping control HPRT-1 by qPCR. *B*: representative micrographs of immunohistochemical stainings for IL-10 and CD3 and for IL-10 and CD45R in lung serial sections from CS-exposed WT mice after 6 mo of CS exposure; scale bar 200 µm. *C*: at 24 h post-cigarette smoke extract (CS) stimulation mRNA expression levels of IL-10 were significantly elevated in the B cell lymphoma line A20 as measured compared with housekeeping control HPRT-1 by qPCR. *D*: IL-10 cytokine secretion in CS stimulated B cell lymphoma line A20 were investigated by ELISA of cell culture supernatants. *E*: MMP12 mRNA expression levels in the macrophage cell line MH-S with and without anti-IL-10 antibody treatment were investigated compared with housekeeping control HPRT-1 by qPCR.

A.Ö.Y. edited and revised manuscript; G.J.-S., K.H., T.M.C., M.I., J.B., O.E., and A.Ö.Y. approved final version of manuscript.

REFERENCES

1. **Aloisi F, Pujol-Borrell R.** Lymphoid neogenesis in chronic inflammatory diseases. *Nat Rev Immunol* 6: 205–217, 2006.
2. **Barnes PJ, Shapiro SD, Pauwels RA.** Chronic obstructive pulmonary disease: molecular and cellular mechanisms. *Eur Respir J* 22: 672–688, 2003.
3. **Biswas SK, Mantovani A.** Macrophage plasticity and interaction with lymphocyte subsets: cancer as a paradigm. *Nat Immunol* 11: 889–896, 2010.
4. **Bosken CH, Hards J, Gatter K, Hogg JC.** Characterization of the inflammatory reaction in the peripheral airways of cigarette smokers using immunocytochemistry. *Am Rev Respir Dis* 145: 911–917, 1992.
5. **Botelho FM, Gaschler GJ, Kianpour S, Zavitz CC, Trimble NJ, Nikota JK, Bauer CM, Stampfli MR.** Innate immune processes are sufficient for driving cigarette smoke-induced inflammation in mice. *Am J Respir Cell Mol Biol* 42: 394–403, 2010.
6. **Bracke KR, Verhamme FM, Seys LJ, Bantsimba-Malanda C, Cunoosamy DM, Herbst R, Hammad H, Lambrecht BN, Joos GF, Brusselle GG.** Role of CXCL13 in cigarette smoke-induced lymphoid follicle formation and chronic obstructive pulmonary disease. *Am J Respir Crit Care Med* 188: 343–355, 2013.
7. **Brusselle GG.** Matrix metalloproteinase 12, asthma, and COPD. *N Engl J Med* 361: 2664–2665, 2009.
8. **Brusselle GG, Demoor T, Bracke KR, Brandsma CA, Timens W.** Lymphoid follicles in (very) severe COPD: beneficial or harmful? *Eur Respir J* 34: 219–230, 2009.
9. **Cantin AM.** Cellular response to cigarette smoke and oxidants: adapting to survive. *Proc Am Thorac Soc* 7: 368–375, 2010.
10. **Carragher DM, Rangel-Moreno J, Randall TD.** Ectopic lymphoid tissues and local immunity. *Semin Immunol* 20: 26–42, 2008.
11. **Churg A, Cosio M, Wright JL.** Mechanisms of cigarette smoke-induced COPD: insights from animal models. *Am J Physiol Lung Cell Mol Physiol* 294: L612–L631, 2008.
12. **D'hulst AI, Maes T, Bracke KR, Demedts IK, Tournoy KG, Joos GF, Brusselle GG.** Cigarette smoke-induced pulmonary emphysema in scid-mice. Is the acquired immune system required? *Respir Res* 6: 147, 2005.
13. **D'hulst AI, Vermaelen KY, Brusselle GG, Joos GF, Pauwels RA.** Time course of cigarette smoke-induced pulmonary inflammation in mice. *Eur Respir J* 26: 204–213, 2005.
14. **Dieu-Nosjean MC, Antoine M, Danel C, Heudes D, Wislez M, Poulot V, Rabbe N, Laurans L, Tartour E, de Chaisemartin L, Lebecque S, Fridman WH, Cadranel J.** Long-term survival for patients with non-small-cell lung cancer with intratumoral lymphoid structures. *J Clin Oncol* 26: 4410–4417, 2008.
15. **DiLillo DJ, Horikawa M, Tedder TF.** B-lymphocyte effector functions in health and disease. *Immunol Res* 49: 281–292, 2011.
16. **Gosman MM, Willemse BW, Jansen DF, Lapperre TS, van Schadewijk A, Hiemstra PS, Postma DS, Timens W, Kerstjens HA, Groningen and Leiden Universities Corticosteroids in Obstructive Lung Disease Study Group.** Increased number of B-cells in bronchial biopsies in COPD. *Eur Respir J* 27: 60–64, 2006.
17. **Halle S, Dujardin HC, Bakocevic N, Fleige H, Danzer H, Willenzon S, Suezer Y, Hammerling G, Garbi N, Sutter G, Worbs T, Forster R.** Induced bronchus-associated lymphoid tissue serves as a general priming site for T cells and is maintained by dendritic cells. *J Exp Med* 206: 2593–2601, 2009.
18. **Hautamaki RD, Kobayashi DK, Senior RM, Shapiro SD.** Requirement for macrophage elastase for cigarette smoke-induced emphysema in mice. *Science* 277: 2002–2004, 1997.
19. **Heo YJ, Joo YB, Oh HJ, Park MK, Heo YM, Cho ML, Kwok SK, Ju JH, Park KS, Cho SG, Park SH, Kim HY, Min JK.** IL-10 suppresses Th17 cells and promotes regulatory T cells in the CD4+ T cell population of rheumatoid arthritis patients. *Immunol Lett* 127: 150–156, 2010.
20. **Hogg JC.** Pathophysiology of airflow limitation in chronic obstructive pulmonary disease. *Lancet* 364: 709–721, 2004.
21. **Hogg JC, Chu F, Utokaparch S, Woods R, Elliott WM, Buzatu L, Cherniack RM, Rogers RM, Sciurba FC, Coxson HO, Pare PD.** The nature of small-airway obstruction in chronic obstructive pulmonary disease. *N Engl J Med* 350: 2645–2653, 2004.
22. **Ireland S, Monson N.** Potential impact of B cells on T cell function in multiple sclerosis. *Mult Scler Int* 2011: 423971, 2011.
23. **Ireland SJ, Blazek M, Harp CT, Greenberg B, Frohman EM, Davis LS, Monson NL.** Antibody-independent B cell effector functions in relapsing remitting multiple sclerosis: clues to increased inflammatory and reduced regulatory B cell capacity. *Autoimmunity* 45: 400–414, 2012.
24. **John G, Kohse K, Orasche J, Reda A, Schnelle-Kreis J, Zimmermann R, Schmid O, Eickelberg O, Yildirim AO.** The composition of cigarette smoke determines inflammatory cell recruitment to the lung in COPD mouse models. *Clin Sci (Lond)* 126: 207–221, 2014.
25. **Kalampokis I, Yoshizaki A, Tedder TF.** IL-10-producing regulatory B cells (B10 cells) in autoimmune disease. *Arthritis Res Ther* 15, *Suppl* 1: S1, 2013.
26. **Kelly-Scumpia KM, Scumpia PO, Weinstein JS, Delano MJ, Cuenca AG, Nacionales DC, Wynn JL, Lee PY, Kumagai Y, Efron PA, Akira S, Wasserfall C, Atkinson MA, Moldawer LL.** B cells enhance early innate immune responses during bacterial sepsis. *J Exp Med* 208: 1673–1682, 2011.
27. **Kitamura D, Roes J, Kuhn R, Rajewsky K.** A B cell-deficient mouse by targeted disruption of the membrane exon of the immunoglobulin mu chain gene. *Nature* 350: 423–426, 1991.
28. **Kroese FG, Timens W, Nieuwenhuis P.** Germinal center reaction and B lymphocytes: morphology and function. *Curr Top Pathol* 84: 103–148, 1990.
29. **Litsiou E, Semitekolou M, Galani IE, Morianos I, Tsoutsa A, Kara P, Rontogianni D, Bellenis I, Konstantinou M, Potaris K, Andreakos E, Sideras P, Zakynthinos S, Tsoumakidou M.** CXCL13 production in B cells via Toll-like receptor/lymphotoxin receptor signaling is involved in lymphoid neogenesis in chronic obstructive pulmonary disease. *Am J Respir Crit Care Med* 187: 1194–1202, 2013.
30. **Lucey EC, Keane J, Kuang PP, Snider GL, Goldstein RH.** Severity of elastase-induced emphysema is decreased in tumor necrosis factor-alpha and interleukin-1beta receptor-deficient mice. *Lab Invest* 82: 79–85, 2002.
31. **Minoprio P, el Cheikh MC, Murphy E, Hontebeyrie-Joskowicz M, Coffman R, Coutinho A, O'Garra A.** Xid-associated resistance to experimental Chagas' disease is IFN-gamma dependent. *J Immunol* 151: 4200–4208, 1993.
32. **Moseman EA, Iannacone M, Bosurgi L, Tonti E, Chevrier N, Tumanov A, Fu YX, Hacohen N, von Andrian UH.** B cell maintenance of subcapsular sinus macrophages protects against a fatal viral infection independent of adaptive immunity. *Immunity* 36: 415–426, 2012.
33. **Motallebzadeh R, Rehakova S, Conlon TM, Win TS, Callaghan CJ, Goddard M, Bolton EM, Ruddle NH, Bradley JA, Pettigrew GJ.** Blocking lymphotoxin signaling abrogates the development of ectopic lymphoid tissue within cardiac allografts and inhibits effector antibody responses. *FASEB J* 26: 51–62, 2012.
34. **Moyron-Quiroz JE, Rangel-Moreno J, Kusser K, Hartson L, Sprague F, Goodrich S, Woodland DL, Lund FE, Randall TD.** Role of inducible bronchus associated lymphoid tissue (iBALT) in respiratory immunity. *Nat Med* 10: 927–934, 2004.
35. **Oliveira HC, Popi AF, Bachi AL, Nonogaki S, Lopes JD, Mariano M.** B-1 cells modulate the kinetics of wound-healing process in mice. *Immunobiology* 215: 215–222, 2010.
36. **Pauwels RA, Buist AS, Calverley PM, Jenkins CR, Hurd SS.** Global strategy for the diagnosis, management, and prevention of chronic obstructive pulmonary disease. NHLBI/WHO Global Initiative for Chronic Obstructive Lung Disease (GOLD) Workshop summary. *Am J Respir Crit Care Med* 163: 1256–1276, 2001.
37. **Perros F, Dorfmuller P, Montani D, Hammad H, Waelput W, Girerd B, Raymond N, Mercier O, Mussot S, Cohen-Kaminsky S, Humbert M, Lambrecht BN.** Pulmonary lymphoid neogenesis in idiopathic pulmonary arterial hypertension. *Am J Respir Crit Care Med* 185: 311–321, 2012.
38. **Popi AF, Godoy LC, Xander P, Lopes JD, Mariano M.** B-1 cells facilitate *Paracoccidioides brasiliensis* infection in mice via IL-10 secretion. *Microbes Infect* 10: 817–824, 2008.
39. **Popi AF, Lopes JD, Mariano M.** Interleukin-10 secreted by B-1 cells modulates the phagocytic activity of murine macrophages in vitro. *Immunology* 113: 348–354, 2004.

39a. **R Development Core Team.** *R: a language and environment for statistical computing*. Vienna, Austria: R Foundation for Statistical Computing, 2013. ISBN 3-900051-07-0; http://www.R-project.org.

40. **Rainer J, Sanchez-Cabo F, Stocker G, Sturn A, Trajanoski Z.** CARMAweb: comprehensive R- and bioconductor-based web service for microarray data analysis. *Nucleic Acids Res* 34: W498–W503, 2006.

41. **Randall TD.** Bronchus-associated lymphoid tissue (BALT) structure and function. *Adv Immunol* 107: 187–241, 2010.
42. **Rangel-Moreno J, Hartson L, Navarro C, Gaxiola M, Selman M, Randall TD.** Inducible bronchus-associated lymphoid tissue (iBALT) in patients with pulmonary complications of rheumatoid arthritis. *J Clin Invest* 116: 3183–3194, 2006.
43. **Rangel-Moreno J, Moyron-Quiroz JE, Hartson L, Kusser K, Randall TD.** Pulmonary expression of CXC chemokine ligand 13, CC chemokine ligand 19, and CC chemokine ligand 21 is essential for local immunity to influenza. *Proc Natl Acad Sci USA* 104: 10577–10582, 2007.
44. **Saetta M, Di Stefano A, Turato G, Facchini FM, Corbino L, Mapp CE, Maestrelli P, Ciaccia A, Fabbri LM.** CD8+ T-lymphocytes in peripheral airways of smokers with chronic obstructive pulmonary disease. *Am J Respir Crit Care Med* 157: 822–826, 1998.
45. **Saetta M, Turato G, Facchini FM, Corbino L, Lucchini RE, Casoni G, Maestrelli P, Mapp CE, Ciaccia A, Fabbri LM.** Inflammatory cells in the bronchial glands of smokers with chronic bronchitis. *Am J Respir Crit Care Med* 156: 1633–1639, 1997.
46. **Stevenson CS, Docx C, Webster R, Battram C, Hynx D, Giddings J, Cooper PR, Chakravarty P, Rahman I, Marwick JA, Kirkham PA, Charman C, Richardson DL, Nirmala NR, Whittaker P, Butler K.** Comprehensive gene expression profiling of rat lung reveals distinct acute and chronic responses to cigarette smoke inhalation. *Am J Physiol Lung Cell Mol Physiol* 293: L1183–L1193, 2007.
47. **Takahashi Y, Horiyama S, Honda C, Suwa K, Nakamura K, Kunitomo M, Shimma S, Toyoda M, Sato H, Shizuma M, Takayama M.** A chemical approach to searching for bioactive ingredients in cigarette smoke. *Chem Pharm Bull (Tokyo)* 61: 85–89, 2013.
49. **Tetley TD.** Inflammatory cells and chronic obstructive pulmonary disease. *Curr Drug Targets Inflamm Allergy* 4: 607–618, 2005.
50. **Thun MJ, Carter BD, Feskanich D, Freedman ND, Prentice R, Lopez AD, Hartge P, Gapstur SM.** 50-Year trends in smoking-related mortality in the United States. *N Engl J Med* 368: 351–364, 2013.
51. **van de Veerdonk FL, Lauwerys B, Marijnissen RJ, Timmermans K, Di Padova F, Koenders MI, Gutierrez-Roelens I, Durez P, Netea MG, van der Meer JW, van den Berg WB, Joosten LA.** The anti-CD20 antibody rituximab reduces the Th17 cell response. *Arthritis Rheum* 63: 1507–1516, 2011.
52. **van der Strate BW, Postma DS, Brandsma CA, Melgert BN, Luinge MA, Geerlings M, Hylkema MN, van den Berg A, Timens W, Kerstjens HA.** Cigarette smoke-induced emphysema: a role for the B cell? *Am J Respir Crit Care Med* 173: 751–758, 2006.
53. **Vestbo J, Hurd SS, Agusti AG, Jones PW, Vogelmeier C, Anzueto A, Barnes PJ, Fabbri LM, Martinez FJ, Nishimura M, Stockley RA, Sin DD, Rodriguez-Roisin R.** Global strategy for the diagnosis, management, and prevention of chronic obstructive pulmonary disease: GOLD executive summary. *Am J Respir Crit Care Med* 187: 347–365, 2013.
54. **Wan WY, Morris A, Kinnear G, Pearce W, Mok J, Wyss D, Stevenson CS.** Pharmacological characterisation of anti-inflammatory compounds in acute and chronic mouse models of cigarette smoke-induced inflammation. *Respir Res* 11: 126, 2010.
55. **Weber MS, Prod'homme T, Patarroyo JC, Molnarfi N, Karnezis T, Lehmann-Horn K, Danilenko DM, Eastham-Anderson J, Slavin AJ, Linington C, Bernard CC, Martin F, Zamvil SS.** B-cell activation influences T-cell polarization and outcome of anti-CD20 B-cell depletion in central nervous system autoimmunity. *Ann Neurol* 68: 369–383, 2010.
56. **Wong SC, Puaux AL, Chittezhath M, Shalova I, Kajiji TS, Wang X, Abastado JP, Lam KP, Biswas SK.** Macrophage polarization to a unique phenotype driven by B cells. *Eur J Immunol* 40: 2296–2307, 2010.
57. **Yadava K, Marsland BJ.** Lymphoid follicles in chronic lung diseases. *Thorax* 68: 597–598, 2013.
58. **Ye J, Coulouris G, Zaretskaya I, Cutcutache I, Rozen S, Madden TL.** Primer-BLAST: a tool to design target-specific primers for polymerase chain reaction. *BMC Bioinformatics* 13: 134, 2012.
59. **Yildirim AO, Muyal V, John G, Muller B, Seifart C, Kasper M, Fehrenbach H.** Palifermin induces alveolar maintenance programs in emphysematous mice. *Am J Respir Crit Care Med* 181: 705–717, 2010.

6 Bibliography

Aaron, S.D., Angel, J.B., Lunau, M., Wright, K., Fex, C., Saux, N.L., and Dales, R.E. (2001). Granulocyte inflammatory markers and airway infection during acute exacerbation of chronic obstructive pulmonary disease. American Journal of Respiratory and Critical Care Medicine *163*, 349–355.

Agapov, E., Battaile, J.T., Tidwell, R., Hachem, R., Patterson, G.A., Pierce, R.A., Atkinson, J.J., and Holtzman, M.J. (2009). Macrophage chitinase 1 stratifies chronic obstructive lung disease. Am. J. Respir. Cell Mol. Biol. *41*, 379–384.

Aloisi, F., and Pujol-Borrell, R. (2006). Lymphoid neogenesis in chronic inflammatory diseases. Nat. Rev. Immunol. *6*, 205–217.

Andreu, P., Johansson, M., Affara, N.I., Pucci, F., Tan, T., Junankar, S., Korets, L., Lam, J., Tawfik, D., DeNardo, D.G., et al. (2010). FcRgamma activation regulates inflammation-associated squamous carcinogenesis. Cancer Cell *17*, 121–134.

Armengol, M.P., Juan, M., Lucas-Martín, A., Fernández-Figueras, M.T., Jaraquemada, D., Gallart, T., and Pujol-Borrell, R. (2001). Thyroid autoimmune disease: demonstration of thyroid antigen-specific B cells and recombination-activating gene expression in chemokine-containing active intrathyroidal germinal centers. Am. J. Pathol. *159*, 861–873.

ATS (1962). [ATS] Committee on Diagnostic Standards for Nontuberculous Respiratory Diseases, American Thoracic Society. Definitions and classification of chronic bronchitis, asthma, and pulmonary emphysema. . *85*, 762–769.

Baggiolini, M, Dewald, B, and Moser, B (1997). Human chemokines: an update. Annual Review of Immunology *15*, 675-705.

Barnes, P. (2008). The cytokine network in asthma and chronic obstructive pulmonary disease. J. Clin. Invest. *118*, 3546–3556.

Barnes, P. (2009). The cytokine network in chronic obstructive pulmonary disease. Am. J. Respir. Cell Mol. Biol. *41*, 631–638.

Barnes, P.J., Shapiro, S.D., and Pauwels, R.A. (2003). Chronic obstructive pulmonary disease: molecular and cellularmechanisms. European Respiratory Journal *22*, 672–688.

Becker, S, Soukup, JM, and Gallagher, JE (2002). Differential particulate air pollution induced oxidant stress in human granulocytes, monocytes and alveolar macrophages. Toxicology in Vitro *16*, 209–218.

Berenson, C., Garlipp, M., Grove, L., Maloney, J., and Sethi, S. (2006). Impaired Phagocytosis of NontypeableHaemophilus influenzaeby Human Alveolar Macrophages in Chronic Obstructive Pulmonary Disease. J infect dis. *194*, 1375-1384.

Bhowmik, A., Seemungal, T.A., Sapsford, R.J., and Wedzicha, J.A. (2000). Relation of sputum inflammatory markers to symptoms and lung function changes in COPD exacerbations. Thorax *55*, 114–120.

Biswas, S.K., and Mantovani, A. (2010). Macrophage plasticity and interaction with lymphocyte subsets: cancer as a paradigm. Nat. Immunol. *11*, 889–896.

Boorsma, C.E., Draijer, C., and Melgert, B.N. (2013). Macrophage heterogeneity in respiratory diseases. Mediators Inflamm. *2013*, 769214.

Botelho, FM, Nikota, JK, and Bauer, C (2011). A mouse GM-CSF receptor antibody attenuates neutrophilia in mice exposed to cigarette smoke. Eur Respir J. *38*, 285-294.

Bracke, K.R., Verhamme, F.M., Seys, L.J., Bantsimba-Malanda, C., Cunoosamy, D.M., Herbst, R., Hammad, H., Lambrecht, B.N., Joos, G.F., and Brusselle, G.G. (2013). Role of CXCL13 in cigarette smoke-induced lymphoid follicle formation and chronic obstructive pulmonary disease. Am. J. Respir. Crit. Care Med. *188*, 343–355.

Brandsma, CA, Hylkema, MN, and Geerlings, M (2009). Increased levels of (class switched) memory B cells in peripheral blood of current smokers. Respir Res. *10*:108.

Brandsma, C.A., Kerstjens, H.A., Geerlings, M., Kerkhof, M., Hylkema, M.N., Postma, D.S., and Timens, W. (2011). The search for autoantibodies against elastin, collagen and decorin in COPD. Eur. Respir. J. *37*, 1289–1292.

Brusselle, G.G. (2009). Matrix metalloproteinase 12, asthma, and COPD. N. Engl. J. Med. *361*, 2664–2665.

Brusselle, G., Demoor, T., Bracke, K., Brandsma, C.-A., and Timens, W. (2009). Lymphoid follicles in (very) severe COPD: beneficial or harmful? Eur. Respir. J. *34*, 219–230.

Brusselle, G.G., Joos, G.F., and Bracke, K.R. (2011). New insights into the immunology of chronic obstructive pulmonary disease. Lancet *378*, 1015–1026.

Bucchioni, E., Kharitonov, S.A., Allegra, L., and Barnes, P.J. (2003). High levels of interleukin-6 in the exhaled breath condensate of patients with COPD. Respir Med *97*, 1299–1302.

Buist, A.S., McBurnie, M.A., Vollmer, W.M., Gillespie, S., Burney, P., Mannino, D.M., Menezes, A.M., Sullivan, S.D., Lee, T.A., Weiss, K.B., et al. (2007). International variation in the prevalence of COPD (the BOLD Study): a population-based prevalence study. Lancet *370*, 741–750.

Burge, S., and Wedzicha, J.A. (2003). COPD exacerbations: definitions and classifications. Eur Respir J Suppl *41*, 46s–53s.

Cassatella, MA, Meda, L, Bonora, S, and Ceska, M (1993). Interleukin 10 (IL-10) inhibits the release of proinflammatory cytokines from human polymorphonuclear leukocytes. Evidence for an autocrine role of tumor necrosis factor and IL-1 beta in mediating the production of IL-8 triggered by lipopolysaccharide. J. Exp. Med. *178*, 2207-2211.

Caughey, GH (1994). Serine proteinases of mast cell and leukocyte granules. Am J Respir Crit Care Med. *150*, 138-142.

Celli, BR, and Barnes, PJ (2007). Exacerbations of chronic obstructive pulmonary disease. European Respiratory Journal *29*, 1224–1238.

Chung, K.F., and Adcock, I.M. (2008). Multifaceted mechanisms in COPD: inflammation, immunity, and tissue repair and destruction. Eur. Respir. J. *31*, 1334–1356.

Churg, A, and Wright, JL (2005). Proteases and emphysema. Current Opinion in Pulmonary Medicine *11*, 153-159.

Churg, A, Wang, RD, Tai, H, Wang, X, and Xie, C (2004). Tumor necrosis factor-α drives 70% of cigarette smoke–induced emphysema in the mouse. Am J Respir Crit Care Med. *170*, 492-498

Cohen, D, Arai, SF, and Brain, JD (1979). Smoking impairs long-term dust clearance from the lung. Science *204*, 514-517.

Colebatch, H.J., Finucane, K.E., and Smith, M.M. (1973). Pulmonary conductance and elastic recoil relationships in asthma and emphysema. J Appl Physiol. *34*, 143–153.

Cosio, M., Ghezzo, H., Hogg, J.C., Corbin, R., Loveland, M., Dosman, J., and Macklem, P.T. (1978). The relations between structural changes in small airways and pulmonary-function tests. N. Engl. J. Med. *298*, 1277–1281.

Cosio, M., Majo, J., and Cosio, M. (2002). Inflammation of the Airways and Lung Parenchyma in COPD* : Role of T Cells. Chest *121*, 160S–165.

Cottin, V, Fabien, N, and Khouatra, C (2009). Anti-elastin autoantibodies are not present in combined pulmonary fibrosis and emphysema. Eur Respir J. *33*, 219-221.

Culpitt, SV, Rogers, DF, and Shah, P (2003). Impaired inhibition by dexamethasone of cytokine release by alveolar macrophages from patients with chronic obstructive pulmonary disease. Am J Respir Crit Care Med. *167*, 24-31.

Curtis, J.L., Freeman, C.M., and Hogg, J.C. (2007). The immunopathogenesis of chronic obstructive pulmonary disease: insights from recent research. Proc Am Thorac Soc *4*, 512–521.

Demirjian, L, Abboud, RT, Li, H, and Duronio, V (2006). Acute effect of cigarette smoke on TNF-α release by macrophages mediated through the erk1/2 pathway. Biochim Biophys Acta. *1762*, 592-597.

Demoor, T., Bracke, K.R., Vermaelen, K.Y., Dupont, L., Joos, G.F., and Brusselle, G.G. (2009). CCR7 modulates pulmonary and lymph node inflammatory responses in cigarette smoke-exposed mice. J. Immunol. *183*, 8186–8194.

Dennis, R.J., Maldonado, D., Norman, S., Baena, E., and Martinez, G. (1996). Woodsmoke exposure and risk for obstructive airways disease among women. Chest *109*, 115–119.

Deshmane, SL, Kremlev, S, and Amini, S (2009). Monocyte chemoattractant protein-1 (MCP-1): an overview. J Interferon Cytokine Res. *29*, 313-326.

DiLillo, D.J., Horikawa, M., and Tedder, T.F. (2011). B-lymphocyte effector functions in health and disease. Immunol. Res. *49*, 281–292.

Doz, E, Noulin, N, Boichot, E, and Guénon, I (2008). Cigarette smoke-induced pulmonary inflammation is TLR4/MyD88 and IL-1R1/MyD88 signaling dependent. J Immunol. *180*, 1169-1178.

D'hulst, A.I., Vermaelen, K.Y., Brusselle, G.G., Joos, G.F., and Pauwels, R.A. (2005a). Time course of cigarette smoke-induced pulmonary inflammation in mice. Eur. Respir. J. *26*, 204–213.

D'hulst, A.I., Maes, T., Bracke, K.R., Demedts, I.K., Tournoy, K.G., Joos, G.F., and Brusselle, G.G. (2005b). Cigarette smoke-induced pulmonary emphysema in scid-mice. Is the acquired immune system required? Respir. Res. *6*, 147.

Epstein, F.H., Border, W.A., and Noble, N.A. (1994). Transforming growth factor in tissue fibrosis. New England Journal of Medicine *331*, 1286–1292.

Facchinetti, F, Amadei, F, and Geppetti, P (2007). α, β-unsaturated aldehydes in cigarette smoke release inflammatory mediators from human macrophages. Am J Respir Cell Mol Biol. *37*, 617-623.

Feghali-Bostwick, CA, and Gadgil, AS (2008). Autoantibodies in patients with chronic obstructive pulmonary disease. Am J Respir Crit Care Med. *177*, 156-163.

Fillatreau, S, Sweenie, CH, McGeachy, MJ, and Gray, D (2002). B cells regulate autoimmunity by provision of IL-10. Nat Immunol. *3*, 944-950.

Finkelstein, R, Fraser, RS, and Ghezzo, H (1995). Alveolar inflammation and its relation to emphysema in smokers. Am J Respir Crit Care Med. *152*, 1666-1672.

Fletcher, C., Peto, R., Tinker, C., and Speizer, F.E. (1976). The natural history of chronic bronchitis and emphysema. An eight-year study of early chronic obstructive lung disease in working men in London. Oxford: Oxford University Press.

Fujii, T, Hayashi, S, Hogg, JC, and Vincent, R (2001). Particulate matter induces cytokine expression in human bronchial epithelial cells. Am J Respir Cell Mol Biol. *25*, 265-271.

Fujii, T, Hayashi, S, Hogg, JC, and Mukae, H (2002). Interaction of alveolar macrophages and airway epithelial cells following exposure to particulate matter produces mediators that stimulate the bone marrow. Am J Respir Cell Mol Biol. *27*, 34-41.

Fujita, M, Shannon, JM, and Irvin, CG (2001). Overexpression of tumor necrosis factor-α produces an increase in lung volumes and pulmonary hypertension. American Journal of ….

Fuke, S., Betsuyaku, T., Nasuhara, Y., Morikawa, T., Katoh, H., and Nishimura, M. (2004). Chemokines in bronchiolar epithelium in the development of chronic obstructive pulmonary disease. Am. J. Respir. Cell Mol. Biol. *31*, 405–412.

Gershon, A.S., Wang, C., Wilton, A.S., Raut, R., and To, T. (2010). Trends in chronic obstructive pulmonary disease prevalence, incidence, and mortality in ontario, Canada, 1996 to 2007: a population-based study. Arch. Intern. Med. *170*, 560–565.

Gilmour, PS, Rahman, I, and Hayashi, S (2001). Adenoviral E1A primes alveolar epithelial cells to PM10-induced transcription of interleukin-8. Am J Physiol Lung Cell Mol Physiol. *281*, L598-606.

Gordon, S. (2003). Alternative activation of macrophages. Nat Rev Immunol *3*, 23–35.

Gosman, M.M., Willemse, B.W., Jansen, D.F., Lapperre, T.S., Schadewijk, A., Hiemstra, P.S., Postma, D.S., Timens, W., and Kerstjens, H. (2006). Increased number of B-cells in bronchial biopsies in COPD. European Respiratory Journal *27*, 60–64.

Green, GM, Jakab, GJ, and Low, RB (1977). Defense mechanisms of the respiratory membrane. Am Rev Respir Dis. *115*, 479-514.

Greene, C., Low, T., O'Neill, S., and McElvaney, N. (2010). Anti–Proline-Glycine-Proline or Antielastin Autoantibodies Are Not Evident in Chronic Inflammatory Lung Disease. Am J Respir Crit Care Med *181*, 3135.

Grumelli, S., Corry, D.B., Song, L.-Z., Song, L., Green, L., Huh, J., Hacken, J., Espada, R., Bag, R., and Lewis, D.E. (2004). An immune basis for lung parenchymal destruction in chronic obstructive pulmonary disease and emphysema. PLoS Medicine *1*, e8.

Hall, M., DeFrances, C.J., Williams, S.N., Golosinskiy, A., and Schwartzman, A. (2010). National hospital discharge survey: 2007 summary. Natl Health Stat Report *29*, 1–20.

Harris, DP, Goodrich, S, and Gerth, AJ (2005). Regulation of IFN-γ production by B effector 1 cells: essential roles for T-bet and the IFN-γ receptor. J Immunol. *174*, 6781-6790.

Hautamaki, R.D., Kobayashi, D.K., Senior, R.M., and Shapiro, S.D. (1997). Requirement for macrophage elastase for cigarette smoke-induced emphysema in mice. Science *277*, 2002–2004.

Hjelmström, P. (2001). Lymphoid neogenesis: de novo formation of lymphoid tissue in chronic inflammation through expression of homing chemokines. J. Leukoc. Biol. *69*, 331–339.

Hogg, JC (2004). Pathophysiology of airflow limitation in chronic obstructive pulmonary disease. The Lancet *364*, 709-721.

Hogg, JC (2008). Lung structure and function in COPD [State of the Art Series. Chronic obstructive pulmonary disease in high-and low-income countries. Edited by G. Marks and M. Chang-Yeung. Int. J. Tuberc. Lung Dis. *12*, 467-479.

Hogg, J.C., Chu, F., Utokaparch, S., Woods, R., Elliott, W.M., Buzatu, L., Cherniack, R.M., Rogers, R.M., Sciurba, F.C., Coxson, H.O., et al. (2004). The nature of small-airway obstruction in chronic obstructive pulmonary disease. N. Engl. J. Med. *350*, 2645–2653.

Howard, D.J., Briggs, L.A., and Pritsos, C.A. (1998). Oxidative DNA damage in mouse heart, liver, and lung tissue due to acute side-stream tobacco smoke exposure. Arch. Biochem. Biophys. *352*, 293–297.

Hulbert, W.C., Walker, D.C., Jackson, A., and Hogg, J.C. (1981). Airway permeability to horseradish peroxidase in guinea pigs: the repair phase after injury by cigarette smoke. Am. Rev. Respir. Dis. *123*, 320–326.

Imaoka, H, Hoshino, T, and Takei, S (2008). Interleukin-18 production and pulmonary function in COPD. Eur Respir J. *31*, 287-297.

Ito, K. (2009). COPD as a Disease of Accelerated Lung Aging. CHEST Journal *135*, 173.

Johnson, MD, Schilz, J, Djordjevic, MV, and Rice, JR (2009). Evaluation of in vitro assays for assessing the toxicity of cigarette smoke and smokeless tobacco. Cancer Epidemiol Biomarkers Prev. *18*, 3263-3304.

Jones, J.G., Minty, B.D., Lawler, P., Hulands, G., Crawley, J.C., and Veall, N. (1980). Increased alveolar epithelial permeability in cigarette smokers. Lancet *1*, 66–68.

Kao, C.-Y.Y., Chen, Y., Thai, P., Wachi, S., Huang, F., Kim, C., Harper, R.W., and Wu, R. (2004). IL-17 markedly up-regulates beta-defensin-2 expression in human airway epithelium via JAK and NF-kappaB signaling pathways. J. Immunol. *173*, 3482–3491.

Karimi, K, Sarir, H, Mortaz, E, Smit, JJ, and Hosseini, H (2006). Toll-like receptor-4 mediates cigarette smoke-induced cytokine production by human macrophages. Respir Res. *7*:66.

Keatings, V.M., Collins, P.D., Scott, D.M., and Barnes, P.J. (1996). Differences in interleukin-8 and tumor necrosis factor-alpha in induced sputum from patients with chronic obstructive pulmonary disease or asthma. American Journal of Respiratory and Critical Care Medicine *153*, 530–534.

Kim, E., Battaile, J., Patel, A., You, Y., Agapov, E., Grayson, M., Benoit, L., Byers, D., Alevy, Y., Tucker, J., et al. (2008). Persistent activation of an innate immune response translates respiratory viral infection into chronic lung disease. Nat Med. *14*, 633-640.

Knowles, MR, and Boucher, RC (2002). Mucus clearance as a primary innate defense mechanism for mammalian airways. J Clin Invest. *109*, 571-577.

Kocks, J.R., Davalos-Misslitz, A.C., Hintzen, G., Ohl, L., and Förster, R. (2007). Regulatory T cells interfere with the development of bronchus-associated lymphoid tissue. J. Exp. Med. *204*, 723–734.

Krausgruber, T., Blazek, K., Smallie, T., Alzabin, S., Lockstone, H., Sahgal, N., Hussell, T., Feldmann, M., and Udalova, I.A. (2011). IRF5 promotes inflammatory macrophage polarization and TH1-TH17 responses. Nat. Immunol. *12*, 231–238.

Kroese, F., Timens, W, and Nieuwenhuis, P (1990). Germinal center reaction and B lymphocytes: morphology and function. Reaction Patterns of the Lymph Node. Curr. Top. Pathol. *84*, 103-148.

Kumar, V., Abbas, A.K., and Fausto, N. (2005). Acute and chronic inflammation. (Robbins and Cortran pathological basis of disease: Elesvier Saunders), pp. 47–86.

Lacoste, J.Y., Bousquet, J., Chanez, P., Van Vyve, T., Simony-Lafontaine, J., Lequeu, N., Vic, P., Enander, I., Godard, P., and Michel, F.B. (1993). Eosinophilic and neutrophilic inflammation in asthma, chronic bronchitis, and chronic obstructive pulmonary disease. J. Allergy Clin. Immunol. *92*, 537–548.

Lappalainen, U., Whitsett, J., Wert, S., Tichelaar, J., and Bry, K. (2005). Interleukin-1β Causes Pulmonary Inflammation, Emphysema, and Airway Remodeling in the Adult Murine Lung. American Journal of Respiratory Cell and Molecular Biology *32*, 311–318.

Leberl, M., Kratzer, A., and Taraseviciene-Stewart, L. (2013). Tobacco smoke induced COPD/emphysema in the animal model-are we all on the same page? Front Physiol *4*, 91.

Lee, S.-H.H., Goswami, S., Grudo, A., Song, L.-Z.Z., Bandi, V., Goodnight-White, S., Green, L., Hacken-Bitar, J., Huh, J., Bakaeen, F., et al. (2007). Antielastin autoimmunity in tobacco smoking-induced emphysema. Nat. Med. *13*, 567–569.

Lieberman, J (2003). The ABCs of granule-mediated cytotoxicity: new weapons in the arsenal. Nat Rev Immunol. *3*, 361-370.

Litsiou, E., Semitekolou, M., Galani, I.E., Morianos, I., Tsoutsa, A., Kara, P., Rontogianni, D., Bellenis, I., Konstantinou, M., Potaris, K., et al. (2013). CXCL13 production in B cells via Toll-like receptor/lymphotoxin receptor signaling is involved in lymphoid neogenesis in chronic obstructive pulmonary disease. Am. J. Respir. Crit. Care Med. *187*, 1194–1202.

MacLennan, I. (1994). Germinal centers. Annu. Rev. Immunol. *30*, 429-457.

MacNee, W (2005). Pathogenesis of chronic obstructive pulmonary disease. Proc Am Thorac Soc. *2*, 258-266.

Mahadeva, R., and Shapiro, S.D. (2002). Chronic obstructive pulmonary disease * 3: Experimental animal models of pulmonary emphysema. Thorax *57*, 908–914.

Majo, J, Ghezzo, H, and Cosio, MG (2001). Lymphocyte population and apoptosis in the lungs of smokers and their relation to emphysema. Eur Respir J. *17*, 946-953.

Manzo, A., Paoletti, S., Carulli, M., Blades, M.C., Barone, F., Yanni, G., Fitzgerald, O., Bresnihan, B., Caporali, R., Montecucco, C., et al. (2005). Systematic microanatomical analysis of CXCL13 and CCL21 in situ production and progressive lymphoid organization in rheumatoid synovitis. Eur. J. Immunol. *35*, 1347–1359.

Martinez, F., Helming, L., and Gordon, S. (2009). Alternative activation of macrophages: an immunologic functional perspective. Annu. Rev. Immunol. *27*, 451–483.

Matera, M., Calzetta, L., and Cazzola, M. (2010). TNF-α inhibitors in asthma and COPD: We must not throw the baby out with the bath water. Pulm. Pharmacol. Ther. *23*, 121–128.

Mathers, C, Fat, DM, and Boerma, JT (2008). The global burden of disease: 2004 update.

Mead, J., Turner, J.M., Macklem, P.T., and Little, J.B. (1967). Significance of the relationship between lung recoil and maximum expiratory flow. J Appl Physiol *22*, 95–108.

Miossec, P, Korn, T, and Kuchroo, VK (2009). Interleukin-17 and type 17 helper T cells. N Engl J Med. *361*, 888-898.

Montuschi, P., Collins, J.V., Ciabattoni, G., Lazzeri, N., Corradi, M., Kharitonov, S.A., and Barnes, P.J. (2000). Exhaled 8-isoprostane as an in vivo biomarker of lung oxidative stress in patients with COPD and healthy smokers. Am. J. Respir. Crit. Care Med. *162*, 1175–1177.

Moore, KW, O'garra, A, and Malefyt, RW (1993). Interleukin-10. Annu. Rev. Immunol. *11*, 165-190.

Morissette, M.C., Jobse, B.N., Thayaparan, D., Nikota, J.K., Shen, P., Labiris, N.R., Kolbeck, R., Nair, P., Humbles, A.A., and Stämpfli, M.R. (2014). Persistence of pulmonary tertiary lymphoid tissues and anti-nuclear antibodies following cessation of cigarette smoke exposure. Respir. Res. *15*, 49.

Moritsugu, K.P. (2007). The 2006 Report of the Surgeon General: the health consequences of involuntary exposure to tobacco smoke. Am J Prev Med *32*, 542–543.

Morris, A., Kinnear, G., Wan, W.-Y., Wyss, D., Bahra, P., and Stevenson, C. (2008). Comparison of cigarette smoke-induced acute inflammation in multiple strains of mice and the effect of a matrix metalloproteinase inhibitor on these responses. J. Pharmacol. Exp. Ther. *327*, 851–862.

Moseman, E.A., Iannacone, M., Bosurgi, L., Tonti, E., Chevrier, N., Tumanov, A., Fu, Y.-X.X., Hacohen, N., and von Andrian, U.H. (2012). B cell maintenance of subcapsular sinus

macrophages protects against a fatal viral infection independent of adaptive immunity. Immunity *36*, 415–426.

Mosser, D., and Edwards, J. (2008). Exploring the full spectrum of macrophage activation. Nat Rev Immunol. *8*, 958-969.

Mullen, J.B., Wright, J.L., Wiggs, B.R., Pare, P.D., and Hogg, J.C. (1985). Reassessment of inflammation of airways in chronic bronchitis. Br Med J (Clin Res Ed) *291*, 1235–1239.

Nadel, JA (2000). Role of neutrophil elastase in hypersecretion during COPD exacerbations, and proposed therapies. CHEST Journal. *117*, 386S-389S

O'Shaughnessy, TC, and Ansari, TW (1997). Inflammation in bronchial biopsies of subjects with chronic bronchitis: inverse relationship of CD8+ T lymphocytes with FEV1. Am J Respir Crit Care Med. *155*, 852-857.

Paredi, P., Kharitonov, A.S., Leak, D., Ward, S., Cramer, D., and Barnes , P.J. Exhaled ethane, a marker of lipid peroxidation, is elevated in chronic obstructive pulmonary disease. *162*, 1175–1177.

Pauwels, RA, and Rabe, KF (2004). Burden and clinical features of chronic obstructive pulmonary disease (COPD). The Lancet *364*, 613-620.

Pauwels, R.A., Buist, A.S., Calverley, P.M., Jenkins, C.R., and Hurd, S.S. (2001). Global strategy for the diagnosis, management, and prevention of chronic obstructive pulmonary disease. NHLBI/WHO Global Initiative for Chronic Obstructive Lung Disease (GOLD) Workshop summary. Am. J. Respir. Crit. Care Med. *163*, 1256–1276.

Penman, R.W., O'Neill, R.P., and Begley, L. (1970). The progress of chronic airway obstruction in relation to measurements of airway resistance and lung elastic recoil. Am. Rev. Respir. Dis. *101*, 536–544.

Pistoia, V (1997). Production of cytokines by human B cells in health and disease. Immunol. Today *18*, 343-350.

Popi, A., Lopes, J., and Mariano, M. (2004). Interleukin-10 secreted by B-1 cells modulates the phagocytic activity of murine macrophages in vitro. Immunology *113*, 348–354.

Prieto, A, Reyes, E, and Bernstein, ED (2001). Defective natural killer and phagocytic activities in chronic obstructive pulmonary disease are restored by glycophosphopeptical (inmunoferon). Am J Respir Crit Care Med. *163*, 1578-1583.

Quement, L.C., Guenon, I, and Gillon, JY (2008). The selective MMP-12 inhibitor, AS111793 reduces airway inflammation in mice exposed to cigarette smoke. Br J Pharmacol. *154*, 1206-1215.

Rabe, KF, Hurd, S, Anzueto, A, and Barnes, PJ (2007). Global strategy for the diagnosis, management, and prevention of chronic obstructive pulmonary disease: GOLD executive summary. Am J Respir Crit Care Med. *176*, 532-555.

Rahman, I., van Schadewijk, A., Crowther, A., Hiemstra, P., Stolk, J., MacNee, W., and Boer, W. (2002). 4-Hydroxy-2-Nonenal, a Specific Lipid Peroxidation Product, Is Elevated in Lungs of Patients with Chronic Obstructive Pulmonary Disease. American Journal of Respiratory and Critical Care Medicine *166*, 490–495.

Randall, T.D. (2010). Bronchus-associated lymphoid tissue (BALT) structure and function. Adv. Immunol. *107*, 187–241.

Reid, L. (1960). Measurement of the bronchial mucous gland layer: a diagnostic yardstick in chronic bronchitis. Thorax *15*, 132–141.

Rennard, S. (2007). Inflammation in COPD: a link to systemic comorbidities. European Respiratory Review *16*, 91–97.

Rodriguez-Roisin, R., Drakulovic, M., Rodríguez, D.A., Roca, J., Barbera, J., and Wagner, P.D. (2009). Ventilation-perfusion imbalance and chronic obstructive pulmonary disease staging severity. Journal of Applied Physiology *106*, 1902–1908.

Rogliani, P, Calzetta, L, Ora, J, and Matera, MG (2015). Canakinumab for the treatment of chronic obstructive pulmonary disease. Pulm. Pharmacol. Ther. *31*, 15-27.

Rutgers, SR, Postma, DS, and Hacken, N. (2000). Ongoing airway inflammation in patients with COPD who do not currently smoke. Thorax *55*, 12-18.

Saetta, M, Baraldo, S, Corbino, L, and Turato, G (1999). CD8+ ve cells in the lungs of smokers with chronic obstructive pulmonary disease. Am J Respir Crit Care Med. *160*, 711-717.

Saetta, M., Di Stefano, A., Maestrelli, P., Ferraresso, A., Drigo, R., Potena, A., Ciaccia, A., and Fabbri, L.M. (1993). Activated T-lymphocytes and macrophages in bronchial mucosa of subjects with chronic bronchitis. Am. Rev. Respir. Dis. *147*, 301–306.

Saetta, M., Turato, G., Facchini, F.M., Corbino, L., Lucchini, R.E., Casoni, G., Maestrelli, P., Mapp, C.E., Ciaccia, A., and Fabbri, L.M. (1997). Inflammatory cells in the bronchial glands of smokers with chronic bronchitis. Am. J. Respir. Crit. Care Med. *156*, 1633–1639.

Salomonsson, S., Jonsson, M.V., Skarstein, K., Brokstad, K.A., Hjelmström, P., Wahren-Herlenius, M., and Jonsson, R. (2003). Cellular basis of ectopic germinal center formation and autoantibody production in the target organ of patients with Sjögren's syndrome. Arthritis Rheum. *48*, 3187–3201.

Sapey, E., Ahmad, A., Bayley, D., Newbold, P., Snell, N., Rugman, P., and Stockley, R. (2009). Imbalances Between Interleukin-1 and Tumor Necrosis Factor Agonists and Antagonists in Stable COPD. Journal of Clinical Immunology *29*, 508–516.

Satoh, T., Takeuchi, O., Vandenbon, A., Yasuda, K., Tanaka, Y., Kumagai, Y., Miyake, T., Matsushita, K., Okazaki, T., Saitoh, T., et al. (2010). The Jmjd3-Irf4 axis regulates M2 macrophage polarization and host responses against helminth infection. Nat Immunol. *11*, 936-944.

Shapiro, SD (2003). Proteolysis in the lung. European Respiratory Journal *22*, 30s–32s.

Shapiro, SD (2012). Elastolytic metalloproteinases produced by human mononuclear phagocytes: potential roles in destructive lung disease. Am J Respir Crit Care Med. *150*, 160-164.

Shaykhiev, R., Krause, A., Salit, J., Strulovici-Barel, Y., Harvey, B.-G., O'Connor, T., and Crystal, R. (2009). Smoking-dependent reprogramming of alveolar macrophage polarization: implication for pathogenesis of chronic obstructive pulmonary disease. J. Immunol. *183*, 2867–2883.

Simani, A.S., Inoue, S., and Hogg, J.C. (1974). Penetration of the respiratory epithelium of guinea pigs following exposure to cigarette smoke. Lab. Invest. *31*, 75–81.

Snider, G.L., Kleinerman, J., Thurlbeck, W.M., and Bengali, Z.K. (1985). The definition of emphysema. Report of a National Heart, Lung, and Blood Institute, Division of Lung Diseases workshop. The American Review of Respiratory Disease *132*, 182–185.

Sommerhoff, C.P., Nadel, J.A., Basbaum, C.B., and Caughey, G.H. (1990). Neutrophil elastase and cathepsin G stimulate secretion from cultured bovine airway gland serous cells. J. Clin. Invest. *85*, 682–689.

Stedman, R.L. (1968). Chemical composition of tobacco and tobacco smoke. Chemical Reviews *68*, 153–207.

Stefano, D.A., Capelli, A, and Lusuardi, M (2001). Decreased T lymphocyte infiltration in bronchial biopsies of subjects with severe chronic obstructive pulmonary disease. Clin Exp Allergy. *31*, 893-902.

Di Stefano, A., Caramori, G., Gnemmi, I., Contoli, M., Vicari, C., Capelli, A., Magno, F., D'Anna, S., Zanini, A., Brun, P., et al. (2009). T helper type 17-related cytokine expression is increased in the bronchial mucosa of stable chronic obstructive pulmonary disease patients. Clinical & Experimental Immunology *157*, 316–324.

Stein, Keshav, Harris, and Gordon (1992). Interleukin 4 potently enhances murine macrophage mannose receptor activity: a marker of alternative immunologic macrophage activation. J Exp Med. *176*, 287-292.

Stevenson, C.S., Coote, K., Webster, R., Johnston, H., Atherton, H.C., Nicholls, A., Giddings, J., Sugar, R., Jackson, A., Press, N.J., et al. (2005). Characterization of cigarette smoke-induced inflammatory and mucus hypersecretory changes in rat lung and the role of CXCR2 ligands in mediating this effect. Am. J. Physiol. Lung Cell Mol. Physiol. *288*, L514–22.

Stevenson, C.S., Docx, C., Webster, R., Battram, C., Hynx, D., Giddings, J., Cooper, P.R., Chakravarty, P., Rahman, I., Marwick, J.A., et al. (2007). Comprehensive gene expression profiling of rat lung reveals distinct acute and chronic responses to cigarette smoke inhalation. Am. J. Physiol. Lung Cell Mol. Physiol. *293*, L1183–93.

Van der Strate, B.W., Postma, D.S., Brandsma, C.-A.A., Melgert, B.N., Luinge, M.A., Geerlings, M., Hylkema, M.N., van den Berg, A., Timens, W., and Kerstjens, H.A. (2006). Cigarette smoke-induced emphysema: A role for the B cell? Am. J. Respir. Crit. Care Med. *173*, 751–758.

Sullivan, A.K., Simonian, P.L., Falta, M.T., Mitchell, J.D., Cosgrove, G.P., Brown, K.K., Kotzin, B.L., Voelkel, N.F., and Fontenot, A.P. (2005). Oligoclonal CD4+ T cells in the lungs of patients with severe emphysema. Am. J. Respir. Crit. Care Med. *172*, 590–596.

Taggart, C.C., Greene, C.M., Carroll, T.P., O'Neill, S.J., and McElvaney, N.G. (2005). Elastolytic proteases: inflammation resolution and dysregulation in chronic infective lung disease. Am. J. Respir. Crit. Care Med. *171*, 1070–1076.

Takeyama, K., Agustí, C., Ueki, I., Lausier, J., Cardell, L.O., and Nadel, J.A. (1998). Neutrophil-dependent goblet cell degranulation: role of membrane-bound elastase and adhesion molecules. Am. J. Physiol. *275*, L294–302.

Tang, Q, and Bluestone, JA (2008). The Foxp3+ regulatory T cell: a jack of all trades, master of regulation. Nat Immunol. *9*, 239-244.

Taylor, A.E., Finney-Hayward, T.K., Quint, J.K., Thomas, C.M., Tudhope, S.J., Wedzicha, J.A., Barnes, P.J., and Donnelly, L.E. (2010). Defective macrophage phagocytosis of bacteria in COPD. Eur. Respir. J. *35*, 1039–1047.

Thomson, E., Williams, A., Yauk, C., and Vincent, R. (2012). Overexpression of Tumor Necrosis Factor-α in the Lungs Alters Immune Response, Matrix Remodeling, and Repair and Maintenance Pathways. The American Journal of Pathology *180*, 1413–1430.

Tinkelman, D.G., Price, D., Nordyke, R.J., and Halbert, R.J. (2007). COPD screening efforts in primary care: what is the yield? Prim Care Respir J *16*, 41–48.

Traves, S.L., and Donnelly, L.E. (2008). Th17 cells in airway diseases. Current Molecular Medicine *8*, 416–426.

Turato, G., Zuin, R., Miniati, M., Baraldo, S., Rea, F., Beghé, B., Monti, S., Formichi, B., Boschetto, P., Harari, S., et al. (2002). Airway inflammation in severe chronic obstructive pulmonary disease: relationship with lung function and radiologic emphysema. Am. J. Respir. Crit. Care Med. *166*, 105–110.

U.S. Environmental Protection Agency. Respiratory Health Effects of Passive Smoking (Also Known as Exposure to Secondhand Smoke or Environmental Tobacco Smoke—ETS). U.S. Environmental Protection Agency, 1992

Vastag, E, Matthys, H, Köhler, D, and Grönbeck, L (1984). The connections between smoking, mucociliary clearance and airway obstruction. *102*, 629–634.

Van de Veerdonk, F.L., Lauwerys, B., Marijnissen, R.J., Timmermans, K., Di Padova, F., Koenders, M.I., Gutierrez-Roelens, I., Durez, P., Netea, M.G., van der Meer, J.W., et al. (2011). The anti-CD20 antibody rituximab reduces the Th17 cell response. Arthritis Rheum. *63*, 1507–1516.

Vestbo, J, and Lange, P (2002). Can GOLD Stage 0 provide information of prognostic value in chronic obstructive pulmonary disease? Am J Respir Crit Care Med. *166*, 329-332.

Vlahos, R., Bozinovski, S., Jones, J., Powell, J., Gras, J., Lilja, A., Hansen, M., Gualano, R., Irving, L., and Anderson, G. (2006). Differential protease, innate immunity, and NF-κB induction profiles during lung inflammation induced by subchronic cigarette smoke exposure in mice. AJP: Lung Cellular and Molecular Physiology *290*, L931–L945.

Vlahos, R., Bozinovski, S., Chan, S., Ivanov, S., Lindén, A., Hamilton, J., and Anderson, G. (2010). Neutralizing granulocyte/macrophage colony-stimulating factor inhibits cigarette smoke-induced lung inflammation. Am. J. Respir. Crit. Care Med. *182*, 34–40.

Vuillemenot, B., Rodriguez, J., and Hoyle, G. (2004). Lymphoid Tissue and Emphysema in the Lungs of Transgenic Mice Inducibly Expressing Tumor Necrosis Factor-α. American Journal of Respiratory Cell and Molecular Biology *30*, 438–448.

Walters, MJ, Paul-Clark, MJ, McMaster, SK, and Ito, K (2005). Cigarette smoke activates human monocytes by an oxidant-AP-1 signaling pathway: implications for steroid resistance. Mol Pharmacol. *68*, 1343-1352.

Wan, W.-Y., Morris, A., Kinnear, G., Pearce, W., Mok, J., Wyss, D., and Stevenson, C. (2010). Pharmacological characterisation of anti-inflammatory compounds in acute and chronic mouse models of cigarette smoke-induced inflammation. Respir. Res. *11*, 126.

Wang, C., Rose-Zerilli, M., Koppelman, G., Sandling, J., Holloway, J., Postma, D., Holgate, S., Bours, V., Syvänen, A.-C., and Dideberg, V. (2012). Evidence of association between interferon regulatory factor 5 gene polymorphisms and asthma. Gene *504*, 220–225.

Weibel, E.R. (1966). Morphometry of the Human Lung. Biometrische Zeitschrift *8*, 143–144.
WHO (1997). Alpha 1-antitrypsin deficiency: memorandum from a WHO meeting. Bull World Health Organ. *75*, 397-415.
WHO (2008). World Health Statistics 2008 (World Health Organization).
Wong, S., Puaux, A., Chittezhath, M., Shalova, I., Kajiji, T., Wang, X., Abastado, J., Lam, K., and Biswas, S. (2010). Macrophage polarization to a unique phenotype driven by B cells. Eur. J. Immunol. *40*, 2296–2307.
Woodruff, P., Koth, L., Yang, Y., Rodriguez, M., Favoreto, S., Dolganov, G., Paquet, A., and Erle, D. (2005). A Distinctive Alveolar Macrophage Activation State Induced by Cigarette Smoking. Am J Respir Crit Care Med. *172*, 1383-1392.
Wright, J.L., and Churg, A. (1990). Cigarette smoke causes physiologic and morphologic changes of emphysema in the guinea pig. Am. Rev. Respir. Dis. *142*, 1422–1428.
Wright, JL, Lawson, LM, Pare, PD, and Wiggs, BJ (1983). Morphology of peripheral airways in current smokers and ex-smokers. Am Rev Respir Dis. *127*, 474-477.
Wright, J.L., Cosio, M., and Churg, A. (2008). Animal models of chronic obstructive pulmonary disease. Am. J. Physiol. Lung Cell Mol. Physiol. *295*, L1–15.
Wynn, TA (2011). Integrating mechanisms of pulmonary fibrosis. J Exp Med. *208*, 1339-1350.
Yamamoto, C, and Yoneda, T (1997). Airway inflammation in COPD assessed by sputum levels of interleukin-8. CHEST *112*, 505-510.
Yang, SR, Chida, AS, and Bauter, MR (2006). Cigarette smoke induces proinflammatory cytokine release by activation of NF-κB and posttranslational modifications of histone deacetylase in macrophages. Am J Physiol Lung Cell Mol Physiol. *291*, L46-57.
Zubler, R. (2001). Naive and memory B cells in T-cell-dependent and T-independent responses. Springer Semin Immunopathol *23*, 405419.

7 Acknowledgements

Mein besonderer Dank gilt Prof. Dr. Oliver Eickelberg für die Möglichkeit, dieses interessante Forschungsthema am Comprehensive Pneumology Center in einem tollen wissenschaftlichen Umfeld bearbeiten zu dürfen sowie für seine hilfreiche Unterstützung und die anregenden Diskussionen.

Insbesondere danke ich meinem Betreuer Herrn Dr. Ali Önder Yildirim für die vielen Diskussionen und Ideen sowie seine Anleitung. Ich danke Ihm für die Freiheit die er mir während der Durchführung dieser Dissertation gewährte und dafür dass er mir die Teilnahme an mehreren Kursen und Kongressen ermöglicht hat. Unter seiner Betreuung habe ich sehr viel gelernt und konnte Erfahrungen sammeln, die anderswo nicht möglich gewesen wären.

Meinem Thesis Committee, Prof. Dr. Oliver Eickelberg, Dr. Ali Önder Yildirim und Prof. Dr. med. Dominik Hartl danke ich für die fruchtbaren Diskussionen und hilfreichen Tipps, die erfolgreich zum Fortschritt dieser Arbeit beigetragen haben.

Allen Mitglieder der Arbeitsgruppe, vor allem Gerrit, Oana, Alex, Tom, Catharina, Rim und Jie möchte ich für die tolle Zeit im Labor und ihre Unterstützungen, die weit über den Laboralltag hinausgingen, sehr herzlich danken! Außerdem danke ich Christine für ihre tatkräftige Hilfe im Labor.

Einen herzlichen Dank auch an die gute Seele des Labors: Marlene! Vielen Dank für Dein immer offenes Ohr sowie die zahlreichen praktischen Tipps!

Dr. Dr. Melanie Königshoff danke ich für ihr Engagement in der Research School „Lung Biology and Disease“, die mir ein solides Grundwissen im Bereich “Lunge” sowie ein besseres Verständnis zur Bearbeitung wissenschaftlicher Fragestellungen vermittelt hat.

Den Koordinatorinnen der Graduiertenschule „Lung Biology and Disease“, Camille Beunèche und Doreen Franke, gilt mein Dank für ihre organisatorische Unterstützung rund um die Doktorarbeit. Allen Doktoranden der Graduiertenschule möchte ich danken für die angenehme Zusammenarbeit und die stets hilfreiche und offene Atmosphäre.

Gerrit John-Schuster und Barbara Berschneider danke ich für das Korrekturlesen der Arbeit, sowie für ihre immerwährende Unterstützung auf unterschiedlichsten Wegen.

Meiner Familie und Freunden danke ich für ihre unermüdliche Unterstützung und Aufmunterungen während der gesamten Zeit von Studium und Doktorarbeit. Ohne eure Hilfe wäre dies alles sicher nicht möglich gewesen.

Philipp, danke für´s Anspornen und danke für Deine Unterstützung in allen Lebenslagen vor allem bei der “Bewältigung” unserer wohl größten Herausforderung ;) .